



<https://theses.gla.ac.uk/>

Theses Digitisation:

<https://www.gla.ac.uk/myglasgow/research/enlighten/theses/digitisation/>

This is a digitised version of the original print thesis.

Copyright and moral rights for this work are retained by the author

A copy can be downloaded for personal non-commercial research or study, without prior permission or charge

This work cannot be reproduced or quoted extensively from without first obtaining permission in writing from the author

The content must not be changed in any way or sold commercially in any format or medium without the formal permission of the author

When referring to this work, full bibliographic details including the author, title, awarding institution and date of the thesis must be given

Enlighten: Theses

<https://theses.gla.ac.uk/>
research-enlighten@glasgow.ac.uk

The Molecular Pathology of Metastasis
with reference to the
SL 12 Murine Lymphoma model

WING ZOU WONG
MB ChB (Glasg), FRCSEd

Submitted for the degree of
Doctor of Medicine (MD)
Faculty of Medicine
University of Glasgow

Research was conducted in the
Department of Surgery
Keele University
North Staffordshire Hospital
Stoke-on-Trent

February 1999

ProQuest Number: 10391240

All rights reserved

INFORMATION TO ALL USERS

The quality of this reproduction is dependent upon the quality of the copy submitted.

In the unlikely event that the author did not send a complete manuscript and there are missing pages, these will be noted. Also, if material had to be removed, a note will indicate the deletion.



ProQuest 10391240

Published by ProQuest LLC (2017). Copyright of the Dissertation is held by the Author.

All rights reserved.

This work is protected against unauthorized copying under Title 17, United States Code
Microform Edition © ProQuest LLC.

ProQuest LLC.
789 East Eisenhower Parkway
P.O. Box 1346
Ann Arbor, MI 48106 – 1346

ABSTRACT

The SL 12 murine T-lymphoma cell line established by MacLeod et. al., has two sister clones SL 12.3 and SL 12.4. These two cell lines with similar amount of DNA have been shown to have different surface antigens, tumorigenicity and pattern of metastasis. This was thought to be due to differential expression of genes, either repressed or activated, by the two cell lines.

This study has re-established the SL 12.3 and SL 12.4 cell lines. In tissue culture, both cell lines grow well in suspension in modified Dulbecco medium (DMEM). SL 12.4 cells grow in clumps whereas SL 12.3 cells grow diffusely in vitro. Growth curves of SL 12.3 and SL 12.4 cell lines over five days show similar characteristics but with wide variation in SL 12.4 cell counts resulting in large standard error of mean. Clumping of SL 12.4 cells may be responsible for this variation due to cell counting difficulties. Therefore, although growth curves between the two cell lines are shown to be similar, it is not possible to conclude that the growth rates and cell doubling times are identical.

In macroscopic studies, mice injected with 10^6 SL 12.3 cells via the tail vein deteriorate over a median of 17 days (range 11 to 24 days). All mice (100%) have huge hepatosplenomegaly. On the other hand, only one mouse (9.1%) injected with similar number of SL 12.4 cells deteriorated with metastases at 22 days. When the inoculum of SL 12.4 cells was increased to 10^7 cells, 78.5% of mice developed metastasis over a median of 48 days (range 31-56

days). Metastases were seen in ovaries, kidneys and lymph nodes macroscopically in contrast to SL 12.3 cells. Microscopically, it was found that both SL 12.3 and SL 12.4 cells were similarly distributed in various organs that were not involved macroscopically indicating that the observed differing pattern of metastasis is more likely to be due to differential 'in-organ' growth rates rather than cells homing to a particular site after injection.

This hypothesis was further investigated by *in vivo* cellular tracking studies using ^{125}I UDR labelled cells. The mean number of SL 12.4 cells per gram of wet tissue was found to be higher in ovarian tissues at 60 minutes post injection but after 3 hours post injection, both cell lines showed no significant differences in tissue distribution. This again suggested no evidence of a 'homing' phenomenon. However, the highest possible mean percentage of incorporation of radioactive label into these cell lines was 6.9% for SL 12.3 cells and 4.8% for SL 12.4 cells at $2.0 \mu\text{Ci/ml}$ of ^{125}I UDR. The percentage of incorporation was poorly reproducible and this markedly reduced the sensitivity of the study producing wide variation making the data interpretation difficult and therefore, conclusion based in the data non-valid.

Molecular characterisation of the two cell lines was performed using the technique of Differential Display to further investigate the possibility of differential gene expression or repression that could be responsible for the differing *in vivo* growth rates. Three cDNAs band of interests were isolated from the two cell lines. Bands A and C were exclusively expressed in

SL 12.4 cells and SL 12.3 cells respectively. Band D is expressed more in SL 12.4 cells.

To further characterise these three cDNAs, reamplification was attempted using the TA cloning system. Despite changing parameters such as vector/insert ratios and PCR cycles, it was not possible to amplify these clones using this technique as multiple attempts repeatedly produced false positive colonies with blunt ligation at the plasmid ECoRI sites. The three cDNAs (bands A, C and D) were finally reamplified directly using PCR with extended primers.

Comparing with available genetic databases (Embank and Genbank), Band A has weak homology to tyrosine kinase gene in *Hydra vulgaris* (66.7 % identity with 63 nucleotide overlap) and ERCC2/XPD gene in *Xiphophorus maculatus* (55.9 % identity with 128 nucleotide overlap). Both these genes are important in cancer as mutation in tyrosine kinase and the ERCC genes can result in uncontrolled cellular proliferation (Cadena, 1992) and impaired DNA repair (Weeda, 1997) respectively. Band C has weak homology to transforming protein gene in *Caenorhabditis elegans* (56.9 % identity with 102 nucleotide overlap). The expressed proteins of these mutated genes are able to interact with other cellular proteins to transform the cells to become cancerous (Darnell, 1990). Lastly Band D has weak homology to the gene for proliferin related protein (59.7 % identity with 159 nucleotide overlap). This protein is known to be homologous to the prolactin growth family and is expressed by several murine cell lines and placenta (Linzer, 1985). Their function is unknown but their association with the prolactin growth family suggests their importance in cancer (Reynolds, 1997).

These three sequences are now available for further studies, initially by Northern blotting to confirm differential expression and subsequently, used to further probe the mouse cDNA libraries to identify the complete gene sequence which then would allow characterisation of their protein function using techniques such as transfection studies and 'knock-out' transgenic mouse models. The technique established in this thesis of differential display and direct sequencing can be extended to investigate human tumour models to isolate cDNAs that are responsible for the tumour pattern of metastasis and tumourigenicity.

QUOTATION

*" When a plant goes to seed,
its seeds are carried in all directions;
but they can only live and grow
if they fall on congenial soil "*

(Mr. Stephen Paget, Lancet 1889)

Dedications

I dedicate this thesis to my wife, Caryne
and my two sons, Justin and Henry.

I am indebted to my wife and sons, who have helped,
supported, endured and encouraged me in the completion
of this thesis.

Many thanks to my parents and sisters
for their continuous support and encouragement

Thanks

I would like to thank Mr. Mark Deakin for his supervision and guidance in the preparation and completion of this thesis.

I would also like to thank Professor Elder for giving me the opportunity to do this research and Mrs. Tracy Holland for preparing all histological slides and her expertise technical assistance in the experiments.

I am grateful to the North Staffordshire Medical Institute and the Nuffield Hospital Foundation for the research grant and salary respectively.

TABLE OF CONTENTS

• Chapter 1	Metastasis : The Process	1
• Chapter 2	Metastasis : The Pattern	19
• Chapter 3	Models of Metastasis	46
• Chapter 4	Aims, Hypothesis & Overview Of Studies Performed	52
• Chapter 5	Establishing the SL 12.3 and SL 12.4 Lymphoma model and in vitro growth rate Comparison	55
• Chapter 6	Macroscopic and Microscopic study of Metastatic pattern	60
• Chapter 7	Cell Tracking Studies	71
• Chapter 8	Molecular Studies	96
• Chapter 9	mRNA Differential Display	106
• Chapter 10	Characterisation of cDNAs of interest	122
• Chapter 11	Comparison sequences obtained with Genbank and Embank data	136
• Chapter 12	Discussion	145
• Chapter 13	Conclusions	184
• References		195

LIST OF FIGURES

• Figure 1.1	The metastatic process	4
• Figure 1.2	The role of plasminogen activator in the degradation of plasma membrane	7
• Figure 1.3	Lodgement at capillary	15
• Figure 2.1	Major families of cellular adhesion molecules (Ilynes 1992)	32
• Figure 4.1	Overview of the study	54
• Figure 5.1	SL 12.3 cells grows diffusely	56
• Figure 5.2	SL 12.4 cells grows in clumps	57
• Figure 6.1	AKR mouse restrained for tail vein injection	61
• Figure 6.2	Examples of findings on abdominal examination on an AKR mouse injected with 10^6 SL 12.3 cells (Median=17 days; Range=11-24 days)	66
• Figure 6.3	Examples of findings on abdominal examination on an AKR mouse injected with 10^7 SL 12.4 cells (Median=48 days; Range=31-56 days)	66
• Figure 7.1	Steps in preparing an autoradiograph	80
• Figure 7.2	Autoradiograph of SL 12.3 cells following labelling with 125 IUDR (<i>Low power</i>)	81
• Figure 8.1	Differential screening	99
• Figure 8.2	Subtractive hybridisation	101
• Figure 8.3	A summary of Polymerase Chain Reaction (PCR)	105

• Figure 9.1	Primers used in differential display. The 3'-primer is an anchoring oligo(dTs) and the arbitrarily chosen 5'-primer anneal randomly	107
• Figure 9.2	Selection of 3'-primer is based on the poly -A tail of mRNAs	108
• Figure 9.3	Electrophoresis of total RNA of SL 12.3 and SL 12.4 cells in 1 % denaturing RNA agarose gel	113
• Figure 9.4	Electrophoresis of Reverse Transcription products of SL 12.3 and SL 12.4 cells	115
• Figure 9.5	mRNA of murine CD44 (Nottenburg 1989)	116
• Figure 9.6	PCR products of SL 12.3 and SL 12.4 without [³⁵ S]dATP α S using either CD44 or LTK3 primers	118
• Figure 9.7	Autoradiogram showing the cDNA ladders of SL 12.3 & SL 12.4 cells using CD44	119
• Figure 9.8	Cutting dried gel out from 3 MM paper	121
• Figure 10.1	Insertion of PCR product into the vector using the overhang 3'-A tail (Insert) and the single 5'-T' nucleotide (vector)	123
• Figure 10.2	pCRII vector with the different genes inserted into it	123
• Figure 10.3	Agar plate showing white and blue colonies in TA cloning	126
• Figure 10.4	First specimen: Comparing sequence of vector PCR II (& insert) and sequence obtained	127
• Figure 10.5	Second specimen: Comparing sequence of vector PCR II (& insert) and sequence obtained	127
• Figure 10.6	Sequencing with 19-mers (5'-end primer)	132
• Figure 10.7	Sequencing with 22-mer (3'-end primer)	132
• Figure 10.8	Sequence of cDNA A using 22-mers as the primer	133
• Figure 10.9	Sequence of cDNA A using 19-mers as the primer	133
• Figure 10.10	Sequence of cDNA C using 22-mers as the primer	134

• Figure 10.11	Sequence of cDNA <i>C</i> using 19-mers as the primer	134
• Figure 10.12	Sequence of cDNA <i>D</i> using 22-mers as the primer	135
• Figure 10.13	Sequence of cDNA <i>D</i> using 19-mers as the primer	135
• Figure 12.1	PCR products using either mRNAs or total RNAs as template	159
• Figure 12.2	The importance of the anchoring device in the 3'-end primer	161
• Figure 12.3	Smearing as a result of old 3'-end primers which have lost their anchoring device	162
• Figure 12.4	PCR products on an Agarose gel using either T ₁₁ CA or T ₁₂ CA anchoring primers showing that as the primers are lengthened the anchorage efficiency increases but to the detriment to the increasing background	164
• Figure 12.5	Triplets seen in cDNAs less than 300 base pairs	167
• Figure 12.6	The Hoefer's gel eluter	170

LIST OF CHARTS

- Chart 5.1 The growth curve for SL 12.3 and SL 12.4 cell lines
(*Error bar = standard error of the mean*) 59
- Chart 6.1 The comparison between mean percentage of
body weight of organs in mice injected with
 10^6 SL 12.3 cells, 10^6 SL 12.4 cells and 10^7 SL 12.4 cells
(*arrows indicate significant differences between
 10^6 SL 12.3 cells and 10^7 SL 12.4*) 68
- Chart 7.1 Mean percentage (*standard error of mean*) of incorporation of
radioactive labels by SL 12.3 and SL12.4 cells at different
concentration of ^{125}I -5-Iodo-2' deoxyuridine. 75
- Chart 7.2 Growth curve of SL 12.3 cells (Set 1) in different
concentrations of ^{125}I UDR over 5 days 77
- Chart 7.3 Growth curve of SL 12.3 cells (Set 2) in different
concentrations of ^{125}I UDR over 5 days 77
- Chart 7.4 Growth curve of SL 12.4 cells (Set 1) in different
concentrations of ^{125}I UDR over 5 days 78
- Chart 7.5 Growth curve of SL 12.4 cells (Set 2) in different
concentrations of ^{125}I UDR over 5 days 78
- Chart 7.6 The mean percentage of total viable SL 12.3 and SL 12.4
cells present in different organs at fifteen minutes 87
- Chart 7.7 The mean percentage of total viable SL 12.3 and SL 12.4
cells present at different organs at one hour 88
- Chart 7.8 The mean percentage of total viable SL 12.3 and SL 12.4
cells present at different organs at 3 hours 89
- Chart 7.9 Mean number of cells (*standard error of mean*) per gram of
tissue at 15 minutes after inoculation 93
- Chart 7.10 Mean number of cells (standard error of mean) per gram of
tissue at 60 minutes after inoculation 94
- Chart 7.11 Mean number of cells (standard error of mean) per gram of
tissue at 3 hours after inoculation 95

LIST OF TABLES

• Table 2.1	Autopsies performed by Paget (Paget 1889) showing the disproportionate distribution of metastases between spleen and liver in breast and uterine tumour cases compared with cases of pyaemia	20
• Table 2.2	A summary of adhesion molecules and their ligands	45
• Table 3.1	Tumourigenicity of SL 12, SL 12.3 and SL 12.4 cells after <i>intravenous</i> inoculation (<i>MacLeod. 1985</i>)	48
• Table 3.2	Tumourigenicity of SL 12, SL 12.3 and SL 12.4 cells after <i>intra</i> dermal inoculation (<i>MacLeod 1985</i>)	48
• Table 3.3	Metastatic pattern of SL 12, SL 12.3 and SL 12.4 cell lines after intravenous inoculation of 10^6 cells	49
• Table 5.1	Daily cell counts for SL 12.3 and SL 12.4 cells	58
• Table 6.1a	Macroscopic pattern of metastasis shown by 10^6 12.3 and 10^6 SL 12.4 cells <i>(p-value calculated using the Exact Probability Test)</i>	64
• Table 6.1b	Macroscopic pattern of metastasis shown by 10^6 12.3 and 10^7 SL 12.4 cells <i>(p-value calculated using the Exact Probability Test)</i>	65
• Table 6.2	The mean percentage of body weight (<i>Standard Deviation</i>) of organs in mice injected with SL 12.3 and SL 12.4 cells	67
• Table 6.3	Macroscopic and microscopic patterns of SL 12.3 and SL 12.4 cells	70
• Table 7.1	Percentage of incorporation of radioactive labels by cells at different concentration of ^{125}I -5-Iodo-2'-deoxyuridine	74
• Table 7.1a	P-values (determined with Student T-test) showed no significance statistically between the incorporation of different concentration of ^{125}I UDR by SL 12.3 and SL 12.4 cells	74
• Table 7.2	Daily cell counts to check viability and growth of SL 12.3 and SL 12.4 cells at varying concentration of ^{125}I -5-Iodo-2'-deoxyuridine	76

• Table 7.3a	Mean number [<i>Standard Deviation</i>] of viable SL 12.3 and SL 12.4 cells estimated to be within each organ at 15 minutes after injection	84
• Table 7.3b	Mean number [<i>Standard Deviation</i>] of viable SL 12.3 and SL 12.4 cells estimated to be within each organ at 60 minutes after injection	85
• Table 7.3c	Mean number [<i>Standard Deviation</i>] of viable SL 12.3 and SL 12.4 cells estimated to be within each organ at 3 hours after injection	86
• Table 7.4a	The mean number [<i>Standard Deviation</i>] of cells per gram of tissues at 15 minutes after injection	90
• Table 7.4b	The mean number [<i>Standard Deviation</i>] of cells per gram of tissues at 60 minutes after injection	91
• Table 7.4c	The mean number [<i>Standard Deviation</i>] of cells per gram of tissues at 3 hours after injection	92
• Table 9.1	Theoretical calculation and experimental data of the number of mRNA species that could be amplified by arbitrary primers with different lengths in combination with an anchored oligo(dTs) that binds to 1/12 of mRNAs 3' termini (<i>From Liang et. al., 1992</i>)	108
• Table 9.2	Total Cellular RNA extracted from SL 12.3 and SL 12.4 cells	112
• Table 11.1	Homologies of Band A ~ 162 nucleotides (nt) (using 22-mer primer)	136
• Table 11.2	Homologies of Band A ~ 176 nucleotides (nt) (using 19-mer primer)	137
• Table 11.3	Homologies of Band C ~ 153 nucleotides (nt) (using 22-mer primer)	138
• Table 11.4	Homologies of Band C ~ 160 nucleotides (nt) (using 19-mer primer)	139
• Table 11.5	Homologies of Band D ~ 197 nucleotides (nt) (using 22-mer primer)	140
• Table 11.6	Homologies of Band D ~ 202 nucleotides (nt) (using 19-mer primer)	141

Chapter I Metastasis: The Process

Introduction

The word 'Metastasis' is Greek in origin and is defined by The Dorland's Medical Dictionary as the transfer of disease from one organ or a part to another not directly connected to it and the transfer could be of pathogenic micro-organism (as in tubercle bacilli) or cells (as in malignant tumours) (Dorland 1981). It was initially used by Reclamer in 1829 (Reclamer 1829) when he applied it to a growth in the brain of a patient who also had breast carcinoma.

In 1903, Schmidt (Schmidt 1903) studied the process in detail and clearly described all its morphological aspects including cellular invasion, intravasation, arrest, extravasation and formation of secondary growths in new sites. Today, from reconstruction of surgical biopsies and post mortem specimens, we believe metastasis to be a complex multistep cascade process with potentially rate limiting steps. Tumour cells have to complete all steps in order to metastasise and failing in any of them will eliminate the process (Liotta 1985). Metastasis is, therefore, not an adaptive process but appears to involve selection of pre-existent tumour cells with higher metastatic potential that could complete all steps (Nicholson 1982; Talmadge 1982). The outcome of the event also depends on factors such as the host's immune response and the compatibility of the new site.

The clinical significance of metastasis

A review on six hundred and forty-five colorectal carcinoma cases by McArdle et al showed that one quarter of patients presenting with colorectal carcinoma for the first time already had distant metastases (McArdle 1990) and one half of patients with tumours showed some signs of tumour fixity at their first presentation. The overall five year survival rate for colorectal carcinomas is about 25-30 % after surgery (Nigam 1994) and the five-year survival rate for 'curative' surgical resection is no more than 50 %. If liver metastases are present, the median survival is about six months (Nigam 1994) and only about 1-3 % of all colorectal carcinoma patients benefits from hepatectomy for liver metastasis (Scheele 1993).

Furthermore, results from other alternative treatments such as regional or systemic chemotherapy for metastases are also poor with only about 15-20% of colorectal carcinomas responding to systemic chemotherapy with marginal benefits in terms of survival (Nigam 1994).

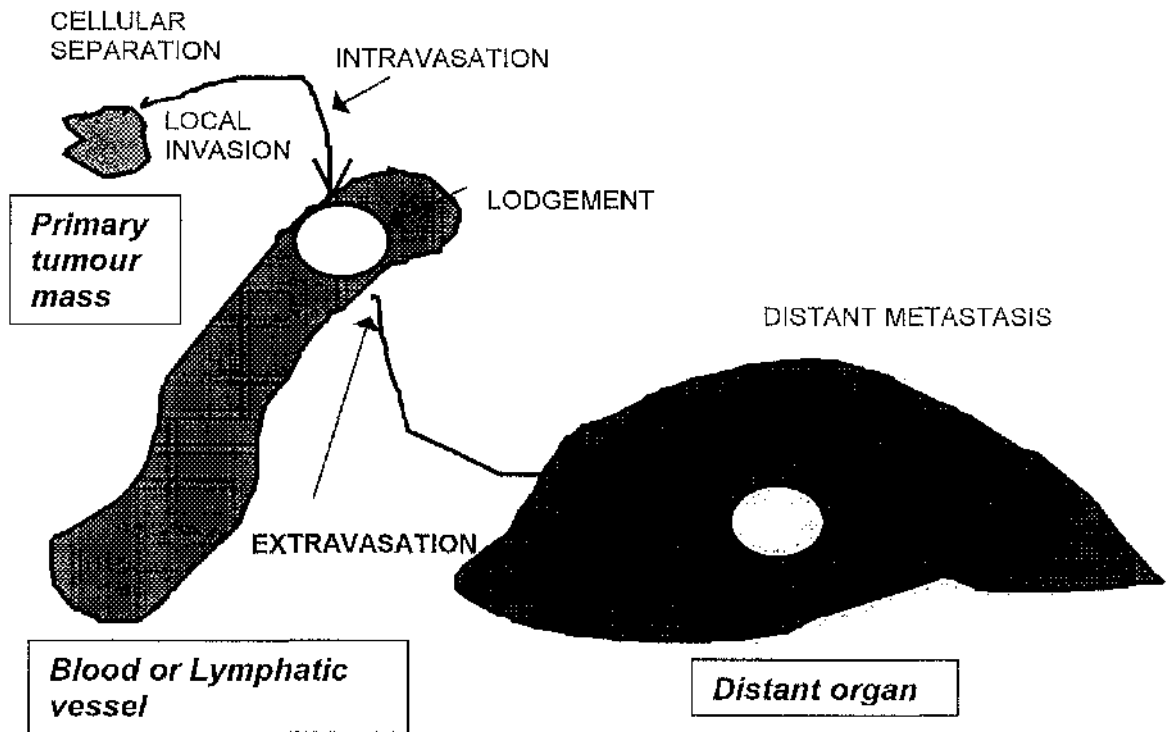
Such poor response to available therapy is not surprising as it has been estimated that by the time visceral metastases are diagnosed, these lesions are about one cubic centimetre containing about a billion cells. Any therapy that could destroy 99.9 % of these cells is, therefore, not sufficient to produce a cure as it still leave a million cells to proliferate and generate further variant resistant cells (Fidler 1985). As a result, most deaths from cancer are due to the uncontrolled growth of metastases resistant to therapy (Poste 1980; Fidler 1985).

The mechanism of metastasis

The process of metastasis involves eight distinct steps: cellular separation, local invasion, angiogenesis, intravasation, distribution, lodgement, extravasation and seeding (Liotta 1985; Fidler 1988; Fidler 1990; Kerbel 1990). These steps are not mutually exclusive to each other and do not necessarily have to occur in the order as described. However, a cell has to complete all steps before it can metastasise (Liotta 1985; Fidler 1990).

Metastatic cells detach themselves from the tumour mass and invade surrounding parenchyma, blood and lymphatic vessels. During this time, new and abnormal blood vessels are developing, feeding the expanding tumour. The metastatic cells then intravasate into blood or lymphatic vessels and are carried to all organs. At the new site, the cells lodge, extravasate and invade the surrounding parenchyma. New deposits begin to grow and later the whole metastatic process can be repeated: metastasis from metastases (Figure 1.1).

Figure 1.1 The metastatic process



(1) Cellular separation

Normally cells, excepting haemopoietic cells, are bound tightly to each other by cellular surface proteins resulting in little or no movement possible between them. Malignant cells, on the other hand, have weaker intercellular binding and a lesser force is required to separate one malignant cell from another (Coman 1944). This weakness in intercellular binding is important as it directly relates to the number of cells that are able to separate from the main tumour mass (Elvin 1982). For example, it has been shown experimentally that trauma or even just massage to a tumour mass can lead

to an increase in the release of tumour cells into the venous outflow (Liotta 1974). Recent studies have shown that adhesion molecules, such as E-Cadherin, play an important role in maintaining this intercellular binding and a decreased in E-Cadherin expression has been associated with an increased metastatic potential (Jiang 1994).

(2) Local invasion

The process of local invasion by tumour cells depends on cellular growth, motility and tissue destruction (Evans 1991). During this period, tumour cells proliferate rapidly resulting in an expanding mass that exerts local pressure on surrounding tissue. Unlike benign tumours (e.g., fibroadenoma of the breast) which stop at this stage, malignant tumours continue to expand. The mechanical pressure, produced by the rapid expansion, forces finger-like cords of tumour cells along the lines of least resistance (Fidler 1987).

Invasion is also an active process of tissue destruction involving degradative enzymes such as proteases. These proteolytic enzymes hydrolyse peptide bonds of connective tissues, thus, facilitating local invasion into surrounding tissues. Tumour cells pass through the basement membrane, eventually making their way to blood or lymphatic vessels. It is now believed that tumour cell invasion is not solely due to the deregulated production of proteases but also to an impaired balance between local concentration of active proteases and the levels of their inhibitors, the tissue inhibitors of metalloproteinase (TIMP) (Waxman 1992).

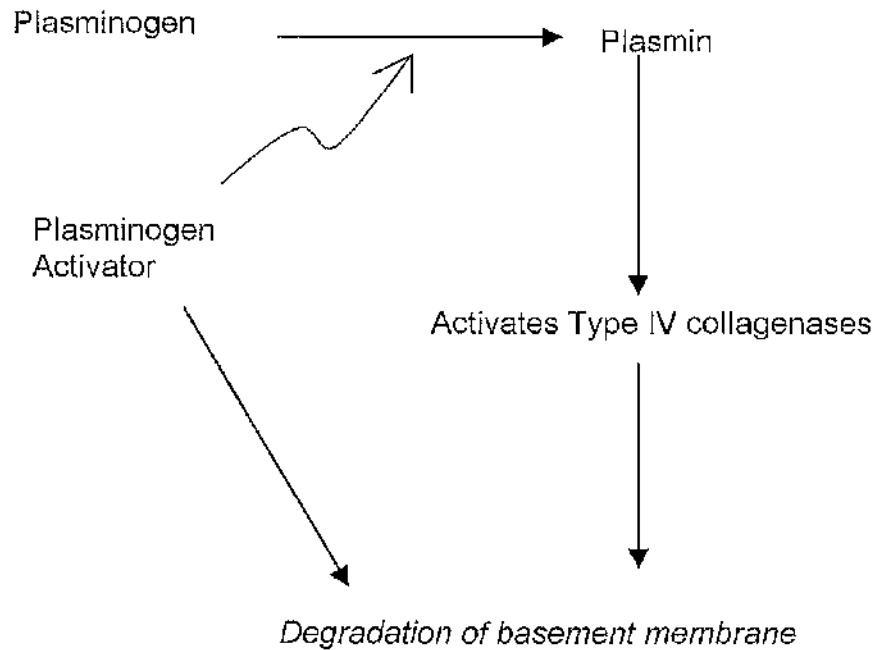
Four major classes of proteases have been described namely Aspartic, Serine, Cysteine and Metalloproteinase. The important proteases involved principally in tumour invasion are serine protease plasminogen activator (Ossowski 1983b), cysteine protease cathepsin B (Sloane 1986) and the metalloproteinase collagenases (Liotta 1979).

Plasminogen activator (PA)

Plasminogen activator may also have a role in the degradation of basement membrane both directly and indirectly (Figure 1.2). Directly, it degrades various glycoprotein and proteoglycan components of basement membranes. Indirectly, it converts plasminogen to plasmin, which in turn activates latent type IV collagenase activity that also results in the degradation of basement membrane (Evans 1991).

The important role of plasminogen activator in local invasion is further supported by studies on the invasion of human amnion by B16-BL6 murine melanoma cells. Invasion is inhibited with anti-urokinase antibodies, plasmin inhibitors and collagenase inhibitors (Mignatti 1986). In addition, plasmin also causes degradation of fibrin and the resulting fibrinolytic activity correlates with the experimental potential of B16 mouse murine melanoma cells to metastasise (Wang 1980).

Figure 1.2 The role of plasminogen activator in the degradation of plasma membrane



Cathepsin B

This cysteine protease is found normally in lysosomes but is also secreted in large amount by tumour cells. Cathepsin B functions optimally at pH 7.0 and degrades basement membrane components such as glycoproteins, proteoglycans and collagen type I-IV. It also appears to be able to activate latent procollagenase (Evans 1991). Cathepsin B-like activity has also been correlated with metastatic potential in B16 melanoma cells (Sloane 1984).

Metalloproteinases

The Metalloproteinases are a group of multidomain, zinc binding and calcium dependent lytic enzymes which cleave tissue collagens (Types I, II, III, IV and V), gelatin, fibronectin, laminin and proteoglycans (Nagase 1992; Yoneda 1994) under normal conditions of body pH and temperature. In local invasion, metalloproteinases also promote cellular separation from the primary tumour. The classification of metalloproteinases is based on their substrate specificity. Two collagenases, two gelatinases, three stromelysins and matrilysin have been described (Nagase 1992; Yoneda 1994).

Interstitial collagenases degrade collagens type I, II and III, gelatinases degrade gelatin and type IV collagen and stromelysins degrade proteoglycans and collagen type IV (Hart 1992). Besides playing an important role in tumour invasion, metalloproteinases have also been associated with normal physiological processes such as morphogenesis, angiogenesis, uterine involution and cervical softening (Waxman 1992)

Increased in tissue concentration of metalloproteinase messenger RNA or immunoreactivity has been described in cancer of the skin, blood, endometrium, ovaries, stomach, colon, prostate, breast, lung, thyroid, head and neck (Yoneda 1994). In these cancers, the increased concentration of metalloproteinases is found to correlate with their invasiveness and their metastatic state (Waxman 1992).

(3) Angiogenesis

Angiogenesis or the formation of new blood vessels is one of the commonest physiological responses of tissues to injury and is seen classically in granulation tissue. In tumour growth angiogenesis is required if the tumour mass were to grow beyond two millimetres in diameter as the transport of nutrients and waste products is not efficient enough beyond this distance by diffusion alone (Hart 1989; Hart 1992). This neovascularisation process is induced either directly by tumours releasing angiogenic factors (Folkman 1989) or by the tumour stimulating host's cells such as macrophages to release the angiogenic factors.

Angiogenic Factors

Regulation of angiogenesis is a balance between the effects of a number of angiogenic factors. Vascular endothelial cells growth factor or VEGF is a known angiogenic inducer in several in vivo systems (Alessandro 1995) and has been shown to be overexpressed in human tumours such as colon, breast, lung and bladder cancer (Alessandro 1995). Intraperitoneal injection of anti-VEGF antibodies inhibited growth of liver metastasis of a human colon carcinoma model (Warren 1995).

The major groups of angiogenic peptides that have been isolated are fibroblast growth factor (FGF) (Shing 1984; Shing 1985), low molecular weight products such as nicotinamide (Kull 1987), platelet derived endothelial cell growth factor (PD-ECGF) (Ishikawa 1989),

epidermal growth factor (EGF) and transforming growth factor - α (TGF- α) (Evans 1991).

(4) Distribution

Metastatic cells can be distributed to distant tissues by direct extension, lymphatics or the haematogenous route (Willis 1973). It is widely recognised that certain tumours (such as sarcomas) prefer to spread by the haematogenous route whereas other tumours such as carcinomas spread by the lymphatic route. However, this is not necessarily true as there is substantial evidence showing that malignant cells pass freely between lymphatics and other vessels (Poste 1980; Fidler 1987).

Direct extension

In this process, tumour cells extend directly and progressively from the primary tumour mass to infiltrate distant tissues via natural routes, fascial planes and neural sheaths (Poste 1980). In body cavities, they may seed directly onto cellular surfaces such as pleural and peritoneal membranes (Poste 1980). Common examples of such transcoelomic spread are often seen in gastric and ovarian tumours.

Spread via lymphatics

In this process, invading tumour cells interact with the exterior surface of the endothelium lining lymphatics (DeBryun 1979; Warren 1980). As lymphatics are thin walled structures, they offer relatively little mechanical resistance to penetration by tumour cells (Poste 1980). Once within the lymphatic system, tumour cells are filtered by groups of intervening nodes. Tumour emboli could either be trapped by the lymph nodes or evade the filtering mechanism and metastasise to distant organs, the "skip" metastasis (Fidler 1987). Eventually, the cells are drained into the systemic circulation.

The lymphatic system in general and lymph nodes in particular, play an important role in controlling metastasis. Lymph nodes are immunologically reactive in patients with neoplasm and usually become clinically enlarged and palpable (Fidler 1987). Unlike angiogenesis, no factors have been described which induce the formation of new lymphatic channels.

(5) Intravasation

In this process, invading tumour cells attach themselves to the collagen Type IV and proteoglycan components of the basement membrane of venules and capillaries. Entry into the circulation is then facilitated by the release of lytic enzymes such as collagenase and heparanase to produce degradation of the basement membrane (DeBryun 1979; Warren 1980). Ultrastructural studies have shown that endothelium of tumour-associated blood vessels are usually

defective and as such are susceptible to tumour cell penetration (Poste 1980).

After intravasation, tumour cells are either carried away passively or may stay at the site of penetration and continue to shed emboli into circulation (Poste 1980). Shedding of emboli is also exacerbated by intermittent changes in venous pressure, by turbulent alteration in blood flow and by movement or manipulation of the neoplasm during diagnostic tests or surgery (Poste 1980).

(6) Lodgement

Circulating tumour cells must be able to lodge at the capillary level before extravasating into distant organs and therefore, any factors which encourage the process of lodgement, such as endothelial damage, will promote metastasis (Cotmore 1973). Mechanical factors such as size and deformability of tumour cells, the diameter and distensibility of capillaries and the interactions of tumour cells with each other and with circulating host cells to create multicellular emboli are important in the lodgement of tumour cells in capillaries (Poste 1980).

Circulating tumour cells interact with endothelial cells both directly and indirectly. It has been proposed that tumour cells are able to lodge in capillaries by mechanical interlocking directly with the vessel surfaces (Weiss 1994). On the other hand, tumour cells may also interact indirectly, by initially binding to normal blood cells such as platelets. When circulating

platelets attach themselves to exposed basement membrane and damaged endothelium lining, they degranulate. This process recruits more platelet to the damaged endothelium and eventually a platelet aggregation is formed. Such platelet aggregation can in turn entrap circulating tumour cells, thus, increasing the chances for tumour cell interaction with the endothelium and basement membrane (Evans 1991).

Size of tumour embolus

Circulating tumour cells that are in aggregation (i.e., larger tumour emboli) have a higher chance to wedge and lodge at capillary level than those that do not aggregate. Even though the presence of tumour cells in circulation does not guarantee metastasis formation (Salsbury 1975; Fidler 1977), there is a good correlation between the size of tumour cell clump, rate of arrest and likelihood of secondary tumour formation (Fidler 1973b; Liotta 1974).

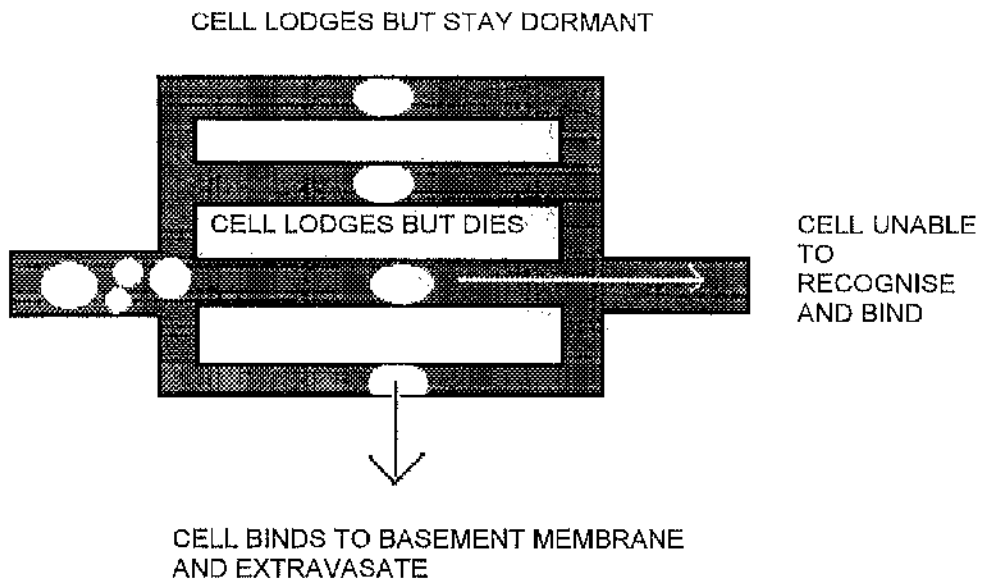
Coagulability of blood

Studies have shown that certain tumours are associated with higher levels of thromboplastin and procoagulant-A activity (Fidler 1988). Procoagulant-A directly activates factor *X* of the clotting cascade, thus, increasing the chance of coagulation at the capillary level. As a result, tumour cells are slowed down in circulation and become entrapped within small capillaries, increasing the chances of lodgement (Fidler 1987). On the contrary, it has also been shown that some metastatic cells are associated with increased fibrinolysis and plasminogen activator production, thus, they may decrease

the coagulability of blood. This is believed to reduce the likelihood of tumour cells becoming enmeshed in a fibrin network, hence, facilitating metastasis (Chew 1976; Donati 1980; Gastpar 1982). In reality, both processes probably happen.

In addition to passive flow and tumour clump size which aid lodgement, tumour cells are also able to recognise and bind specifically to endothelium or basement membrane receptors (Zetter 1990). After lodgement at the capillary bed, four possible outcomes for tumour cells have been suggested (Figure 1.3). Firstly, the cell may lodge and form a metastasis. Secondly, cells may lodge but become dormant. Thirdly, cells may lodge but do not survive. Finally, cells may fail to lodge. Little is known about tumour dormancy. In normal cells a form of dormancy has been reported. When thyroid cells were injected intravenously, they lodge in the lung and remained dormant until the host animal becomes thyroxine deficient (Taptiklis 1968; Taptiklis 1969). It has been shown that only 1 % tumour cells in circulation survive to develop metastases. This could be due to the expression of incompatible growth factors or that the cells are destroyed by the host immune system

Figure 1.3 Lodgement at capillary



(7) Extravasation

Extravasation is the process where tumour cells leave the circulation and pass into surrounding tissue. It is usually preceded by cellular lodgement except in those rare situations where haemorrhage has occurred. The mechanism of extravasation is similar to the process of intravasation but in reverse and involves cellular motility and enzymatic degradation of intercellular structure.

Extravasation can be broadly divided into two main processes. Firstly, tumour cells divide within the lumen and invade outwards *en masse* (Chew 1976). This usually means that tumour cells extravasate by destruction of capillaries rather than by active migration. In the second process tumour cells move actively between endothelial cells and degrade intercellular

matrix and basement membrane using lytic enzymes such as the matrix metalloproteinases (Dingermans and Weerman 1980).

Having extravasated, tumour cells begin to invade the extracellular matrix. A three-step hypothesis of extracellular matrix invasion by tumour cells has been described (Liotta 1986). Firstly, tumour cells bind specifically to exposed extracellular matrix via cell surface receptors (Attachment). The anchored cells then secrete hydrolytic enzymes that can locally degrade the matrix (Dissolution). Finally, tumour cells relocate into the region of the matrix by proteolysis (Locomotion).

(8) Further development of metastases

The ability of tumour cells to grow in the new environment depends on the capability of the cells to evade the host immune system and to express appropriate matrix metalloproteinases and angiogenic factors. In addition, the cells must also express appropriate growth factor receptors. Under favourable conditions, tumour cells proliferate, invade and eventually, metastasise to other organs.

Host's defence system

It is becoming increasingly realised that cellular immunity is an important factor in the prevention of metastases. It is well known that when host immunity is reduced by either T-lymphocyte depletion or by bone marrow ablation, the metastatic potential of certain tumour cell lines is greatly

increased (Alexander 1976; Frost 1983; Schirmacher 1985). In vivo, clones of tumours known to vary in their metastatic capacity, metastasise equally in nude or irradiated mice (Eisenbach 1985).

In circulation, the host's defence system consists of the non-immune and the immune defence system. The non-immune system is non specific and includes phenomena such as intravascular turbulence which can be traumatic enough to account for rapid tumour cell death. Tumour cells may overcome this phenomenon by clumping with each other (homotypic aggregation) or with host's cells such as platelets and lymphocytes (heterotypic aggregation) to form multicellular emboli.

On the other hand, the immune defence system is more complicated and can be subdivided broadly into specific (lymphocytes and antibodies) and non specific (for example, natural killer cells and macrophages) elements. The mechanism of immune surveillance for metastatic cells is similar to that responsible for graft rejection.

Both the Natural killer cells (NK) and macrophages play important role in preventing metastasis. Natural killer cells inhibit tumour colony formation (Hanna 1982a) and their absence is related to increased colony formation. For example, in vivo, tumour cells that were unable to form colonies in the spleens of healthy mice were able to do so if the mouse was pre-treated with anti-NK cell antibodies. Furthermore, when NK cells are inactivated with cyclophosphamide, marked enhancement of both lung and extrapulmonary colonies were observed but these effects could be reversed by the transfer of normal spleen cells to cyclophosphamide treated mice (Hanna 1980).

The effects of NK cells on the primary tumour have been observed to be different from that on metastatic lesions. It is believed that metastatic lesions which are more resistant to the effects of NK cells may have different surface antigens from the primary tumour (Fogel 1979).

Macrophages are important in the immune system as the absence of an intact macrophage system is lethal (Fidler 1985). These cells are able to recognise and discriminate between "self" from "nonself" and they phagocytose and destroy any effete cells and foreign invaders. Frequently, macrophages provide the first line of defence against microbial infections and parasite infestations (Fidler 1987). When activated by lymphokines such as IFN- γ , macrophages are capable of lysing virus-infected or tumourigenic cells and not normal cells (Fidler 1985). It has been shown that macrophages activated by intravenous administration of lymphokines encapsulated with liposomes can enhance the host destruction of metastases (Fidler 1985).

In spite of a competent immune system, some tumour cells manage to complete the metastatic process by escaping the immune system. One possible explanation is that highly metastatic cells are able to shed off surface antigens compared to poorly metastatic cells. Shed antigens may then inhibit lymphocyte mediated cytotoxicity (Alexander 1974; Currie 1974; Kim 1975).

Chapter 2 Metastasis: The Pattern

Introduction

The distribution of metastatic tumours has always fascinated clinicians and pathologists. It has been observed that some organs, such as the liver, lung and bone, are more involved in metastasis than others (Paget 1889). The liver, for example, is a common site for metastasis for a number of cancers. Some arise from nearby tissue such as colonic carcinoma while other distant cancer such as choroidal melanoma bypass several organs to metastasise to the liver. On the other hand, well vascularised organs such as the heart, skin and muscles are unfavourable sites for metastasis (Zetter 1990; Miyasaka 1995).

The interest in metastatic pattern began at the end of the nineteenth century. Studies attempted to answer questions such as “What is it that decides what organs shall suffer in a case of disseminated?” asked by clinicians such as Langenbeck and Billroth (Paget 1889). In 1882, Fuch proposed the ‘Theory of Predisposition’ claiming that certain organs maybe more predisposed to growth of secondary cancers than others. Fuch observed that in choroidal sarcoma, sarcomatous elements were found in the capillary vessels of the retina and metastases developed as far afield as the liver and spleen but not in nearby retinal tissue (Paget 1889).

This was followed by Paget in 1889, who performed necropsies in 735 cases of breast cancer, 244 cases of uterine cancer and 340 cases of pyaemia. He

noted that out of 735 cases of breast carcinoma at post mortem, secondary disease was found in the liver in 241 patients, in spleen in only 17 patients and in the renals and suprarenals in 30 patients (Table 2.1). Despite equally good blood supply to both liver and spleen, the spleen appeared to be a less favourable site for metastasis. Comparing to cases of pyaemia, Paget found that secondary abscesses were found in almost equal proportion in both liver and spleen. He then proposed the 'Seed and Soil Hypothesis' drawing the analogy that when the plant (the primary tumour) goes to seeds (metastases), its seeds are carried in all directions (disseminations); but they can only live and grow if they fall on congenial soil (predisposed organ) (Paget 1889).

Table 2.1. Autopsies performed by Paget (Paget 1889) showing the disproportionate distribution of metastases between spleen and liver in breast and uterine tumour cases compared with cases of pyaemia

AUTOPSIES	LIVER	SPLEEN	KIDNEYS AND SUPRARENALS	LUNGS
735 BREAST CARCINOMA	241 (32.7%)	17 (2.3 %)	30 (4 %)	70 (9.5 %)
244 UTERINE CARCINOMA	35 (14.3 %)	1 (0.4 %)	6 (2.5 %)	8 (3.3 %)
340 PYAEMIA	66 (27.1 %)	39 (16 %)		

Half a century later, Ewing proposed a second model for the metastatic pattern on the basis of circulatory anatomy. His concept formed the basis of the 'Mechanical Hypothesis' of metastasis. In this hypothesis, the pattern of tumour spread is entirely due to the route of blood flow and that various tissues are passive receptacles for tumour cells. The ability of cells to grow

in an organ depends on the number of viable cells delivered to it (Ewing 1928; Coman 1953).

Evidence for 'Seed and Soil' Hypothesis

In the 'Seed and Soil' hypothesis, metastasis is a non-random process and each cancer has its own specific metastatic pattern. The growth of metastases in target organ depends on both the cellular intrinsic genetic make-up and the compatibility of the new tissue environment. Evidence supporting this hypothesis falls into the following observations:

(a) *Discrepancies between the relative blood supply and the relative incidence of metastases in various organs*

If tumour emboli are disseminated in the blood stream, then they should be distributed to the different viscera in proportion to their relative blood supply. Thus, one should expect richly vascular tissues be involved in metastases more frequently than poorly vascular ones. However, this is not so as organs with the richest vascular supply such as adrenals, thyroid, gastrointestinal tract, skeletal muscles and spleen are infrequent sites of metastasis compared to the liver, lung and bone (Fidler 1987).

(b) *Tissues specificity shown by tumour cells*

Certain primary tumours such as lung, prostate, breast and kidneys frequently metastasise specifically only to bone bypassing other organs. Studies have suggested that such tissue specificity could be due to soluble

growth factors released by cells of the target organs allowing specific tumour cells to proliferate and grow (Horak 1986; Nicholson 1986; Naito 1987). For example, mouse mammary tumour cells that normally form pulmonary metastases are unable to survive in medium enriched with liver or thyroid extract. However, when the same tumour cells are cocultured with pieces of lung, they survive and adhere to the substratum. These effects can be transferred from one culture to another with cell-free media 'conditioned' by the organ (Horak 1986).

Furthermore, when B16 melanoma cells were injected into C57BL/6 mice, metastases were found in fragments of pulmonary or ovarian tissue implanted intramuscularly. In contrast, metastatic lesions did not develop in renal tissue implanted intramuscularly as 'control' or within the scar (Hart 1981). The same author also showed that extracts taken from mouse lung stimulated growth of lung-colonising tumour cells whereas extracts from other organs inhibited their growth. Similar results were obtained using extracts or conditioned medium from mouse ovary, lung, brain, liver and thyroid (Hart 1982). Another reason for such tissue specificity may lie in the ability of tumour cells to 'home' to various target organs. This phenomenon will be discussed later under 'Homing'.

The "Seed and Soil" hypothesis therefore assumes that tissues provide optimal chemical and metabolic conditions for the growth of particular secondary tumours and that different tumours may have differing optimal requirements. Hence, each tumour has its own preferential sites of metastasis. *Different "seeds" require different "soils" and in poor "soil" the "seeds" fail to germinate.*

Evidence for the 'Mechanical Hypothesis'

The mechanical hypothesis proposes that the development of secondary tumours in common sites such as the lung, liver and bone is non random and can be explained by a combination of blood flow and the number of viable tumour cells reaching these sites via venous and arterial channels (Coman 1953). Having 'escaped' from the primary tumour, tumour cells gain access to either lymphatic and/or venous system. They then travel to various organs via different routes.

Both the liver and lung are organs that are frequently involved with metastasis as they receive venous drainage from the portal system and the caval system respectively. In addition, the liver and lung might also receive tumour emboli through the hepatic and bronchial arteries respectively (Coman 1953). In the lung, tumour cells could either enter the pulmonary veins or the pulmonary arteriovenous anastomosis to enter the arterial circulation (Coman 1953; Sugarbaker 1981) to metastasise to organs such as kidneys, adrenals, spleen and muscle.

Tumour cells could reach the skull and axial bones via the communications between vertebral venous system of Batson and systemic venous system. Vertebral veins form an extensive system from the pelvis to skull anastomosing freely with the caval system at each segmental level providing an explanation for the spread of breast, thyroid and prostatic cancers to the axial bones bypassing other organs (Batson 1940; Coman 1953). Furthermore, the mammary veins communicate with the vertebral system

through the intercostal and subclavian veins providing a route for the spread of breast cancer to the vertebrae (Coman 1953).

Lastly, tumour cells that gained access to the lymphatic channels form metastases in the lymph nodes that they encountered. From there, tumour cells could join the venous system via lymphaticovenous channels or the thoracic duct that drains into the main systemic venous system (Sugarbaker 1981)

The mechanical hypothesis was supported by Coman in 1951 and 1953 when he injected suspension of rabbit V₂ carcinoma cells (a tumour that rarely produces spontaneous metastases in organs other than lungs) into the left ventricle of a rabbit. He found that tumour cells 'appeared and grew in virtually all organs'. He concluded that the reason metastases failed to develop widely was not due to the various organs offering an unfavourable chemical environment but because inadequate number of cells did not reach those organs that did not develop metastases (Coman 1951; Coman 1953).

The mechanical hypothesis was further supported by the observation made by Weiss. He found that when 4×10^6 Walker 256 tumour cells were injected into the rats via the tail vein, 90 % of the rats had secondaries in their lungs but only 10% of them had extrapulmonary tissues metastases, mainly in the liver. However, when he repeated the experiment by injecting 1×10^3 Walker 256 tumour cells into the rats via intrahepatic/portal vein, he found that 90% of the rats had liver metastases. Using radiolabelled cells, Weiss was able to show that tumour cells, after tail vein injection, reached the liver after being filtered by the lungs and came to the conclusion that the

liver is not an unfavourable soil for tumour cells to grow but most cells reaching it were dead (Hart 1982; Weiss 1985).

'Seed and Soil' Vs 'Mechanical' hypothesis

In the mechanical hypothesis, the development of metastasis is dependent solely upon the dose of viable tumour cells delivered to the appropriate organs but these anatomical and haemodynamic considerations do not explain all the metastatic patterns of spontaneous tumours (Poste 1980; Fidler 1987; Pauli 1988; Fidler 1990). Moreover, the mere presence of viable tumour cells does not predict that the cells will proliferate to produce metastases (Fidler 1970; Fidler 1990).

A review by Sugarbaker suggested that the two hypothesis are both active and can be reconciled if due consideration is paid to the manner in which the data to support these hypothesis have been obtained (Sugarbaker 1981; Hart 1982). For early-stage tumours of moderate and low metastatic potential, the initial sites of metastasis are almost exclusively determined by the mechanical hypothesis. Once generalised metastasis has occurred, the autopsy pattern of metastasis indicates that for a given histological primary tumour, organ specificity can be demonstrated. On the other hand, tumours with high potential that metastasise rapidly to all organs by the time of clinical diagnosis and treatment, no apparent seed and soil mechanisms are apparent (Sugarbaker 1981).

Tumour Heterogeneity

Cancers were once thought to be monoclonal in nature: 'Tumour cells simply bred true and a monoclonal tumour grew into a bigger version of itself' (Dexter 1982). However, in 1977, Fidler and Kripke provided the first experimental demonstration of the metastatic heterogeneity of neoplasm using B16 melanoma cells. Using a modification of the fluctuation assay devised by Luria and Delbruck in 1943 for analysing the origin of microbial mutants, Fidler and Kripke were able to show that individual cells from the parent tumour varied dramatically in their ability to metastasise and that subpopulations of tumour cells of differing metastatic potential existed within the parent tumour (Fidler and Kripke 1977).

It is now widely accepted that both human and animal tumours are heterogeneous in nature containing subpopulations of cells with different phenotypes (Evans 1991; Dexter 1982; Heppner 1984). Such heterogeneity is not confined to cells in the primary tumours and is equally prominent among cells populating metastases (Fidler 1985). These subpopulations of cells within a single neoplasm or metastatic lesion may vary in their metastatic potential, surface antigens, morphology, immunological properties, growth rates, metabolic characteristics, hormone receptors, radiosensitivity and susceptibility to cytotoxic drugs (Heppner 1984; MacLeod 1985; Fidler 1990).

In vivo, the tumourigenicity and the metastatic potential may vary between clones from a same tumour mass. For example, clones isolated from murine melanoma model K1735 differed greatly from each other and from the

parent tumour in their ability to produce lung metastases (Fidler 1980). Similarly, clones from the SL 12 murine lymphoma model, despite equal DNA content confirmed by flow cytometry, vary in their surface antigens, tumourigenicity and metastatic patterns (MacLeod 1984; MacLeod 1985). Such biological heterogeneity exhibited by both primary and secondary tumours forms a major barrier in the treatment of cancer resulting in poor response of cancers to current therapies (Heppner 1984; Fidler 1990, Dexter 1982).

The mechanism of tumour heterogeneity

The mechanism of how a single tumour mass achieve its heterogeneity would be easier to understand if tumours were multicellular in origin. However, not all tumours are multicellular in origin (Heppner 1984) and it is more difficult to perceive the source of heterogeneity in neoplasms that are unicellular in origin (Fidler 1987).

Foulds introduced the 'Theory of Progression' to try to explain the progression of premalignant to malignant lesions in the breast (Foulds 1975; Weiss 1985). Extensive studies on the progression of mouse mammary tumours led Foulds to believe that tumours undergo a series of permanent and irreversible changes during the course of the disease (Nicholson 1982; Fidler 1987). Ultimately, this results in a heterogeneous tumour mass with subpopulations of cancer cells that are related but not identical. According to Foulds, the 'neoplasia tends to go from bad to worse' (Foulds 1949; Foulds 1969).

Fould's theory of progression was further refined by Nowell in 1976, who suggested that tumour progression results from genetic instability such as point mutations, genomic rearrangements, chromosome losses and gene amplification. As a result, emerging variants with increasing genetic instability are produced in an expanding tumour (Nowell 1976; Fidler 1978; Heppner 1984). This model of tumour evolution was further supported by an observation that clones of highly metastatic murine fibrosarcoma are more unstable with a significantly higher rate of spontaneous mutation compared to poorly metastatic potential clones (Evans 1991; Cifone 1981; Dexter 1982).

It is also possible to isolate one or more clones of high grade metastatic potential from a tumour using single cell-cloning methods if the frequency of metastatic variants is high enough (Fidler 1977; Kerbel 1990). However, in some cases, initially highly metastatic clones become phenotypically unstable and tend to revert to the less metastatic parental wild-type after weeks to months in culture. Such behavioural trait of tumour cell clones in vitro is sometimes referred as "phenotypic drift". This phenomenon can be explained by heritable (but unstable) epigenetic events such as DNA methylation, transcriptional and translational control processes (Evans 1991; Neri 1981; Kerbel 1990).

Phenotypic differences between cells are not found only within the primary tumour but even with metastases themselves, thus, explaining why multiple metastases in the same patient, even within the same organ, show biological diversity (Dexter 1982; Fidler 1986; Kerbel 1990).

Homing

In 1960, Kinsey showed that when mice were injected intravascularly by either intravenous, intra-arterial or intraventricular routes, with melanoma S91 Cloudman (a lung-homing melanoma tumour model), the S91 persisted its preference to metastasise to the host lung and also to ectopically transplanted lung tissue but not to other organs (Kinsey 1960; Zetter 1990). Such site specificity displayed by tumour cells is also observed clinically in patients who have peritoneovenous shunts for malignant ascites. These patients develop metastasis at specific sites and rarely within the lung or cardiovascular system (Tarin; Price 1984b; Fidler 1990). Furthermore, when K-1735 murine melanoma cells and B-16 murine melanoma cells were injected directly into the carotid artery of mice, it was shown that K-1735 cells metastasised to the brain parenchyma whereas B-16 cells only produced meningeal secondaries even though clinically they are both murine melanomas (Schackert 1988).

Mechanisms

It is believed that tumour cells exhibit non-random metastatic patterns because they are able to 'home' to their target organs (Zetter 1990). Such homing processes are not unique to tumour cells alone as normal cells also display homing. For example in embryonic patterning and leucocyte trafficking, cells travel selectively to distant tissues for further growth, differentiation and maturation (Picker 1992).

Like leucocytes trafficking, circulating tumour cells are able to recognise and attached specifically to endothelial cells, basement membrane and

extracellular matrix. Having interacted, tumour cells begin to extravasate and invade with the help of degradative enzymes. Their cellular motility is also influenced by motogens produced by the host tissue. Angiogenesis and host tissue factors facilitate further growth of the cells at the new site (Jiang 1994).

Selective recognition

The flow of circulating tumour cells slows down at the capillary level. As a result of diminishing flow, it is believed that tumour cells lodge and arrest passively, an important event preceding potential extravasation. However, this non-specific mechanism is insufficient to explain why certain organs are bypassed and metastases develop selectively in other sites downstream with similar sized capillary beds (Hart 1982). Fidler showed that only 1 % circulating cells after intravenous injection survived to form metastases and that the first encountered organ was not necessarily involved. Cells are also noticed to recirculate through organs without forming metastases (Fidler 1970; Fidler 1990). Therefore, more specific mechanisms must be involved.

In 1964, Greene and Harvey proposed that the localisation of tumour cells at target organs might involve formation of an initial bond between tumour cells and the adhesion molecules on the luminal side of the vascular endothelium of that organ. Furthermore, the strength of this adhesive bond varies with different tumours and also with the vascular endothelium at different sites (Greene 1964). Auerbach et al., subsequently demonstrated that when tumour cells are incubated with cultured endothelial cells from

different organs, they stick selectively to the endothelial cells derived from their preferred secondary site (Auerbach 1987). When tumour cells are exposed to histological sections, they also stick to sections prepared from their preferred site of metastasis (Netland 1984).

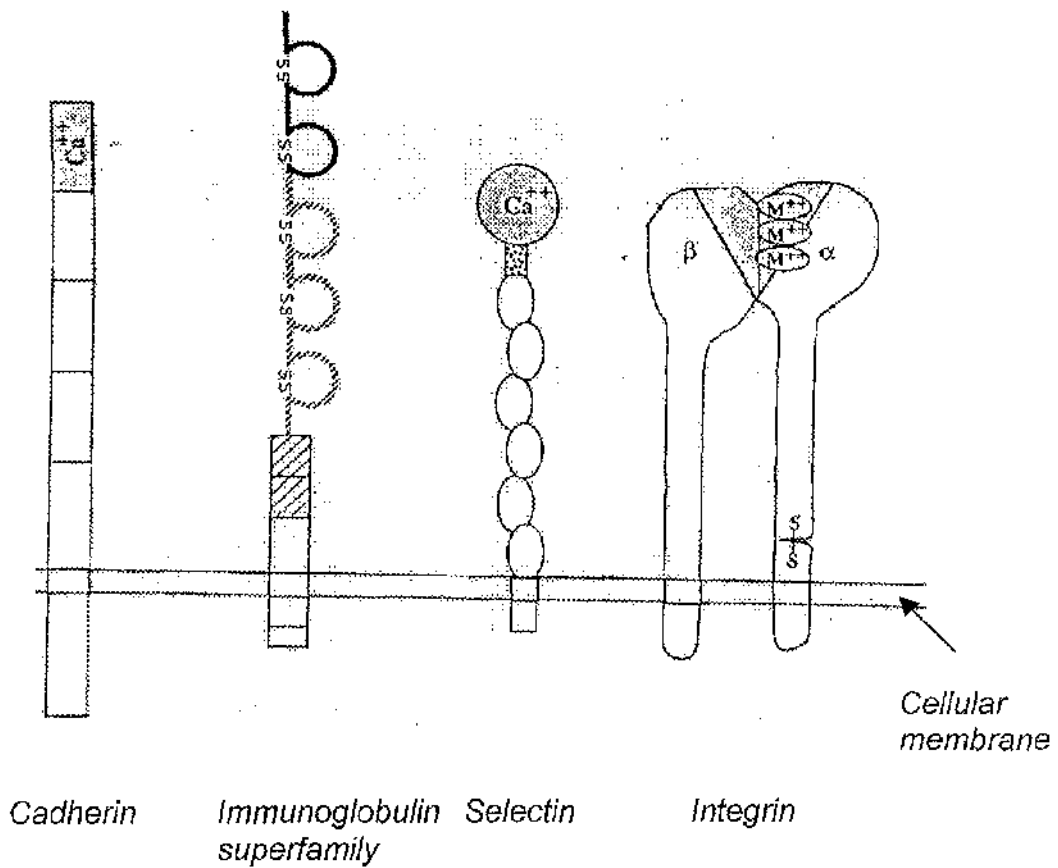
Increasing evidence now suggests that adhesion molecules play an important role in tumour cell homing (Zetter 1990; Miyasaka 1995). Similar to T-lymphocytes homing to primary and secondary lymphoid organs for differentiation and maturation (Picker 1992), tumour cells have also been shown to express cell surface receptors or adhesion molecules that are able to recognise and interact specifically to their counterparts on endothelial cells, exposed basement membrane and extracellular matrix (Zetter 1990). Selective adhesion between these molecules allows tumour cells to bind firmly to the vascular endothelium, leading to specific entrapment and later site-specific metastases. It has also been demonstrated that such firm binding can even protect tumour cells from cytotoxic T-cells and natural killer cells, thus, prolonging their half life and increasing their chances of forming metastases (Kaminski 1988).

Adhesion molecules

Adhesion molecules are cell surface receptors that mediate cell-cell and cell-extracellular matrix interactions (Nigam 1993). Recent studies have shown that adhesion molecules play important roles in the metastatic cascades. Their down regulation allows cellular detachment from the primary and their upregulation allows specific recognition and attachment to endothelial

cellular ligands in target organs. Molecules that maybe involve in tumour cell homing are the integrins, the members of the immunoglobulin superfamily (VCAM, ICAM-1, ICAM-2, NCAM etc.), CD44, selectins and addressins.

Figure 2.1 Major families of cellular adhesion molecules (Hynes 1992)



Integrins

The integrin family is divided into at least three subfamilies, each consists of heterodimers with a common β subunit (90-110 kDa). The common β subunit is noncovalently associated with a specific group of α subunits (120-180 kDa) as shown in Figure 2.1 (Jiang 1994, Hynes 1992; Maemura 1994). Most β subunits can associate with several different α subunits, whereas, α subunits usually bind to one particular β subunit (Roos 1991).

Integrins are transmembrane receptors expressed by most cells (Nigam 1994). They bind to ligands such as the immunoglobulin superfamily on the endothelial surfaces (VCAM, ICAM 1 & 2), components of basement membrane (collagen IV and laminin) and extracellular matrix proteins found during early development, inflammation and wound healing (fibronectin, fibrinogen, vitronectin, thrombospondin and peptide sequence such as the RGD sequence) (Hynes 1987; Hynes 1992; Albelda 1993). The RGD-peptides sequence was originally identified as the cell attachment promoting sequence in fibronectin but now has been found in a number of matrix proteins including fibrinogen, thrombospondin, vitronectin, laminin and type I collagen (Hynes 1992; Maemura 1994). In vitro, when integrin receptors are blocked by synthetic RGD-peptides sequence (*Arg-Gly-Asp*), invasion of human melanoma cells across amniotic basement membranes is inhibited (Gehlsen 1988) and in vivo, coinjection of RGD-peptides sequence and B₁₆F₁₀ murine melanoma cells reduced the number of metastatic lung nodules in mice (Humphries 1986). These studies suggest that RGD-peptides sequence act as ligand analogues, competing for adhesion receptor

binding sites and thereby decreasing the amount of integrin-mediated attachment between metastatic tumour cells and extracellular matrix (Maemura 1994).

In metastasis, integrins play an important role in tumour cell attachment to extracellular matrix and invasion after extravasation as they provide a link between cytoskeleton and extracellular matrix (Maemura 1994). They are found to be expressed in tumours of the breast, colon, pancreas, stomach, kidneys, prostate, lung and the skin (Nigam 1994).

β_1 subfamily

The β_1 subfamily contains 7 heterodimers ($\alpha_1\beta_1$ to $\alpha_6\beta_1$ and $\alpha_v\beta_1$) and is the largest integrin subfamily (Maemura 1994). They are also known as the VLAs (Very late after activation) subfamily and its members are also called by their VLA- α subunit number (Hynes 1992; Miyasaka 1995). The ligands for the β_1 subfamily are extracellular matrix proteins such as laminin (VLA-1, -2, -3 and -6), collagen (VLA-1, -2 and -3) and fibronectin (VLA -3, -4, -5 and -v) (Maemura 1994; Miyasaka 1995). Unlike VLA-1, -2, -3 and -6 which are expressed by most cells, VLA-5 (fibronectin receptor) is poorly expressed in most tissues.

Both VLA-5 and 6 are important in metastasis. VLA-5 is a fibronectin receptor and is responsible for migration of tumour cells whereas VLA-6 is a laminin receptor and adhesion to laminin, an important component of basement membrane, has been shown to be essential in metastasis (Roos 1991).

Abnormal expression of β_1 has been correlated with increased metastatic ability of tumour cells (Miyasaka 1995). For example, increased expression of VLA-2 has been associated with metastatic behaviour of rhabdomyosarcoma cells and VLA-3 with melanoma progression. VLA-4, on the other hand, is expressed mainly by lymphoid and myeloid cells. Besides being a fibronectin receptor, VLA-4 also binds specifically to immunoglobulin VCAM-1 (Vascular adhesion molecule-1) (Miyasaka 1995).

β_2 subfamily

The β_2 integrins have three members, LFA-1 (CD11a/CD18), Mac-1 (CD11b/CD18) and gp150/95 (CD11c/CD18) which are expressed exclusively on white blood cells, thus, gaining the name "leucocyte integrins" (Roos 1991). Their primary role is in intercellular adhesion such as leucocyte-leucocyte or leucocyte-endothelial cell interactions" (Roos 1991; Maemura 1994). In addition to intercellular adhesion, Mac-1 and gp150/95 maybe involved in adhesion to substrates as well.

LFA-1 (Lymphocyte functioning antigen-1 or $\alpha_4\beta_2$)

LFA-1 is the most extensively characterised β_2 integrins. It is widely expressed by leucocytes and plays an essential role in inflammation (Roos 1991). LFA-1 binds to endothelial ligands of the immunoglobulin superfamily, ICAMs (Intercellular adhesion molecules), with a higher affinity for ICAM-1 than ICAM-2 (Roos 1991).

LFA-1 is also expressed by many metastatic lymphomas. Adhesion and consequently, invasion of these lymphoma cells in hepatocyte and fibroblast monolayers is inhibited by anti LFA-1 antibody, suggesting that LFA-1 is required for efficient metastasis formation (Roos 1991; Maemura 1994). Furthermore, lymphoma cell variants deficient in LFA-1 are unable to invade and metastasise in vivo (Roosien 1989), and in vitro, LFA-1 deficient mutant cells were less invasive than their parental cells in hepatocyte and fibroblast monolayers. This provides strong evidence for an essential role of LFA-1 in metastasis of these cells (Roos 1991; Maemura 1994).

Mac-1 (CD11b/CD18 or $\alpha_M\beta_2$) and gp150/95 (CD11c/CD18 or $\alpha_X\beta_2$)

Mac-1 and gp150/95 expression is largely limited to myeloid cells and they appear to be involved in interaction with endothelial cells and extracellular matrix, thus, probably involved in extravasation. They probably play an important role in tumour formation for myeloid tumours (Roos 1991).

β_3 subfamily

This subfamily has two members namely $\alpha_{IIb}\beta_3$ and $\alpha_6\beta_3$. The integrin $\alpha_{IIb}\beta_3$, a fibrinogen receptor is expressed primarily by platelets and is involved in platelet aggregation (Albelda 1993). It is also found to be expressed by certain tumours and plays a crucial role in tumour cell-platelet-endothelial interactions. Such interactions could be reversed by antibodies to $\alpha_{IIb}\beta_3$. Tumour platelet aggregation helps in the lodgement and arrest of

tumour cells at capillary levels, thus, facilitating metastasis (Maemura 1994; Tang 1994). On the other hand, induction of thrombocytopenia, is associated with a decrease of metastasis (Albelda 1993).

$\alpha_v\beta_3$, on the other hand, is a vitronectin receptor (Maemura 1994) but is also found to bind fibronectin, fibrinogen, thrombospondin, osteopontin and von Willebrand factor (Garrod 1993). Both integrins have been found to be expressed in human melanoma cells but not in benign melanocytes. There seems to be a direct relationship between their expression and tumour metastasis (Maemura 1994; Tang 1994).

Immunoglobulin superfamily

In this large family, all molecules share a common structural feature, the immunoglobulin homology unit (Figure 2.1) and they exhibit both haemophilic and heterophilic interactions.

VCAM-1 (Vascular cellular adhesion molecules-1) is expressed by endothelial cells that are activated by cytokines. It is a ligand for integrin VLA-4 ($\alpha_4\beta_1$). As a result, tumour cells such as melanoma (Albelda 1993) that expressed VLA-4 could bind specifically to activated endothelium via VLA-4/VCAM-1 interactions (Maemura 1994). Furthermore, VCAM-1 is also expressed by bone marrow stromal cells, thus, explaining the metastasis of lymphoma cells to the bone marrow and the retention of leukaemia cells in the bone marrow (Juneja 1993).

ICAM-1 (intercellular adhesion molecules 1) contains 5 extracellular immunoglobulin-like domains and a short cytoplasmic tail. It has been recognised as an endothelial ligand for integrin, LFA-1 (lymphocyte functioning antigen-1) (Maemura 1994) but recently, has also been found to act as receptor for Mac-1 and rhinovirus (Miyasaka 1995). ICAM-1 is also expressed in non-endothelial cells such as in melanomas and squamous cell carcinoma (Maemura 1994; Miyasaka 1995). In melanoma, it correlates with tumour progression and increased risk of metastasis (Johnson 1989; Natali 1990; Maemura 1994). It has been speculated that melanoma cells which expressed ICAM-1 could bind to lymphocytes via LFA-1, thus, able to disseminate throughout the blood stream in analogy to lymphocytes (Maemura 1994).

Other important immunoglobulin superfamily includes NCAM, L1 and CEA. NCAM (Neural cell adhesion molecule) is a homophilic calcium-dependent cell-cell adhesion molecule that is expressed primarily in the nervous system (Albelda 1993). It has been found to be expressed in many neural and neuroendocrine tumours including Wilm's tumour, pituitary adenomas, phaeochromocytomas, small cell lung carcinoma and frequently in bile duct cancer (Albelda 1993; Miyasaka 1995). Its circulating form may be a potential marker for small cell lung carcinoma (Jaques 1993) and there is also a correlation between its expression and neural invasion of bile duct cancer (Seki 1993)

L1 is also a homophilic neural adhesion molecule and is expressed by lymphomas. Its expression correlates negatively with metastatic capacity of lymphomas (Kowitz et al. 1993). CEA (carcinoembryonic antigen) was

described as an oncofetal glycoprotein found in the serum of patients with colonic carcinoma but was subsequently found to be associated with other tumours (Albelda 1993). Recently, CEA has been recognised to be a member of the immunoglobulin superfamily and function as a true cell adhesion molecule. It still remains unclear how the increased expression of CEA on tumour cells is related to the development of malignancy. One possible explanation is that the presence of excess CEA could interfere with the function of the normally present cell-cell adhesion molecules by downregulating integrin and cadherin molecule expression (Albelda 1993; Nigam 1994)

CD 44 (Hermes antigen, H-CAM, pgp-1 antigen)

CD 44 is a membrane glycoprotein (37-kD core protein) with an amino-terminal domain homologous to the cartilage link protein (Miyasaka 1995). It is present in many cell types including epithelial and haemopoietic cells (Guo 1994; Miyasaka 1995) and functions as a receptor mediating cell-cell and cell-matrix interactions by binding to ligands such as hyaluronic acid, collagen and fibronectin (Aruffo 1990; Lesley 1990; Underhill 1992). In lymphocyte trafficking, CD 44 behaves as a lymph node homing molecule by helping lymphocytes to bind selectively to high endothelial venules found in mucosal lymph node tissue (Maemura 1994; Miyasaka 1995).

At molecular level, the transcription of CD 44 is by alternative splicing, thus producing many variants and some of these variants are important in tumour cell homing and invasion. Transfection studies showed that tumour cells

which acquire CD 44 variant cDNA increase their metastatic potential (Underhill 1980; Underhill 1981; Haynes 1983; Namec 1987; Horst 1990; Stamenkovic 1991; Dougherty 1992; Jalkanen 1992; Matsumura 1992; Albelda 1993). For example, Gunthert identified a variant, pMeta-1 cDNA, which is expressed in a highly metastatic pancreatic carcinoma cell line in rats but not in a poorly metastatic variant. This variant CD 44 contains an additional extracellular domain of 162 amino acids, probably introduced by alternative splicing (Albelda 1993). By transfecting this heavier cDNA to the non-metastasising cell line, the cells were able to express both the normal and variant CD 44 and became metastatic (Gunthert 1991). In vivo, antibodies against CD 44E were found to have inhibitory effects on tumour growth and metastasis (Seiter 1993) supporting the hypothesis proving that interactions between CD 44 variant and its ligands are important in metastasis.

Evidence showed that the higher molecular weight of CD 44 variant is a distinct form with different adhesion potential. It is possible that this higher weight form confers metastatic potential by allowing the cells to adhere strongly to hyaluronic acid, thus, aiding tumour implantation (Albelda 1993). Another explanation is that this additional extra extracellular domain could also be found in activated T-cells. Thus, expression of this variant CD 44 could act as a "molecular disguise" that helps the tumour cells to mimic circulating activated lymphocytes (Kahn 1992; Albelda 1993). Such molecular disguise or "wolves in lamb clothing" helps the tumour cells to evade immune system (Nigam 1994). For example, when tumour cells are transfected to overexpress the epithelial variant CD 44R1, they readily gain

access to lymph nodes and distant metastatic sites in animal models (Stamenkovic 1989; Tanabe 1993).

Selectins

The Selectins are adhesion molecules that share a common structure characterised by an amino-terminal lectin domain area, an epidermal growth factor-like domain, a variable number of complement regulatory protein repeat sequences and a short cytoplasmic domain as shown in Figure 2.1. They bind to carbohydrate ligands and consist of P-selectin (GMP140 or PADGEM), E-selectin (ELAM-1) and L-selectin (LECAM-1).

P-selectin is expressed on platelets and endothelial cells (Maemura 1994) and possibly play a role in tumour invasiveness as it was found to bind to tumour sections of the breast, colon and lung (Aruffo 1990; Albelda 1993; Miyasaka 1995).

E-selectin (Endothelial Leucocyte Adhesion Molecule 1 or ELAM-1) is found to be expressed by endothelium activated by interleukin-1 (IL-1), tumour necrosis factor α (TNF- α) and other cytokines and not in unstimulated endothelium. It binds to a carbohydrate ligand containing sialyl Lewis x (SLe^x) or sialyl Lewis a (SLe^a) structure on leucocytes. As several carcinoma cells also express sialyl Lewis x (SLe^x), these malignant cells have the potential to bind to endothelial cells via E-selectin (Maemura 1994). Antibodies against E-selectin has been shown to inhibit adhesion of seven colon carcinoma cell lines to activated endothelium (Lauri 1991)

Selectins also play an important role in lymphocyte trafficking (Picker and Butcher 1992). L-selectin (Leucocyte adhesion molecule 1 or LECAM-1) is a lymph node homing receptor and helps lymphocytes to bind specifically to peripheral lymph node addressins (PNA_d) expressed by the high endothelial venules of lymph nodes (Bartgatze 1987; Picker 1992; Garrod 1993). It has also been suggested that L-selectin is a predictor of the haematogenous dissemination of murine lymphomas (Miyasaka 1995)

Cadherins

Cadherins form a group of cell-cell adhesion molecules which are calcium-dependent transmembrane proteins. They mediate cell-cell adhesion mainly by homotypic interaction (Takeichi 1991; Jiang 1996) and are responsible for establishing and maintenance of intercellular connections (Takeichi 1991). There are four subclasses of Cadherins which share a common basic structure but display a unique tissue distribution pattern: E-cadherin (epithelial cadherin), P-cadherin (placenta cadherin), N-cadherin (neural cadherin) and L-CAM (liver cell adhesion molecule) (Takeichi 1991; Miyasaka 1995).

E-cadherin (also known as uvomorulin, Arc-1 and cell-CAM 120/80), is one of the best characterised cadherins. This 120-kDa transmembrane protein is confined to all epithelia originating from ectodermal, mesodermal and endodermal tissue (Behrens 1993; Jiang 1996). The intracellular domain of E-cadherin interacts with a group of cytoplasmic proteins called catenin, which consists of alpha, beta and gamma subunits.

E-cadherin is a key intercellular adhesion molecule. Cells without E-cadherin / catenins do not aggregate or adhere to each other (Takeichi 1991) and this non-adhesive state could be reversed by transfecting E-cadherin negative cells with E-cadherin cDNA (Jiang 1996). Furthermore, a loss of E-cadherin / catenins expression correlates with poorly differentiated and invasive malignant tumours (Takeichi 1991; Albelda 1993; Behrens 1993; Dorudi 1993; Garrod 1993; Kinsella 1993; Maemura 1994; Jiang 1996). Hence, E-cadherin / catenins have been regarded as a tumour suppressor (Jiang 1996).

Addressins

Lymphocytes homing to different organs are regulated by adhesion molecules (homing receptors) recognising tissue specific vascular addressins on endothelium such as peripheral lymph node addressins (PNAd) and mucosal vascular addressins (Mad) (Picker 1992).

Peripheral lymph node addressin, a mixture of glycoproteins, is a group of adhesion molecule that is selectively expressed in the high endothelial venules (HEV) of peripheral lymph node. They play an important role in the homing of lymphocytes to peripheral lymph nodes by binding to LECAM-1, a selectin adhesion molecule on circulating lymphocytes. Antibodies to either LECAM-1 or PNAd markedly reduce lymphocyte binding in vitro to peripheral lymph node (Picker 1992)

Mucosal vascular addressin (Mad), on the other hand, is a group of adhesion molecule that is selectively expressed in the high endothelial venules (HEV)

in gut-associated lymphoid tissue (GALT) such as Peyer's patches and appendix. They bind to mucosal-homing and not lymph node specific lymphocytes (Picker 1992).

Table 2.2 A summary of adhesion molecules and their ligands

Adhesion molecule family	Adhesion molecule	Ligand
Integrin (α and β subunits)		Ig superfamily, Extracellular matrix proteins, Basement membrane
	β_1 : VLA-1	Laminin, Collagen
	β_1 : VLA-2	Laminin, Collagen
	β_1 : VLA-3	Laminin, Collagen, Fibronectin
	β_1 : VLA-4	VCAM -1, Fibronectin
	β_1 : VLA-5	Fibronectin
	β_1 : VLA-6	Laminin
		β_2 : LFA-1
	β_2 : MAC-1	ICAM-1
Immunoglobulin superfamily	ICAM-1	LFA-1, MAC-1
	VCAM-1	VLA-4
CD 44		Hyaluronic acid, Collagen, Fibronectin, MAd
Selectin	L-selectin (LAM-1)	Endothelium of lymph node, PNA _d
	E-selectin (ELAM-1)	Carbohydrate, Sialyl Lewis x/a
	P-selectin (PADGEM)	Carbohydrate
Cadherins		Cadherins (Homotypic)
	P-cadherin (Placenta)	P-cadherin (Placenta)
	E-cadherin (Epithelial)	E-cadherin (Epithelial)
	N-cadherin (Nerve)	N-cadherin (Nerve)

Chapter 3 Models of metastasis

Various models of metastasis have been described such as those used by Hart, Fidler, Wang and Mignatti as previously described (Wang 1980; Fidler 1985; Mignatti 1986; Hart 1992).

In 1984, MacLeod described a murine T-cell lymphoma model (MacLeod 1984).

The SL 12 cell lines

AKR mice are an inbred strain that develop thymic lymphomas at high frequency after six months of age and usually die within two weeks after the clinical onset (Hays 1982). In this animal model, lymphoma originates in the thymus and then metastasise to liver, spleen, kidneys and lymph nodes.

In 1984, MacLeod et. al., were able to isolate and establish a T-lymphoma cell line (SL 12) from the femoral bone marrow of an eight month old female AKR mouse with disseminated spontaneous lymphoma. By using the technique of limiting dilution on the SL 12 cells in tissue culture, two cloned cell lines, SL 12.1 and SL 12.4, were further established. These cell lines were maintained with DMEM supplemented with 10 % to 20 % Foetal calf serum, glutamine, penicillin and streptomycin (MacLeod 1984; MacLeod 1985)

SL 12.1 and SL 12.4 cells appeared to be less tumourigenic than their parental SL 12 cells in vivo. When reinjected intravenously into AKR mice via the lateral tail vein, neither SL 12.1 nor SL 12.4 nor both cells at different mixed proportions produced the same rapid onset and progression of disease observed with the parental cell line SL 12 (MacLeod 1984). Subsequently, a further T-cell lymphoma clone, SL 12.3, was established from recultured cells from the spleen of a six week old AKR mouse six days after intravenous injection of 10^6 SL 12 cells followed by limiting dilution cloning.

In vivo characteristics of SL 12.3 and SL 12.4 cell lines

In vivo, the tumourigenicity of SL 12.3 was found to be similar to the SL 12 parent cell line. Compared with the SL 12.4 cell line, in studies by MacLeod, SL 12.3 produced tumours in all animals after inoculation of 10^4 cells whereas only one-half of the animals were affected after an inoculation of 10^6 SL 12.4 cells (Table 3.1) (MacLeod 1985). The differences in tumourigenicity were not affected by the age and sex of the recipient animal.

The difference in tumourigenicity and the latent period between inoculation and tumour formation between SL 12.3 and SL 12.4 cells was further demonstrated by intradermal inoculation (Table 3.2).

Table 3.1 Tumourigenicity of SL 12, SL 12.3 and SL 12.4 cells after *intravenous* inoculation (MacLeod, 1985)

No. of cells inoculated	SL 12		SL 12.3		SL 12.4	
	% of animals developed lymphoma	Latency period between inoculation and disease	% of animals developed lymphoma	Latency period between inoculation and disease	% of animals developed lymphoma	Latency period between inoculation and disease
10^6	100	9-12 days	100	10-16 days	43.3	34-79 days
10^5	100	12-16 days	100	14-18 days	8.3	49 days
10^4	100	16-24 days	100	23-27 days	0	-
10^3	100	21-30 days	40	23-45 days	0	-

Table 3.2 Tumourigenicity of SL 12, SL 12.3 and SL 12.4 cells after *intra-dermal* inoculation (MacLeod 1985)

No. of cells inoculated	SL 12		SL 12.3		SL 12.4	
	% of animals developed lymphoma	Latency period between inoculation and 2 mm nodule	% of animals developed lymphoma	Latency period between inoculation and 2 mm nodule	% of animals developed lymphoma	Latency period between inoculation and 2 mm nodule
10^6	100	4 days	100	5 days	100	8 days
10^5	100	5 days	100	9 days	0	-
10^4	100	9 days	100	13 days	0	-
10^3	100	11 days	50	-	0	-
10^2	100	14 days	Not tested	-	0	-

Furthermore, the macroscopic pattern of metastasis in vivo also differ between the SL 12, SL 12.3 and SL 12.4 cell lines after intravenous inoculation of 10^6 cells. SL 12.3 cell line produced diffuse splenomegaly with occasional hepatomegaly whereas SL 12.4 cell line appeared to produce diffuse involvement of the liver (37 % of animals) and the spleen (58 % of animals) (MacLeod 1985).

In addition to hepatosplenic involvement, SL 12.4 cell line has been shown to produce extranodal tumours which consisted of massive nodules in the kidneys, tumour mass in the thigh muscle and around the knee joint, subcutaneous tumour nodules, orbital and intracerebral tumours and massive bilateral ovarian tumours in about 95 % of animals (Table 3.3) (MacLeod 1985).

Table 3.3 Metastatic pattern of SL 12, SL 12.3 and SL 12.4 cell lines after intravenous inoculation of 10^6 cells

	SL 12	SL 12.3	SL 12.4
Muscle	0 %	0%	37 %
Liver	100 % (diffuse)	87 % (diffuse)	37 % (diffuse)
Spleen	100 % (diffuse)	100 % (diffuse)	58 % (diffuse)
Ovaries	0 %	0 %	95 % (>1 cm)
Mean latent period in days	13	13	39

Microscopically, all tumour cells had large and pleomorphic nuclei but no detailed microscopic analysis of individual organ was documented (MacLeod 1985).

In vitro characteristics of SL 12.3 and SL 12.4 cell lines

In tissue culture both SL 12.3 and SL 12.4 cells grow in suspension. SL 12.3 cells grow diffusely whereas SL 12.4 cells grow in clumps (MacLeod 1985).

The *in vitro* phenotypic characterisation of SL 12.3 and SL 12.4 cell lines has shown that both the cell lines differ in their expression of mRNAs for several surface antigens. The SL 12.4 cell line expresses mRNAs for almost all the components of TCR/CD3 complex. The TCR or T-cell receptor antigen is expressed in association with the CD3 complex proteins by all developing thymocytes in order to become functional in the immune system. Furthermore, SL 12.4 cells also express surface antigen TdT, which is found in cortical thymocytes. SL 12.3 cell line, on the other hand, expresses very few of the genes required for T-cell function and does not express TdT (MacLeod 1990).

However, both cell lines were found to have no expression of the surface antigens Lyt-1 (which is commonly found on cortical thymocytes) and Lyt-2 (which is found on medullary thymocytes and on functional T-cells). These surface markers are known to be present in primary spontaneous lymphoma (Lyt-1) and virus accelerated lymphomas (Lyt-2).

In summary, SL 12.4 cell line appears to be the most differentiated and least tumourigenic clone with surface markers of immature cortical thymocytes. On the other hand, the SL 12.3 cell line appears to be the least differentiated and most tumourigenic clone with surface antigens of even more immature thymocytes (MacLeod 1985).

One of the most interesting aspects of the SL 12.3 / SL 12.4 model of metastasis is that these two closely related clones appear to exhibit completely different metastatic pattern in vivo. One clone, SL 12.3, producing diffusely hepatic involvement and SL 12.4 apparently producing predominantly nodal disease and nodular deposits. Detailed microscopic analysis was not performed however in MacLeod's initial studies but these two patterns of metastasis are frequently seen in human tumours for example, metastatic adenocarcinoma of the colon.

This metastatic model was therefore chosen for further investigation and characterisation.

Chapter 4 Aims, Hypothesis & Overview of Studies Performed

Studies on the Molecular Pathology of Metastasis with particular reference to the SL 12 murine lymphoma model

Aim :

The aim of these studies is to investigate the molecular pathology of metastasis focusing on the homing phenomenon of tumour cells and the possible genes responsible in the metastatic process.

Hypothesis :

Variation in metastatic potential between clones of the same tumour cell population is due in part to the differentiation of genes, which after either being activated or repressed, favour the selective growth of the certain cells in organ specific environments. Furthermore, differences in gene expression may allow immune evasion, “homing” of particular clones to specific distant tissues and favour implantation.

Overview of the studies :

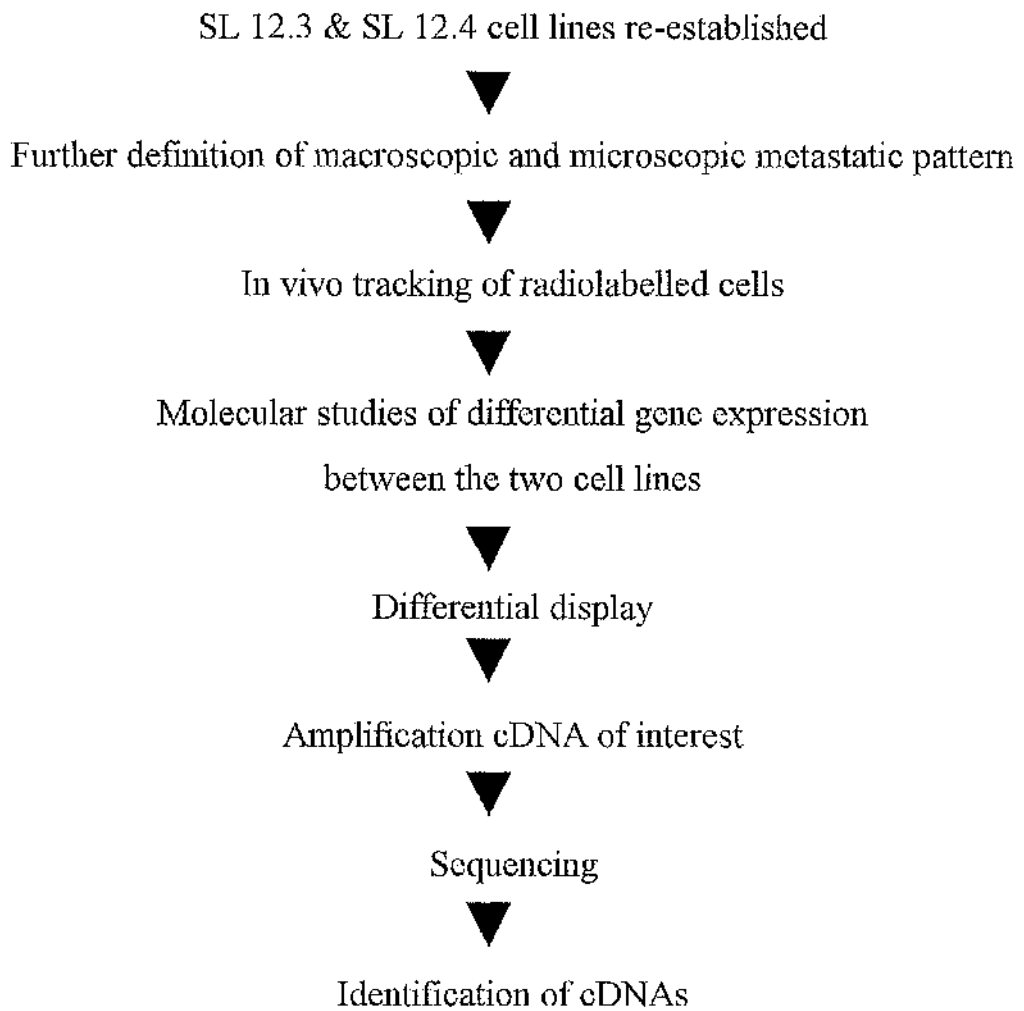
The study is divided into three 3 sections as shown in figure 4.1. In the first section, the SL 12.3 / SL12.4 model of metastasis was re-established in

AKR mice. The growth rate in vitro, tumourigenicity, microscopic and macroscopic pattern of metastasis of the SL 12.3 / SL 12.4 model was studied in detail in AKR mice.

In the second section, radiolabelled cells were used to study the metastatic pattern and the dissemination of the two cell lines of interest to different organs after intravenous injection.

In the third section, the technique of differential display was used to identify and isolate cDNAs expressed in one cell line and not in the other. This study then concludes with the amplification and comparison of cDNAs of interest with known sequences in gene databanks.

Figure 4.1 Overview of the study



Chapter 5 Establishing the SL 12.3 and SL 12.4 Lymphoma model and in vitro growth rate comparison

The SL 12.3 and SL 12.4 cell lines were re-established in tissue culture from frozen storage supplied as a kind gift of Professor MacLeod (UC, San Diego).

Both SL 12.3 and SL 12.4 cells were grown in Dulbecco's modified Eagle medium (DMEM, *Imperial*) supplemented with 10 % foetal calf serum (*Imperial*), L-glutamine (20 mls of 200 mM/L of medium, *Sigma*) penicillin (100,000 units/L of medium, *Sigma*) and streptomycin (100 mg/L of medium, *Sigma*). The cells were cultured at 37°C with an atmosphere containing 5 % CO₂.

10⁶ cells were initially transferred into 6 mls of supplemented DMEM in 25 cm³ tissue culture flasks (*Costar*). Subsequently, cells were recultured with passage of 1 ml of medium plus cells into 5 mls of fresh supplemented DMEM every 48 to 72 hours.

In vitro growth characteristics

Methods

2 X 10⁶ SL 12.3 and SL 12.4 cells were introduced into 75 cm² tissue culture flask (*Costar*) with 10 mls of DMEM each. Each day 90 µls of cells

was pipetted out and mixed with 10 μ ls of 0.4 % Trypan Blue. 15 μ ls of this mixture was used to fill two counting wells. Live cells were counted in duplicate from the 25 squares of two counting chambers with a total volume of 0.1 mm^3 or 10^{-4} ml (1 mm X 1 mm X 0.1 mm) each. The mean value of the two counts were multiplied by 10^4 (for a volume of 1 ml) and 10 (for 10mls) to give the number of live cells per 10 mls of sample. This is then further corrected for the volume of Trypan Blue that was 10 % of the total volume. No further medium was added after each daily count. Growth curves were estimated in triplicate.

Results:

SL 12.3 and SL 12.4 grow in suspension in supplemented DMEM. Unlike SL 12.3 cells, SL 12.4 cells tend to grow in clumps (Figure 5.1 and 5.2).

Figure 5.1: SL 12.3 cells grows diffusely

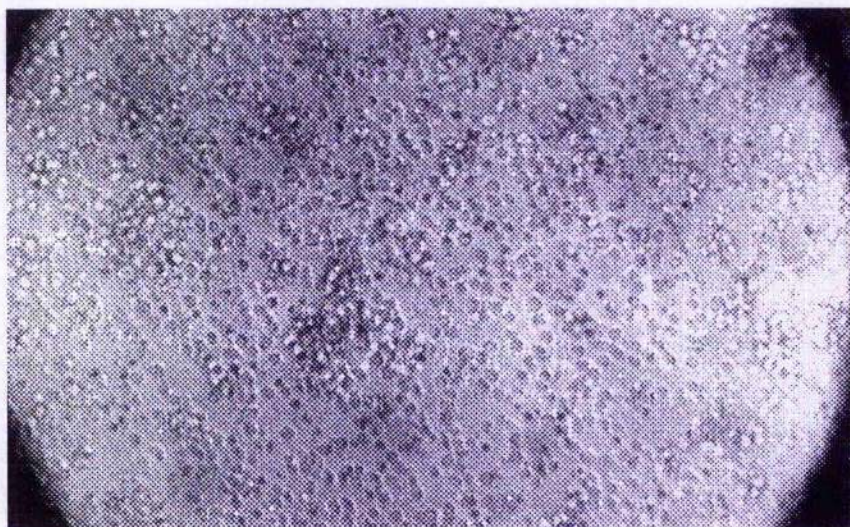
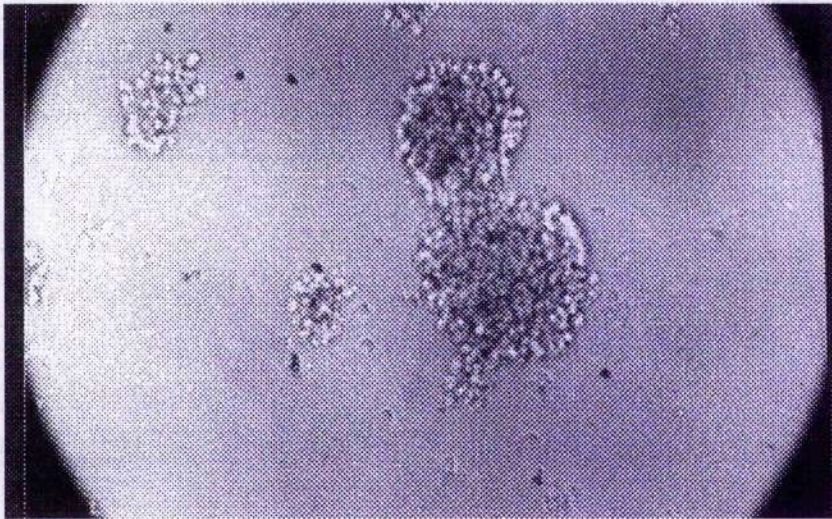


Figure 5.2: SL 12.4 cells grows in clumps

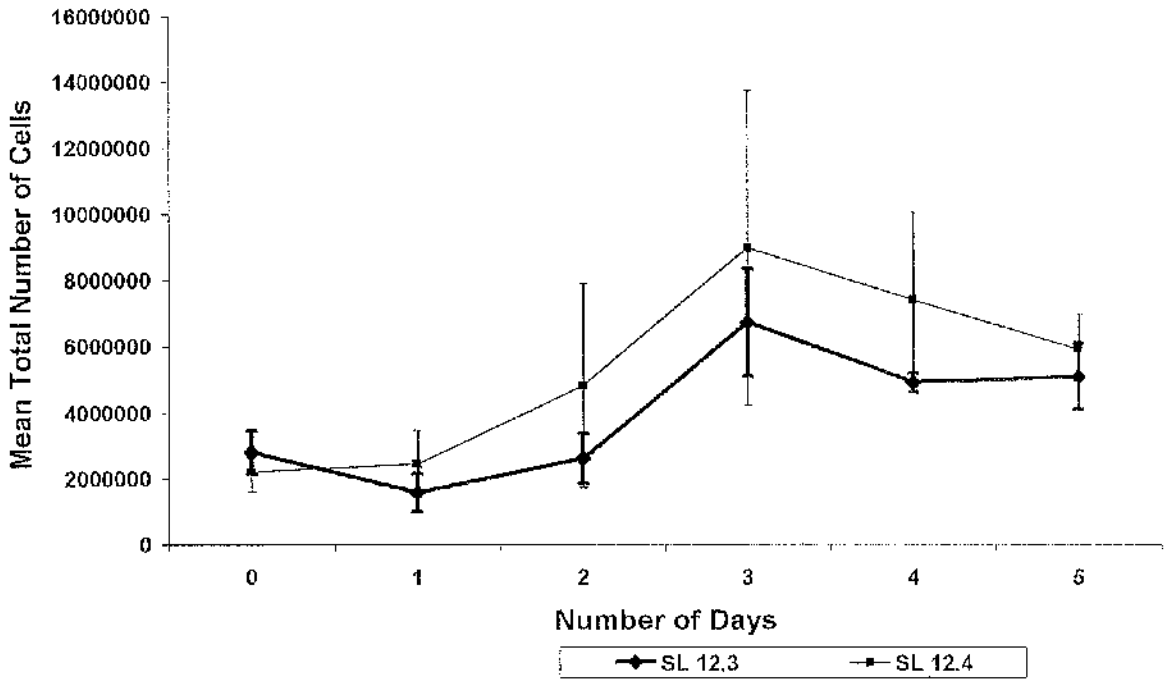


Daily cell counts (Table 5.1) and growth curves (Figure 5.3) for the SL 12.3 and SL 12.4 showed that both the cell lines grow at a similar rate with cells reaching exponential growth rate between forty-eight to seventy-two hours before medium exhaustion. Doubling time for both cell lines is approximately sixty hours

Table 5.1. Daily cell counts for SL 12.3 and SL 12.4 cells

<i>SL 12.3</i>					
Days	Study 1	Study 2	Study 3	Mean	Standard error of mean
0	2610000	1770000	4000000	2793333	650239
1	1420000	654000	2620000	1564667	572126
2	2430000	1400000	4000000	2610000	755932
3	5410000	4820000	9950000	6726667	1620641
4	5300000	5090000	4350000	4913333	288116
5	4100000	6090000		5095000	995000
<i>SL 12.4</i>					
Days	Study 1	Study 2	Study 3	Mean	Standard error of mean
0	2700000	2880000	1000000	2193333	598925
1	2450000	654000	4250000	2451333	1038076
2	2700000	864000	10900000	4821333	3085199
3	4170000	4280000	18500000	8983333	4758439
4	4770000	4770000	12700000	7413333	2643333
5	6990000	4830000		5910000	1080000

Chart 5.1 The growth curve for SL 12.3 and SL 12.4 cell lines
(Error bar = standard error of the mean)



Chapter 6 Macroscopic and microscopic study of metastatic pattern

Introduction

Although earlier studies (MacLeod 1985; MacLeod 1990) demonstrated a difference in metastatic pattern, no microscopic analysis was performed. The studies were not randomised and differing numbers of cells were inoculated. The previous studies of MacLeod were therefore expanded with full macro and microscopic analysis.

Methods :

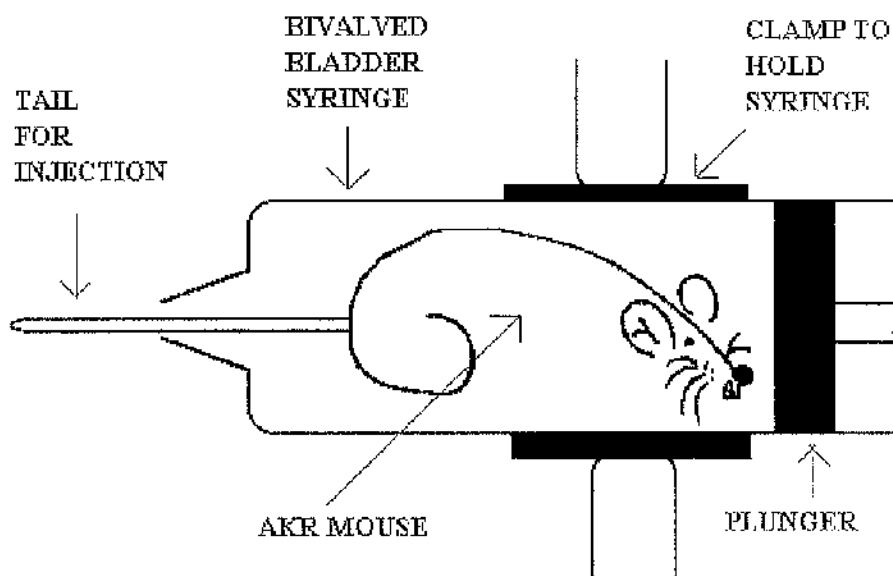
Either 10^6 SL 12.3 or 10^6 SL 12.4 cells was injected via the tail veins into twenty two 8-10 week old AKR mice. Subsequently the study was repeated using 14 AKR mice inoculated with 10^7 SL 12.4 cells.

Injection of cells into AKR mice

SL 12.3 and SL 12.4 cells during the exponential growth phase (48 to 72 hours after starting culture) were pelleted and re-suspended in Phosphate Buffered Saline (PBS) at appropriate concentrations. The mouse was restrained in a bivalved 50 mls bladder syringe (Figure 6.1). 10^6 SL 12.3 cells, 10^6 SL 12.4 cells or 10^7 SL 12.4 cells in 200 μ L of Phosphate

Buffered Saline (PBS) were injected into the tail veins of 11, 11 and 14 AKR female mice respectively. In the initial set of mice with 10^6 SL 12.3 or SL 12.4 cells, the injection order was randomised to avoid bias due to errors in injection technique.

Figure 6.1: AKR mouse restrained for tail vein injection



Post injection, the mice were kept on a standard diet, observed and weighed daily. Any mouse showing signs of distress (e.g., hunched and piloerection), losing more than 10% of their original weight or surviving beyond 8 weeks was euthanised and had an autopsy performed. Organs from each mouse (i.e., liver, spleen, lymph node, ovaries, lungs, kidneys and brain) were weighed and their macroscopic appearances recorded before being fixed with acetic methanol (1:3) for 1 hour. All tissues were preserved with formal saline (Bancroft 1990) until further use.

Microscopic study

Two sections of different plane (horizontal and vertical) of 3 to 5 mm thick were cut randomly from each organ. The specimens were dehydrated through alcohol before being embedded into wax. Sections of 4 μm were cut with a standard microtome on each tissue biopsy and all specimens were stained with haematoxylin-eosin dye. The stained specimens were then analysed in conjunction with a consultant histo-pathologist. Sections were scored as either 'definitely positive', if there were groups of eight to nine large lymphoblasts seen infiltrating the tissue or as 'definitely negative' if there were none or less than five lymphoblasts. When there are any doubts about a slide, another random section was cut from the wax block and re-analysed.

Results

Macroscopic analysis

The results of the macroscopic analysis on the metastatic patterns of SL 12.3 and SL 12.4 within 8 weeks of injection are shown in Table 6.1a and b. Injecting 10^6 SL 12.3 cells intravenously into each of the 11 AKR mice produced 100 % incidence of metastases. The mice deteriorated over 17 days (median) with a range between 11 to 24 days. SL 12.3 cells appeared to produce metastases mainly within the liver (100 %) and spleen (100 %) causing diffuse organ enlargement as shown in Figure 6.2. Only 1 mouse

(9.1 %) of this group had renal and subcutaneous secondaries. No mice had ovarian enlargement.

In contrast, 10^6 SL 12.4 cells injected intravenously into each of 11 AKR mice only produced metastasis in one mouse only at 22 days. The remaining mice survived up to 8 weeks with no apparent distress when the study was terminated. On repeating this section of the study with 10^7 SL 12.4 cells injected intravenously into 14 AKR mice, the incidence of metastasis increased to 78.5 % (11/14). Unlike SL 12.3 cells, mice developed large ovarian metastasis (greater than 1 cm in diameter) in one of the eleven mice following injection of 10^6 SL 12.4 cells and in six out of fourteen mice following injection of 10^7 SL 12.4 cells. The other major differences macroscopically were a higher incidence of nodular renal metastasis (5/14, 35.7 %) and also massive retroperitoneal lymph node involvement, (8/14, 57.1 %) again following the injection of 10^7 SL 12.4 cells. An example of the macroscopic findings in mice injected with SL 12.4 cells is shown in Figure 6.3. The involved ovaries were found to be enlarged, haemorrhagic and diffusely involved with metastases. Gross hepatosplenomegaly after SL 12.4 injection was not seen in contrast to SL 12.3 injection (figure 6.2).

Table 6.1a. Macroscopic pattern of metastasis shown by 10^6 12.3 and 10^6 SL 12.4 cells
 (*p*-value calculated using the Exact Probability Test)
 (***) = *p*<0.001)

Mouse	SL 12.3	SL 12.4
Number of Cells	10^6	10^6
Liver	*** 11/11 (100.0 %)	1/11 (9.1 %)
Spleen	*** 11/11 (100.0 %)	1/11 (9.1 %)
Kidneys	1/11 (9.1 %)	1/11 (9.1 %)
Ovaries	0/11 (0.0 %)	1/11 (9.1 %)
Lungs	0/11 (0.0 %)	0/11 (0.0 %)
Retroperitoneal lymph nodes	0/11 (0.0 %)	1/11 (9.1 %)
Brain	0/11 (0.0 %)	0/11 (0.0 %)
Thymus	0/11 (0.0 %)	0/11 (0.0 %)
Subcutaneous metastasis	1/11 (9.1 %)	0/11 (0.0 %)
Median Latent Period days (Range)	17 days (11-24 days)	^{##} 56 days (22-56 days)

(*p*-value for Median Latent Period was obtained using the Wilcoxon Rank Sum Test)
 (## = *p*<0.01)

Table 6.1b. Macroscopic pattern of metastasis shown by 10^6 SL 12.3 and 10^7 SL 12.4 cells
(p-value calculated using the Exact Probability Test)
*(** = $p < 0.01$, * = $p < 0.05$)*

Mouse	SL 12.3	SL 12.4
Number of Cells	10^6	10^7
Liver	11/11 (100.0 %)	11/14 (78.5 %)
Spleen	11/11 (100.0 %)	11/14 (78.5 %)
Kidneys	1/11 (9.1 %)	5/14 (35.7 %)
Ovaries	0/11 (0.0 %)	* 6/14 (42.9 %)
Lungs	0/11 (0.0 %)	0/14 (0.0 %)
Retroperitoneal lymph nodes	0/11 (0.0 %)	** 8/14 (57.1 %)
Brain	0/11 (0.0 %)	1/14 (7.1 %)
Thymus	0/11 (0.0 %)	0/14 (0.0 %)
Subcutaneous metastasis	1/11 (9.1 %)	2/14 (14.3 %)
Median Latent Period days (Range)	<i>17 days (11-24 days)</i>	<i>## 48 days (31-56 days)</i>

(p-value for Median Latent Period was obtained using the Wilcoxon Rank Sum Test)
(## = $p < 0.01$)

Figure 6.2 Example of findings on an abdominal examination on an AKR mouse injected with 10^6 SL 12.3 cells (median = 17 days; range = 11-24 days)

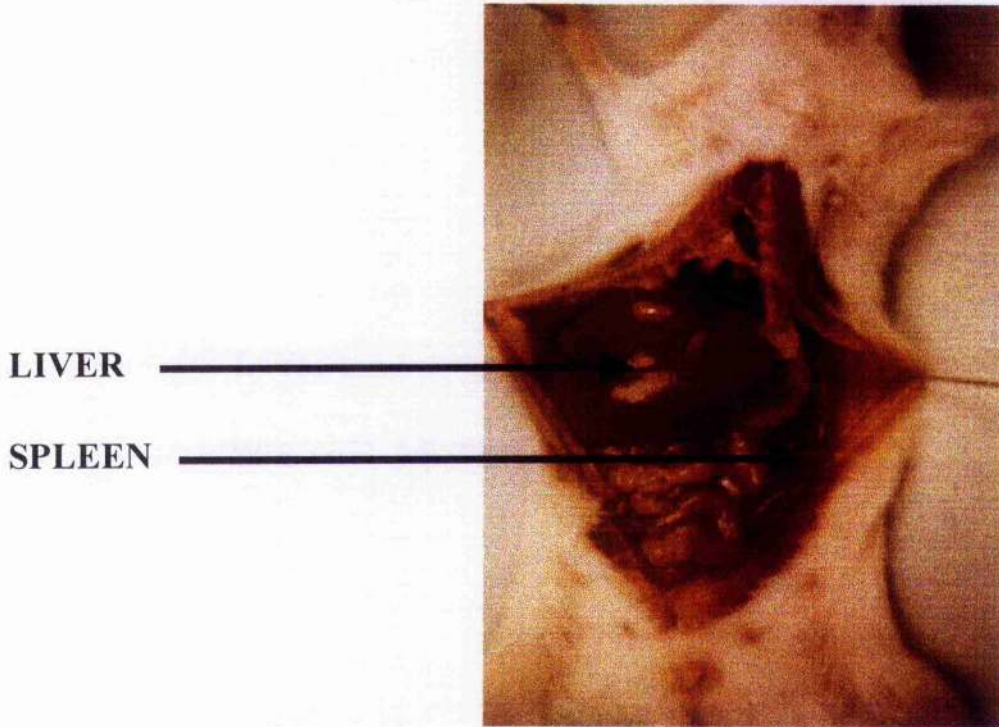
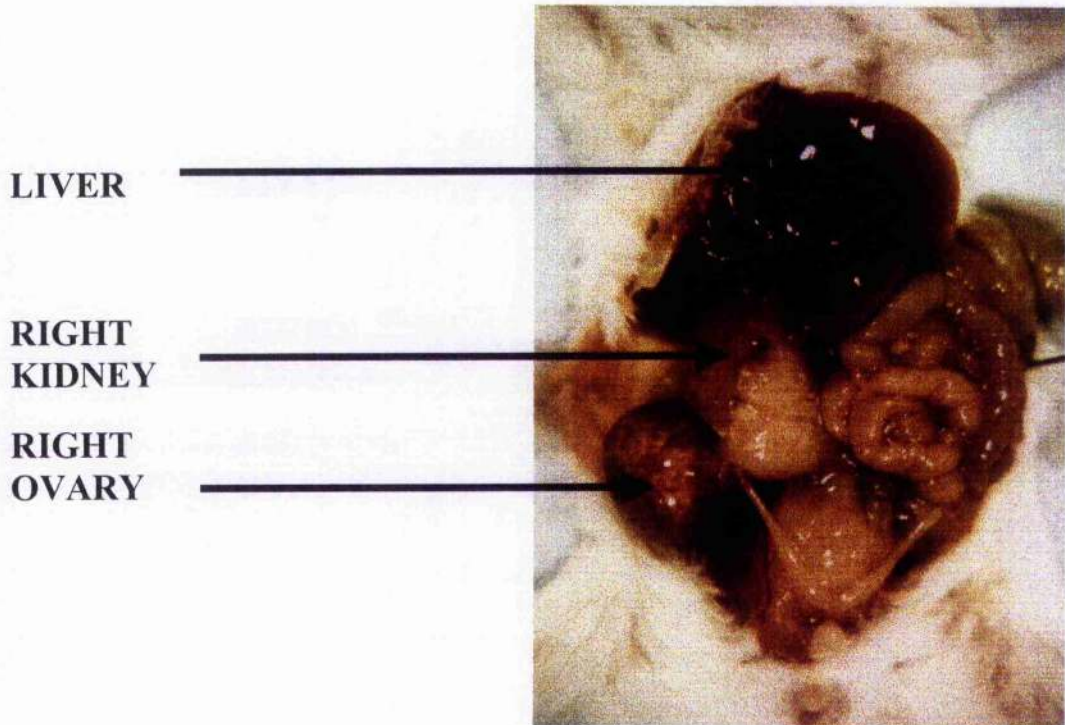


Figure 6.3 Example of findings on an abdominal examination on an AKR mouse injected with 10^7 SL 12.4 cells (median = 48 days; range = 31-56 days)



The macroscopic differences between organs of mice injected with SL 12.3 and SL 12.4 cells are also demonstrated when the mean percentage body weight of individual organs are compared as shown in Table 6.2 and graphically in Chart 6.1

Table 6.2 The mean percentage of body weight (*Standard Deviation*) of organs in mice injected with SL 12.3 and SL 12.4 cells

Organs	SL 12.3 (10^6 cells)	SL 12.4 (10^6 cells)
Liver	** 11.080 (3.246)	5.806 (0.508)
Spleen	* 2.237 (0.505)	0.513 (0.598)
Right Kidney	0.838 (0.069)	0.775 (0.089)
Left Kidney	0.794 (0.055)	0.745 (0.058)
Right Lung	0.790 (0.241)	0.555 (0.170)
Left Lung	0.427 (0.184)	0.273 (0.078)
Right ovary	0.122 (0.044)	0.074 (0.026)
Left ovary	0.128 (0.048)	0.064 (0.018)

Organs	SL 12.3 (10^6 cells)	SL 12.4(10^7 cells)
Liver	** 11.080 (3.246)	6.024 (1.086)
Spleen	** 2.237 (0.505)	0.600 (0.418)
Right Kidney	0.838 (0.069)	0.786 (0.124)
Left Kidney	0.794 (0.055)	0.721 (0.084)
Right Lung	** 0.790 (0.241)	0.532 (0.165)
Left Lung	0.427 (0.184)	0.331 (0.130)
Right ovary	0.122 (0.044)	0.890 (1.367)
Left ovary	0.128 (0.048)	0.601 (0.820)

** = $p < 0.01$

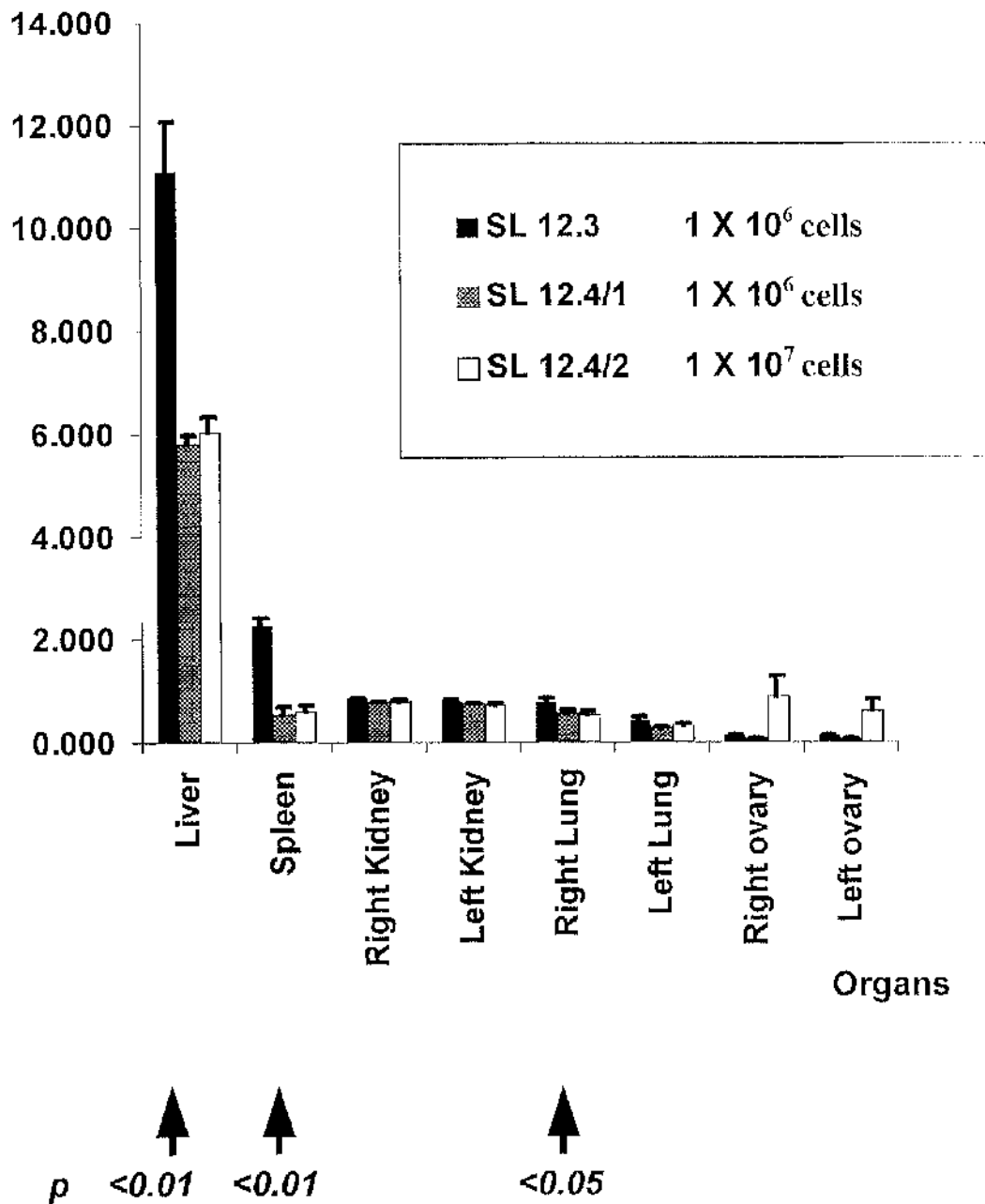
* = $p < 0.05$

(*p-values were obtained using the Wilcoxon Rank Sum Test*)

Chart 6.1

The comparison between mean percentage of body weight of organs in mice injected with 10^6 SL 12.3 cells, 10^6 SL 12.4 cells and 10^7 SL 12.4 cells (arrows indicate significant differences between 10^6 SL 12.3 cells and 10^7 SL 12.4)

Mean percentage of total body weight



Microscopic analysis

Microscopic analysis differs from the macroscopic pattern in certain organs (Table 6.3). Microscopic analysis confirmed the macroscopic appearance in liver and spleen involvement. Although renal tissue was not enlarged following SL 12.3 injection, microscopic metastases were present in 7/11 (63.6%) kidneys and in particular, although, the ovaries were not enlarged in SL 12.3 mice microscopic metastases were present in all ovarian tissue examined. This is in contrast to the obvious massive involvement of ovarian tissue by SL 12.4 cells although in 5/14 no microscopic ovarian disease was detected. Similarly, microscopic infiltration was seen following SL 12.3 injection in both lungs and retroperitoneal lymph nodes.

Furthermore, microscopic studies showed that the pattern of infiltration differs between organs. For example, in the lungs, tumour cells were found to be in the interstitial tissues and in the brain, the meninges were the site of involvement compared to parenchymal involvement in most organs.

Table 6.3. Macroscopic and microscopic patterns of SL 12.3 and SL 12.4 cells

	SL12.3		SL12.4		SL12.4	
Cells (X 10 ⁶)	1		1		10	
	<i>Macro</i>	<i>Micro</i>	<i>Macro</i>	<i>Micro</i>	<i>Macro</i>	<i>Micro</i>
Liver	11/11 (100%)	9/11 (81.8%)	1/11 (9.1%)	1/11 (9.1%)	11/14 (78.5%)	10/14 (71.4%)
Spleen	11/11 (100%)	11/11 (100%)	1/11 (9.1%)	1/11 (9.1%)	11/14 (78.5%)	8/14 (57.1%)
Kidneys	1/11 (9.1%)	7/11 (63.6%)	1/11 (9.1%)	1/11 (9.1%)	5/14 (35.7%)	5/14 (35.7%)
Ovaries	2/11 (18.2%)	11/11 (100%)	1/11 (9.1%)	2/11 (18.2%)	6/14 (42.9%)	9/14 (64.3%)
Lungs	0/11 (0.0%)	11/11 (100%)	0/11 (0.0%)	0/11 (0.0%)	0/14 (0.0%)	8/14 (57.1%)
Retroperitoneal lymph nodes	0/11 (0.0%)	11/11 (100%)	1/11 (9.1%)	1/11 (9.1%)	8/14 (57.1%)	6/14 (42.9%)
Brain	0/11 (0.0%)	3/11 (27.3%)	0/11 (0.0%)	1/11 (9.1%)	1/14 (7.1%)	5/14 (35.7%)
Thymus	0/11 (0.0%)	5/11 (45.5%)	0/11 (0.0%)	0/11 (0.0%)	0/14 (0.0%)	6/14 (42.9%)
Subcutaneous metastasis	1/11 (9.1%)	1/11 (9.1%)	0/11 (0.0%)	0/11 (0.0%)	2/14 (14.3%)	2/14 (14.3%)

Chapter 7 Cell tracking studies

Introduction

To study the distribution of SL 12.3/SL 12.4 cells after re-injection into AKR mice cell tracking studies were performed. The study of cellular dissemination and arrest in metastasis requires a suitable technique that permits the identification and quantification of tumour-cell emboli. One method of doing this is to label living cells with radioisotopes as described by Fidler (Fidler 1970). Several criteria must be satisfied when radioisotopes are used for labelling living cells. Firstly, the radioactive label should bind firmly to the cells while they are still viable. When labelled cells die, the isotope must not be re-utilised by other cells, but excreted rapidly. Secondly, the radioactive label must not alter the biological behaviour of the tumour cells when bound. Thirdly, the quantity of radioactive label used should be sufficient to allow a few cells to be detected sensitively in vivo but not to be in excess to kill both the host and the tumour cells.

^3H -thymidine, ^{51}Cr and 5-(^{25}I)odo-2'-deoxyuridine ($^{125}\text{IUdR}$) have all been used in such studies. Results using ^3H -thymidine and ^{51}Cr are controversial as they do not meet the ideal criteria. For example, when ^3H or ^{51}Cr are released from dead cells, they can be re-utilised by adjacent normal host stromal cells. Furthermore, the rate of escape of ^{51}Cr from viable tumour cells is rapid and up to 60 % can be lost. ^{51}Cr can also be re-utilised and absorbed by the normal host's cells within 24 hours. As a result, tissue

counts may not represent the true number of viable circulating tumour cells (Fidler 1970).

5-(¹²⁵I)odo-2'-deoxyuridine (¹²⁵IUDR), which has a half life of 59.6 days, tends to fit the ideal selection criteria slightly better. Being an analogue of thymidine, ¹²⁵IUDR is incorporated exclusively into DNA of actively dividing cells. When the cells die, unlike thymidine, ¹²⁵IUDR is released and is not re-utilised by other cells. Released and unused ¹²⁵IUDR is degraded quickly in the liver and the degradative products are largely excreted in the urine (Fidler 1970). Furthermore, ¹²⁵I is suitable for autoradiographic studies. This is useful when determining the quality of radiolabelling and the percentage of radiolabelled cells.

For each cell line studied in this manner, the optimum concentration of the isotope must be determined and labelling efficiency checked by autoradiography. Subsequently tracking studies were performed following the inoculation of labelled cells into AKR mice.

Determination of the optimal concentration of ¹²⁵I-5-Iodo-2'-deoxyuridine for labelling SL 12.3 and SL 12.4 cells

Method

10 petri dishes containing 10⁶ SL 12.3 cells per 6 mls of medium each and 10 petri dishes containing 10⁶ SL 12.4 cells per 6 mls of medium each were incubated at 37°C with 5 % carbon dioxide for 24 hours. ¹²⁵I-5-Iodo-2'-

deoxyuridine ($^{125}\text{IUDR}$) was added to each of the petri dishes at the following concentrations: 0 (control), 0.5, 1.0, 2.0 and 5.0 $\mu\text{Ci/ml}$ in duplicate.

Incubation was continued and after 24 hours, the cells were pelleted and washed three times with phosphate buffered saline (PBS). The washed radiolabelled cells were then analysed by gamma counter to determine the amount of $^{125}\text{IUDR}$ incorporation. The cells were then returned to normal medium before re-incubation and daily cell counts were performed to monitor cell viability and growth over a five-day period.

Results

The radiolabelled cells from each petri dishes containing either 10^6 SL 12.3 or 10^6 SL 12.4 with varying concentration of $^{125}\text{I-5-Iodo-2'-deoxyuridine}$ were analysed with the gamma counter. The percentage of incorporation of radioactivity was calculated using the formula:

$$\% \text{ of incorporation} = \frac{\text{Counts per minute of } \textit{Washed Cells}}{\text{Counts per minute of } \textit{Unwashed Cells + Medium}}$$

The percentage of incorporation of $^{125}\text{IUDR}$ by SL 12.3 and SL 12.4 cells are shown in Table 7.1 and graphically in Chart 7.1

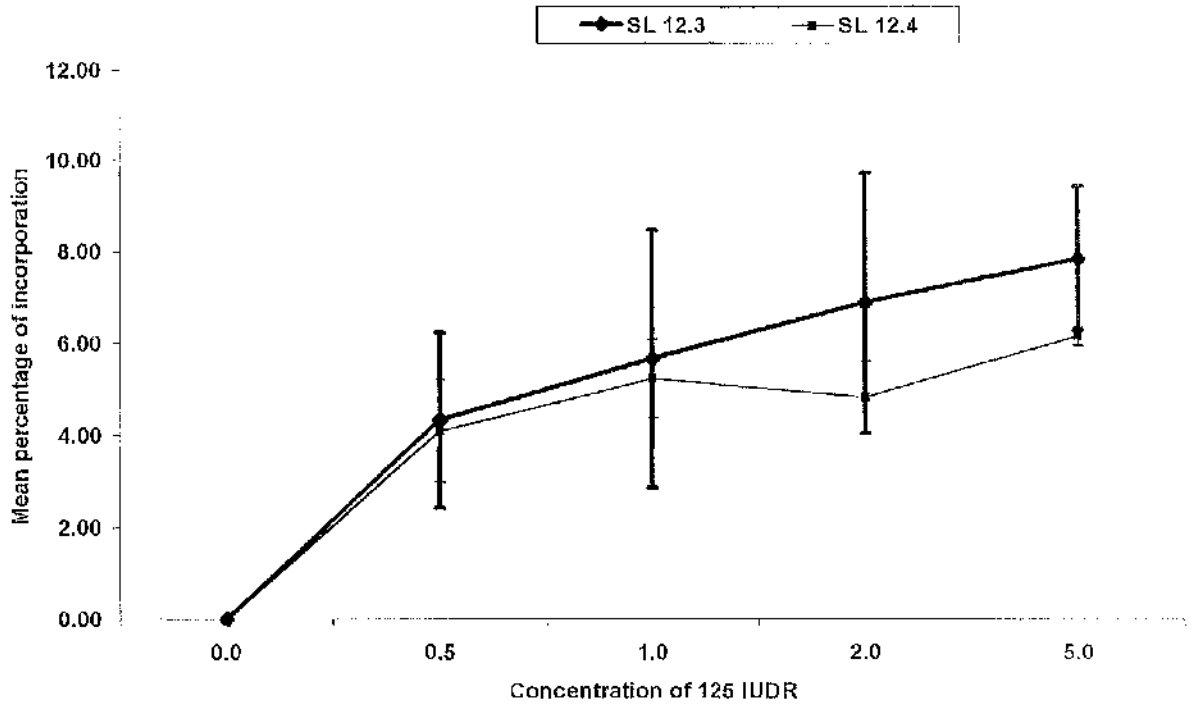
Table 7.1. Percentage of incorporation of radioactive labels by cells at different concentration of ^{125}I -5-Iodo-2'-deoxyuridine

Petri dish (6 mls of medium)	Concentration of $^{125}\text{TUDR}$ ($\mu\text{Ci/ml}$)	% incorporation	% incorporation	Mean	Standard error of mean
<i>SL 12.3</i>		<i>(SET 1)</i>	<i>(SET 2)</i>		
	0	0.00	0.00	0.00	0.00
	0.5	2.43	6.24	4.34	1.91
	1.0	2.85	8.47	5.66	2.81
	2.0	4.04	9.72	6.88	2.84
	5.0	6.28	9.43	7.86	1.57
<i>SL 12.4</i>		<i>(SET 1)</i>	<i>(SET 2)</i>		
	0	0.00	0.00	0.00	0.00
	0.5	5.22	2.99	4.11	1.12
	1.0	6.08	4.38	5.23	0.85
	2.0	5.61	4.04	4.83	0.78
	5.0	6.35	5.97	6.16	0.19

Table 7.1a. p-values (determined with Student T-test) showed no significance statistically between the incorporation of different concentration of $^{125}\text{IUDR}$ by SL 12.3 and SL 12.4 cells

Concentration of $^{125}\text{TUDR}$ ($\mu\text{Ci/ml}$)	Mean % of incorporation for SL 12.3	Mean % of incorporation for SL 12.4	P value using Student T-test
0	0	0	-
0.5	4.34	4.11	0.9
1.0	5.66	5.23	0.9
2.0	6.88	3.83	0.6
5.0	7.86	6.16	0.4

Chart 7.1: Mean percentage (*standard error of mean*) of incorporation of radioactive labels by SL 12.3 and SL12.4 cells at different concentration of ^{125}I -5-Iodo-2' deoxyuridine.



To check that $^{125}\text{IUDR}$ incorporation did not affect cell growth rates, daily cell counts for 5 days were performed and the results are as shown in table 7.2 and graphically in charts 7.2, 7.3, 7.4 and 7.5

Table 7.2. Daily cell counts to check viability and growth of SL 12.3 and SL 12.4 cells at varying concentration of ¹²⁵I-5-Iodo-2'-deoxyuridine

SL12.3	(SET 1)	Day 0	Day 1	Day 2	Day 3	Day 4	Day 5
Petri Dish	Concentration (μCi/ml)	X 10 ⁶ cells					
1	0	1.0	0.12	0.74	0.99	1.31	1.46
2	0.5	1.0	0.12	0.29	0.64	1.77	1.29
3	1.0	1.0	0.18	0.56	0.35	1.88	1.46
4	2.0	1.0	0.18	1.59	1.04	2.05	1.48
5	5.0	1.0	0.18	0.44	1.19	1.88	2.35
SL12.3	(SET 2)	Day 0	Day 1	Day 2	Day 3	Day 4	Day 5
6	0	1.0	0.12	0.41	1.19	1.10	1.29
7	0.5	1.0	0.12	0.47	0.81	1.80	1.43
8	1.0	1.0	0.12	0.62	0.84	0.66	2.04
9	2.0	1.0	0.12	0.77	0.87	2.39	2.04
10	5.0	1.0	0.18	0.24	0.81	1.48	2.80
SL12.4	(SET 1)	Day 0	Day 1	Day 2	Day 3	Day 4	Day 5
11	0	1.0	0.06	2.18	2.61	3.56	3.16
12	0.5	1.0	0.12	1.24	4.32	6.56	5.43
13	1.0	1.0	0.12	0.92	2.67	3.31	4.86
14	2.0	1.0	0.12	2.24	3.71	4.45	2.66
15	5.0	1.0	0.12	0.35	1.94	2.14	2.63
SL12.4	(SET 2)	Day 0	Day 1	Day 2	Day 3	Day 4	Day 5
16	0	1.0	0.12	0.74	0.98	10.3	7.62
17	0.5	1.0	0.12	0.29	0.64	7.61	7.25
18	1.0	1.0	0.12	0.68	4.99	9.09	6.22
19	2.0	1.0	0.06	2.30	7.02	4.16	5.74
20	5.0	1.0	0.18	2.66	7.08	6.73	6.24

Chart 7.2. Growth curve of SL 12.3 cells (Set 1) in different concentrations of ^{125}I UDR over 5 days

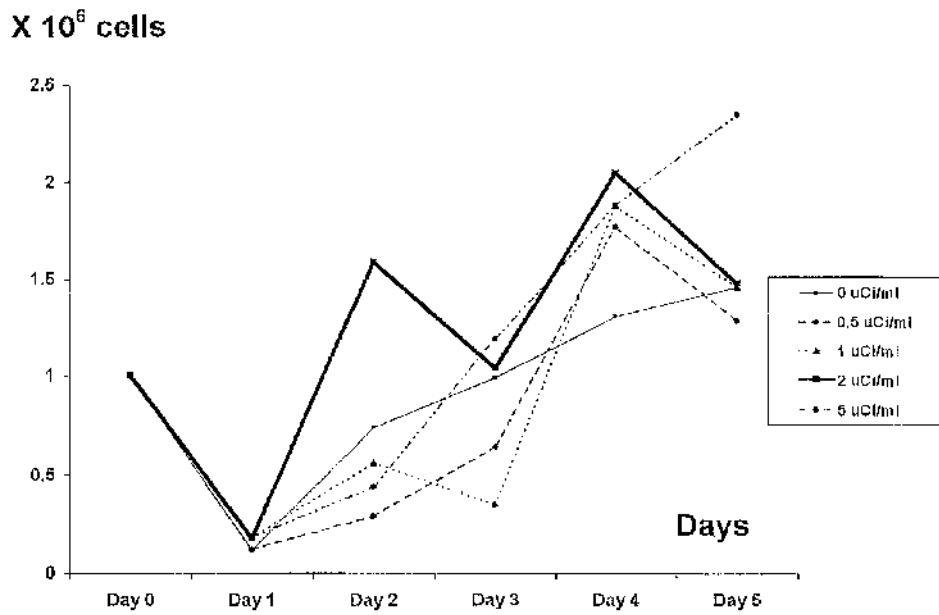


Chart 7.3. Growth curve of SL 12.3 cells (Set 2) in different concentrations of ^{125}I UDR over 5 days

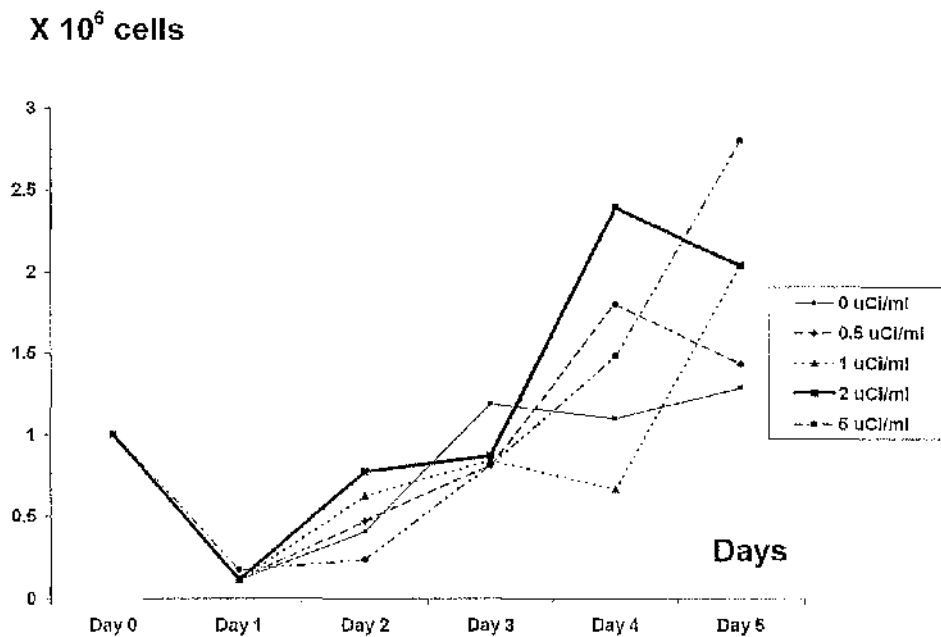


Chart 7.4 Growth curve of SL 12.4 cells (Set 1) in different concentrations of ^{125}I UDR over 5 days

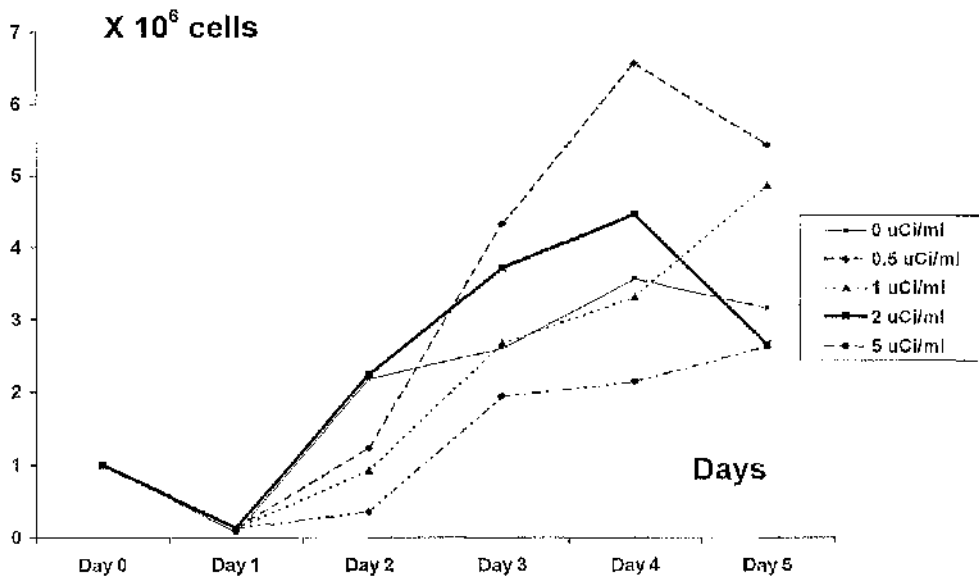
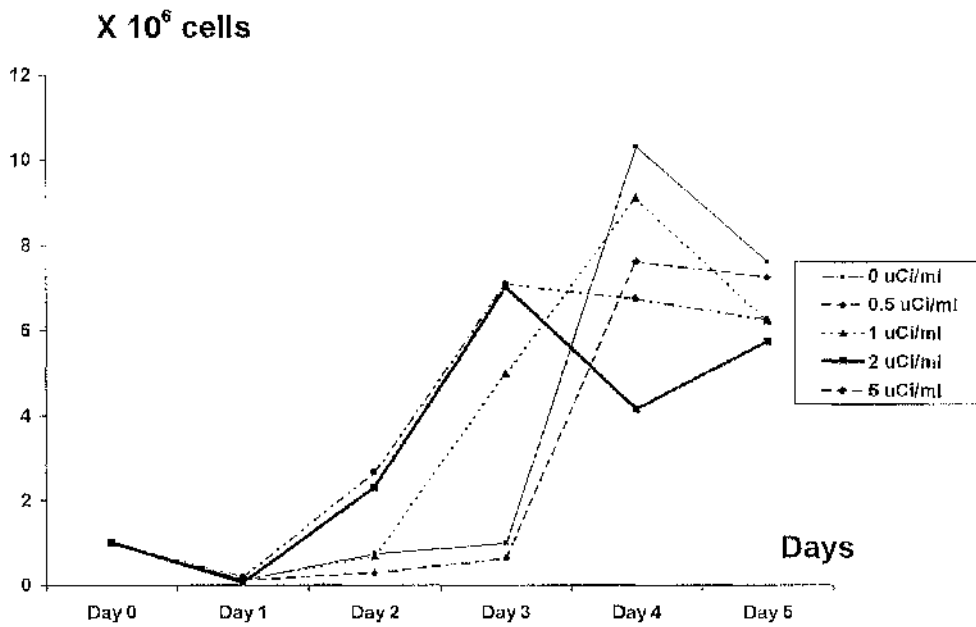


Chart 7.5. Growth curve of SL 12.4 cells (Set 2) in different concentrations of ^{125}I UDR over 5 days



The above results show that a concentration of 2 $\mu\text{Ci/ml}$ of ^{125}I UDR results in a high percentage of isotope incorporation without loss of cell viability. Five $\mu\text{Ci/ml}$ of ^{125}I UDR also resulted in good incorporation but a reduction in cell growth in one set of cells studied. Taking into account these results and economy of isotope used, a labelling concentration of 2 $\mu\text{Ci/ml}$ of ^{125}I UDR was chosen for further study.

Autoradiography

Method:

Preparation of emulsion for autoradiography

Under red safe light in the dark room, the emulsion (*Kodak NTB2*) was diluted 50:50 with distilled de-ionised water and the mixture heated in a 40^oC water bath for thirty minutes without boiling.

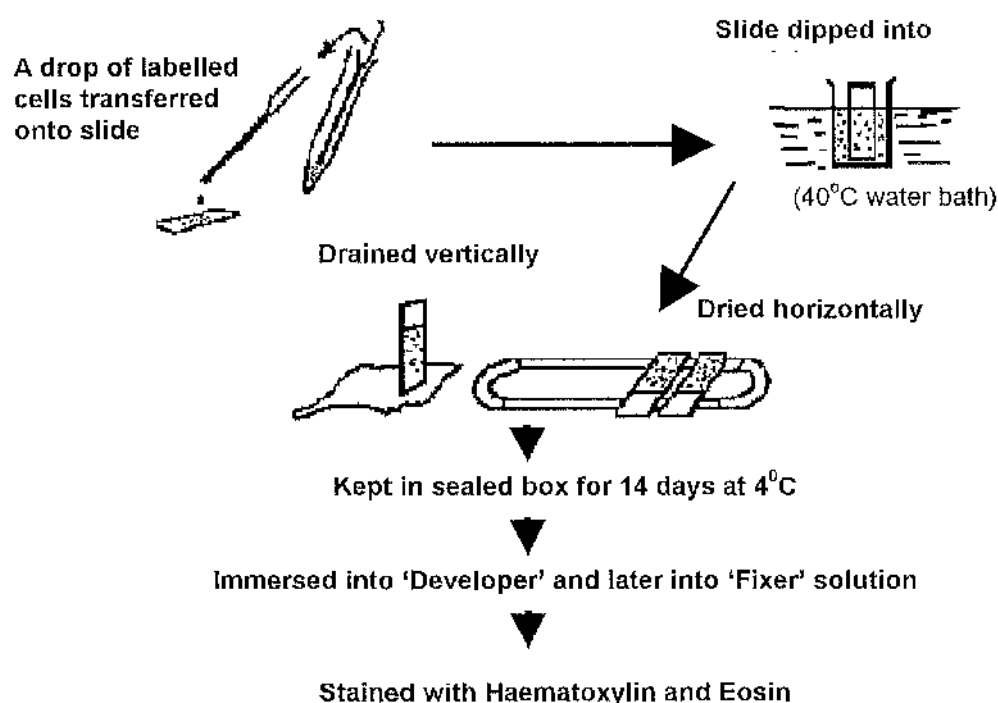
Autoradiography

SL 12.3 and SL 12.4 cells at exponential growth were radiolabelled with 2 $\mu\text{Ci/ml}$ of ^{125}I UDR as described above. A drop of washed labelled cells was smeared onto a glass slide. The slide was air dried for one hour before being fixed with freshly prepared chilled acetic acid/methanol (1:3) for

fifteen minutes. Under red safe light, the lower two-thirds of the slide with the specimen was immersed into the prepared emulsion for two seconds. The slide was withdrawn slowly and left to drain vertically for five minutes and horizontally for thirty minutes (Figure 7.1) before being stored in a light tight microscopic slide box containing a desiccant. The whole box was sealed and kept in 4°C for fourteen days.

The slide was exposed to atmospheric temperature and humidity for two minutes before being immersed into photographic developer solution (Aculux). After five minutes, the slide was briefly washed in distilled deionised water before being immersed into photographic fixer solution (Acufix) for five minutes. The prepared slide was then be stained with Haematoxylin and Eosin dyes.

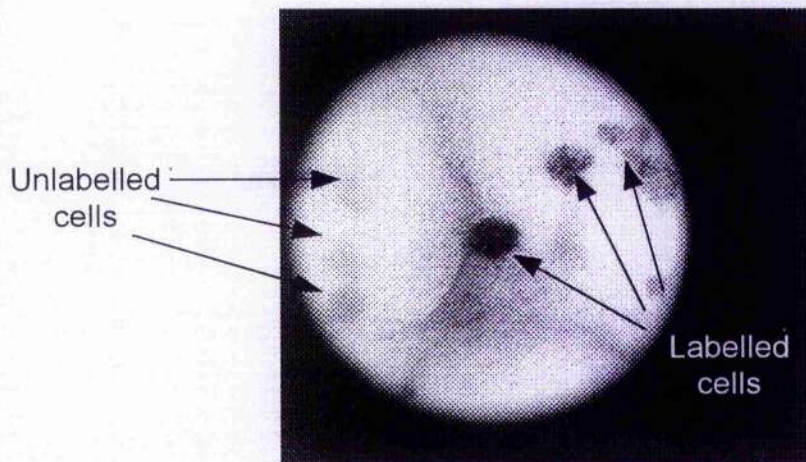
Figure 7.1 Steps in preparing an autoradiograph



Results

Figure 7.2 show a representative autoradiogram. ^{125}I UDR is taken into the nucleus and therefore, labelled viable cells appeared to have dark granules in their nuclei. Cells which do not take up ^{125}I UDR are either dead or remain unlabelled. This study confirmed that nuclear labelling had occurred.

Figure 7.2 : Autoradiograph of SL 12.3 cells following labelling with ^{125}I UDR (*Low power*)



In vivo studies of cell dissemination and arrest

Methods

Mice

36, eight to ten weeks old inbred female AKR strain mice were used in this study. All mice were maintained on a standard mouse diet. All mice were given water supplemented with 0.1 % sodium iodide to saturate their thyroid gland three days before injection, thus, preventing thyroid uptake of the $^{125}\text{IUDR}$

In vivo tracking

SL 12.3 and SL 12.4 cells at exponential growth rate were radiolabelled with 2 $\mu\text{Ci/ml}$ of $^{125}\text{IUDR}$ as described above. The cells were pelleted and total radioactivity counted before being re-suspended to produce an inoculum of 10^6 cells in 200 μl of sterile phosphate buffer (PBS). The total counts per minute of the pelleted cells were recorded which enabled a count per cell to be calculated.

Mice were randomly assigned to be injected with SL 12.3 or SL 12.4 cells and a time point to be sacrificed.

The selected mouse for injection was restrained in a modified bivalved 50 mls bladder syringe and radiolabelled cells were injected into the mouse via the tail vein. Eighteen mice received radiolabelled SL 12.3 cells while the other eighteen mice received radiolabelled SL 12.4 cells.

Post injection, the mice from both groups were euthanised at different time point as follows:

- six mice at fifteen minutes,
- six mice at one hour
- six mice at three hours.

Autopsies were performed on all the mice and the following tissues and organs were harvested, weighed and contained radioactivity counted:

* Brain biopsy	* Kidneys	* Lungs	* Thymus
* Liver	* Ovaries	* Spleen	
* Retroperitoneal lymph nodes			

The number of counts per minute for each organ was divided by the wet tissue weight in grams to give a figure for counts per gram of wet tissue. This was related to the number of either SL 12.3 or SL 12.4 cells present by division by the previously calculated counts per cell.

Results

The mean number of viable cells in the organs harvested at fifteen minutes, sixty minutes and three hours are shown in table 7.3 (a, b and c) and

graphically in charts 7.6, 7.7 and 7.8. Mean number of viable cells per gram of organs harvested are given in table 7.4 (a, b and c) and shown graphically in charts 7.9, 7.10 and 7.11.

Table 7.3a: Mean number [Standard Deviation] of viable SL 12.3 and SL 12.4 cells estimated to be within each organ at 15 minutes after injection

	SL 12.3 (15 minutes)	SL 12.4 (15 minutes)
	(n=6 mice)	n=6 mice
BRAIN	1654 [1101] (0.17 %)	2512 [3120] (0.25 %)
RIGHT KIDNEY	10769 [16587] (1.08 %)	17108 [25175] (1.71 %)
LEFT KIDNEY	18991 [21380] (1.90 %)	14931 [21152] (1.49 %)
RIGHT LUNG	123714 [255257] (12.37 %)	76796 [107035] (7.68 %)
LEFT LUNG	98022 [159576] (9.80 %)	50800 [73031] (5.08 %)
LIVER	481494 [610953] (48.15 %)	153511 [162121] (15.35 %)
LYMPH NODES	1788 [1205] (0.18 %)	2593 [3284] (0.26 %)
OVARIES	3063 [2713] (0.31 %)	4643 [7745] (0.46 %)
SPLEEN	10625 [17426] (1.06 %)	4082 [5937] (0.41 %)
THYMUS	2152 [1167] (0.22 %)	11047 [19069] (1.10 %)

(p-values were obtained using the Wilcoxon Rank Sum Test)

Table 7.3b : Mean number [Standard Deviation] of viable SL 12.3 and SL 12.4 cells estimated to be within each organ at 60 minutes after injection

	SL 12.3 (1 hour)	SL 12.4 (1 hour)
	n=6 mice	n=6 mice
BRAIN	1517 [1352] (0.15 %)	* 8994 [7676] (0.90 %)
RIGHT KIDNEY	15566 [27083] (1.56 %)	16041 [15335] (1.60 %)
LEFT KIDNEY	15263 [24409] (1.53 %)	12016 [8785] (1.20 %)
RIGHT LUNG	6393 [6574] (0.64 %)	21860 [17160] (2.19 %)
LEFT LUNG	10042 [12246] (1.00 %)	16326 [15655] (1.63 %)
LIVER	120585 [213535] (12.06 %)	55725 [40259] (5.57 %)
LYMPH NODES	1974 [132] (0.20 %)	2144 [228] (0.21 %)
OVARIES	1724 [1780] (0.17 %)	11015 [10166] (1.10 %)
SPLEEN	11085 [20471] (1.11 %)	15187 [10266] (1.52 %)
THYMUS	4016 [7401] (0.40 %)	*13757 [12248] (1.38 %)

* = $p < 0.05$

(*p-values were obtained using the Wilcoxon Rank Sum Test*)

Table 7.3c : Mean number [Standard Deviation] of viable SL 12.3 and SL 12.4 cells estimated to be within each organ at 3 hours after injection

	SL 12.3 (3 hours)	SL 12.4 (3 hours)
	n=6 mice	n=6 mice
BRAIN	1979 [85] (0.20 %)	2061 [138] (0.21 %)
RIGHT KIDNEY	3245 [1585] (0.32 %)	3385 [1874] (0.34 %)
LEFT KIDNEY	2738 [1008] (0.27 %)	3443 [1715] (0.34 %)
RIGHT LUNG	7508 [4834] (0.75 %)	* 4072 [4276] (0.41 %)
LEFT LUNG	4593 [2002] (0.46 %)	2549 [1100] (0.25 %)
LIVER	13158 [5838] (1.32 %)	12910 [7020] (1.29 %)
LYMPH NODES	1931 [72] (0.19 %)	2024 [78] (0.20 %)
OVARIES	2572 [1139] (0.26 %)	2105 [79] (0.21 %)
SPLEEN	3909 [2377] (0.39 %)	3987 [1850] (0.40 %)
THYMUS	2406 [606] (0.24 %)	2993 [954] (0.30 %)

* = $p < 0.05$

(*p-values were obtained using the Wilcoxon Rank Sum Test*)

Chart 7.6. The mean percentage of total viable SL 12.3 and SL 12.4 cells present in different organs at fifteen minutes

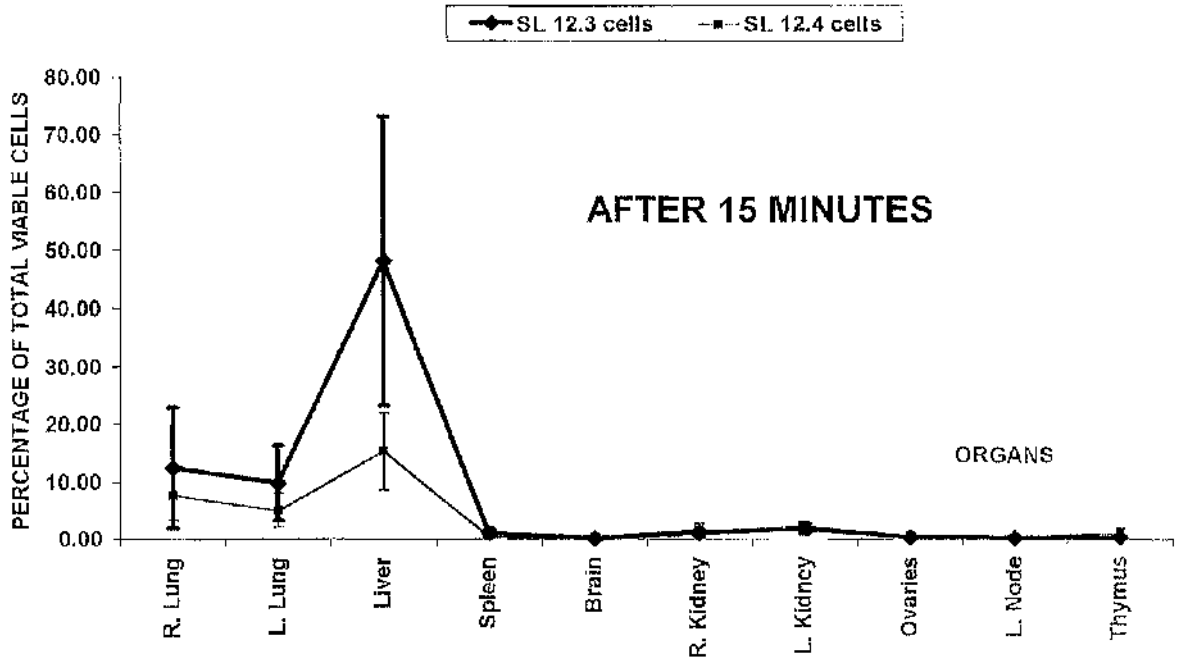


Chart 7.7. The mean percentage of total viable SL 12.3 and SL 12.4 cells present at different organs at one hour

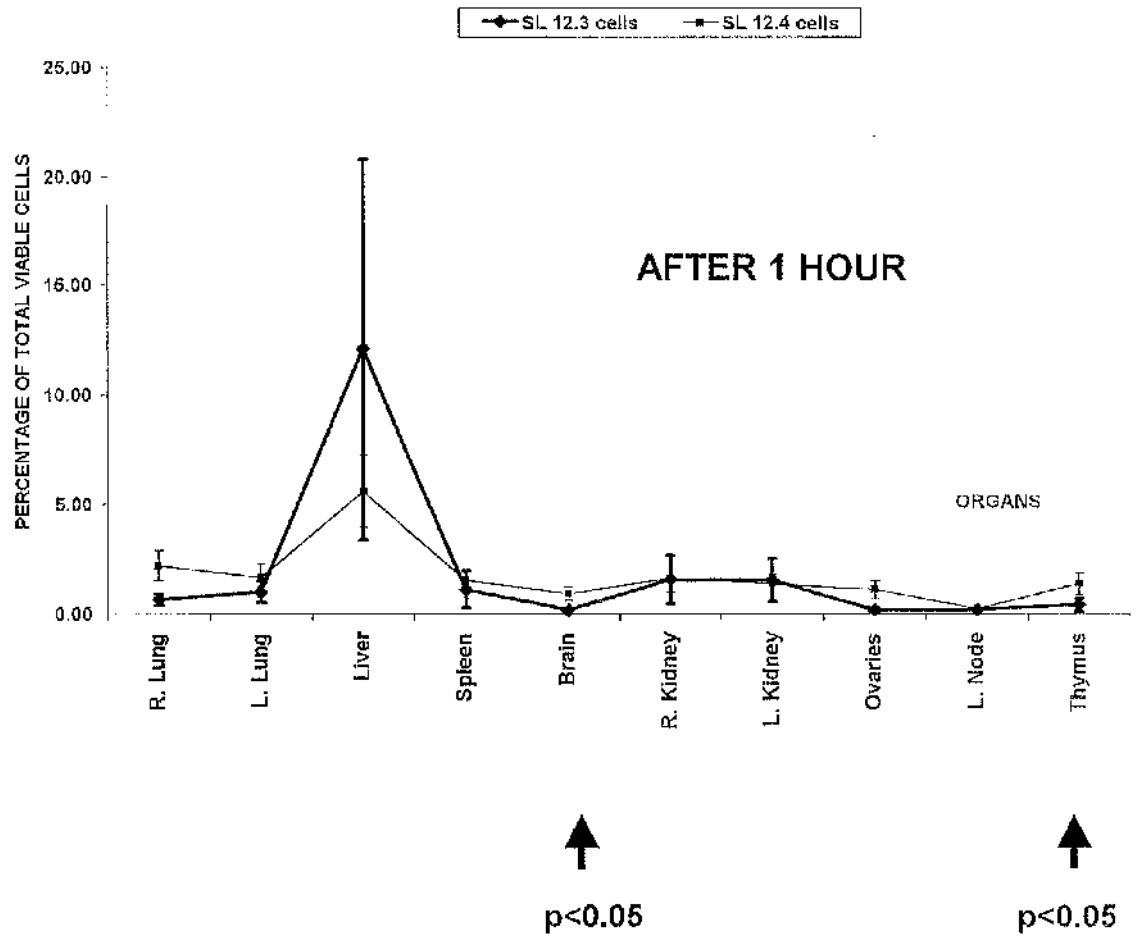
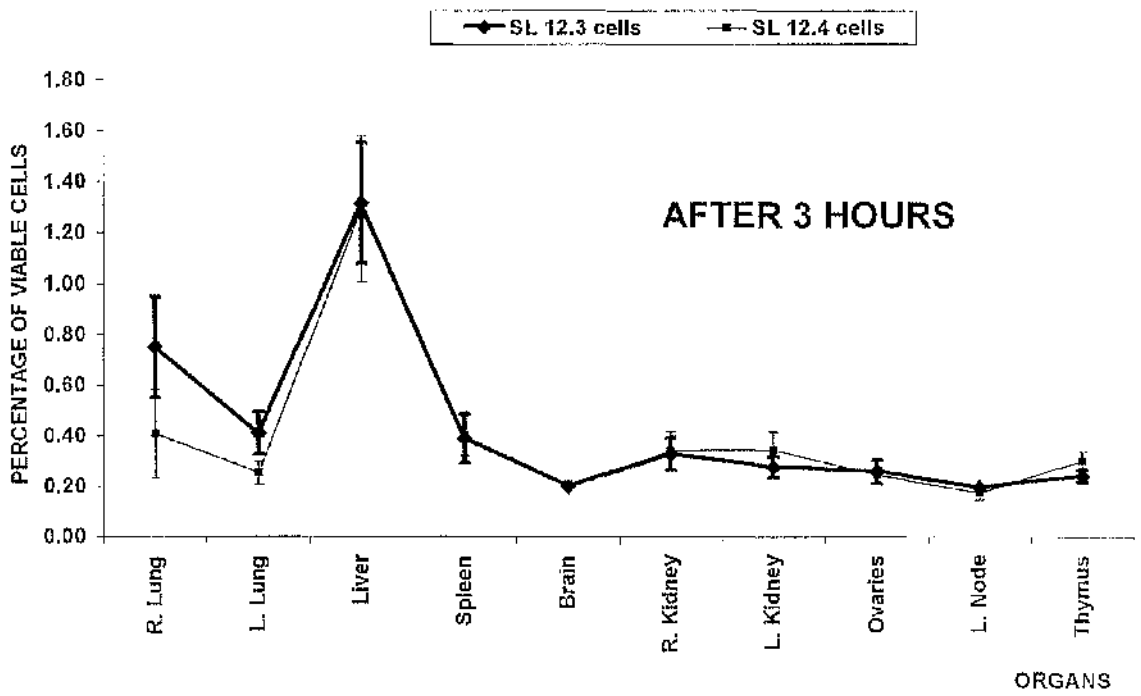


Chart 7.8

The mean percentage of total viable SL 12.3 and SL 12.4 cells present at different organs at 3 hours



↑
 $p < 0.05$

Table 7.4a The mean number [Standard Deviation] of cells per gram of tissues at 15 minutes after injection

	SL 12.3	SL 12.4
Time	15 minutes	15 minutes
Brain	6172 [4909]	9188 [10285]
Right Kidney	42046 [71779]	54705 [80343]
Left Kidney	62280 [71317]	42486 [44439]
Right Lung	553679 [1181070]	548264 [727499]
Left Lung	691522 [906105]	462446 [499957]
Liver	210064 [236553]	130353 [157852]
Lymph nodes	75426 [91085]	161547 [142638]
Ovaries	29974 [24158]	64261 [96857]
Spleen	52120 [86520]	20685 [21545]
Thymus	27802 [29658]	49939 [64047]

(p-values were obtained using the Wilcoxon Rank Sum Test)

Table 7.4b The mean number [Standard Deviation] of cells per gram of tissues at 60 minutes after injection

	SL 12.3	SL 12.4
Time	1 hour	1 hour
Brain	6976 [8424]	41730 [41611]
Right Kidney	44405 [68349]	65403 [61444]
Left Kidney	64371 [109600]	61164 [60083]
Right Lung	61572 [60716]	242724 [238955]
Left Lung	193607 [224528]	404964 [390931]
Liver	119794 [166719]	30359 [15507]
Lymph nodes	94032 [68996]	278555 [268727]
Ovaries	20016 [24259]	* 394082 [428686]
Spleen	66371 [123718]	126253 [91735]
Thymus	50026 [63076]	99505 [85883]

* = $p < 0.05$

(*p*-values were obtained using the Wilcoxon Rank Sum Test)

Table 7.4c The mean number [*Standard Deviation*] of cells per gram of tissues at 3 hours after injection

	SL 12.3	SL 12.4
Time	3 hours	3 hours
Brain	5774 [1286]	6723 [1964]
Right Kidney	17926 [8477]	15577 [10312]
Left Kidney	12484 [4911]	15375 [6432]
Right Lung	43834 [31885]	29178 [22828]
Left Lung	54363 [18996]	38580 [32801]
Liver	9255 [4432]	8124 [4102]
Lymph nodes	130532 [151178]	108475 [115692]
Ovaries	30117 [10876]	41073 [23902]
Spleen	26449 [19443]	22036 [18612]
Thymus	31143 [26565]	16880 [11825]

(p-values were obtained using the Wilcoxon Rank Sum Test)

Chart 7.9

Mean number of cells (*standard error of mean*) per gram of tissue at 15 minutes after inoculation

Mean number of cells per gram of tissue

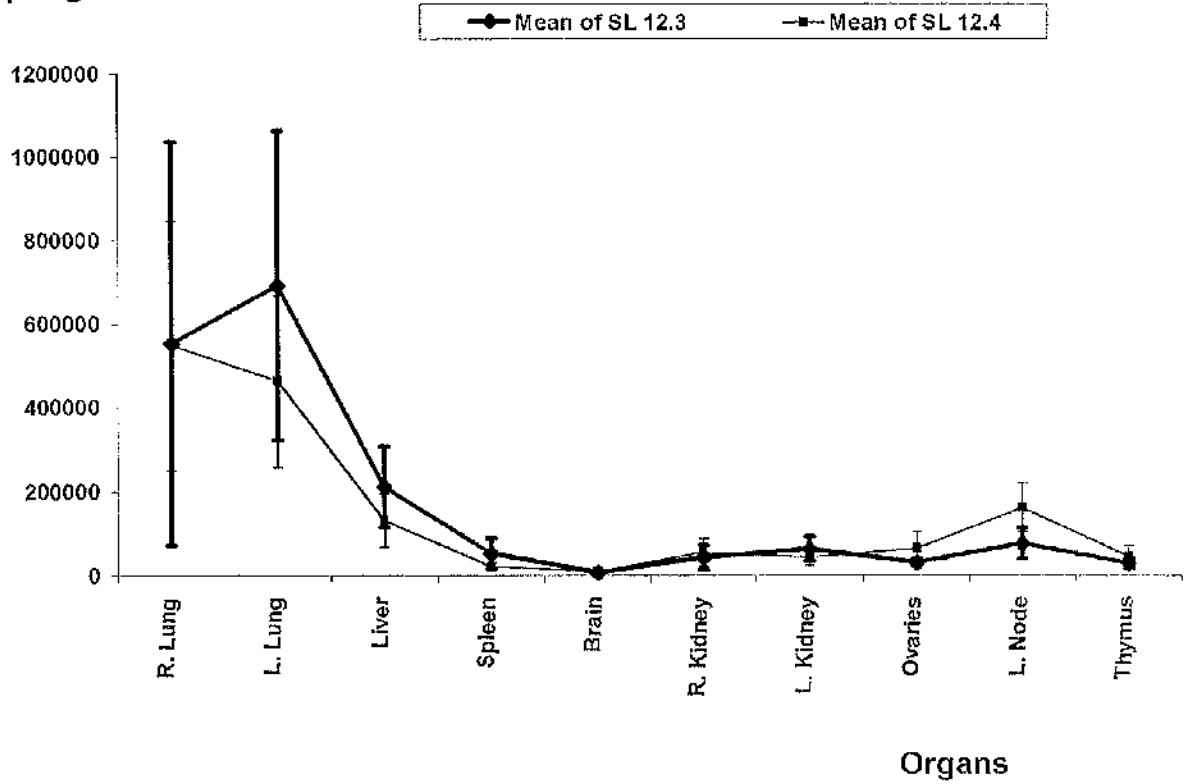


Chart 7.10 Mean number of cells (standard error of mean) per gram of tissue at 60 minutes after inoculation

Mean number of cells per gram of tissue

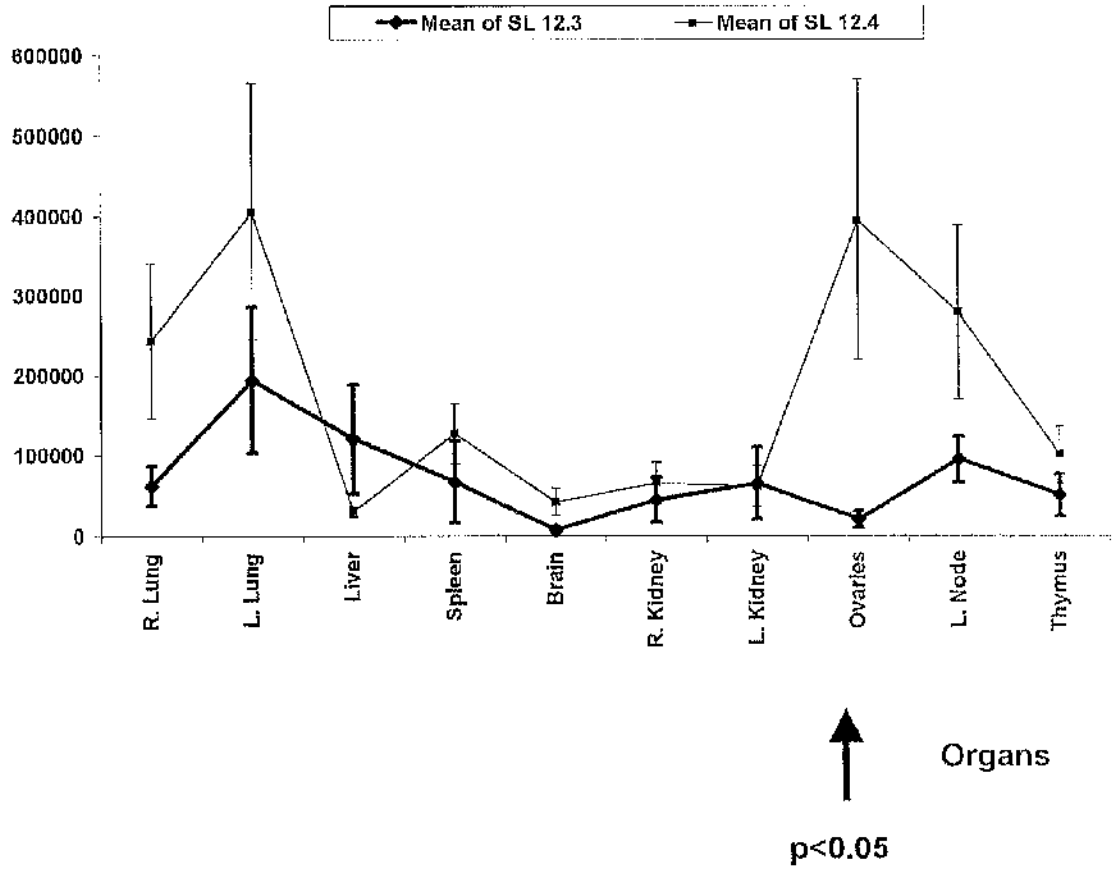
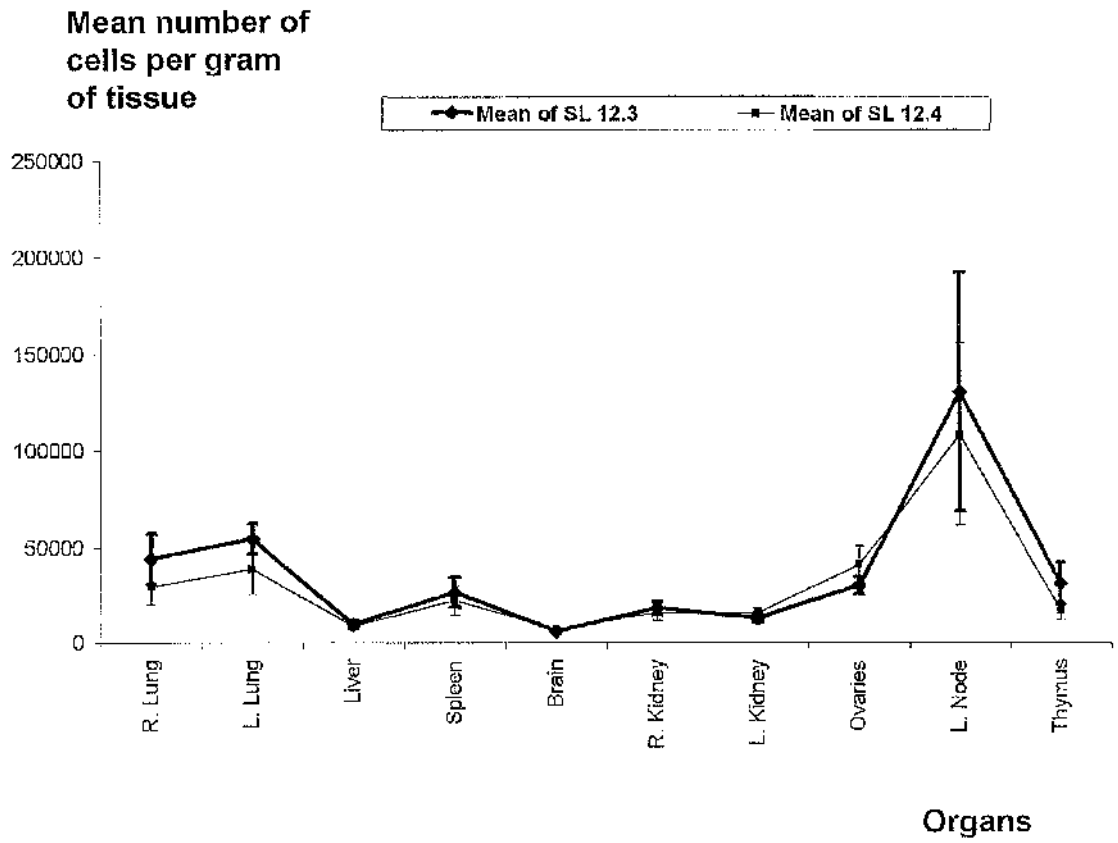


Chart 7.11 Mean number of cells (standard error of mean) per gram of tissue at 3 hours after inoculation



Chapter 8 Molecular Studies

Introduction

Studies thus far have confirmed a difference in tumourigenicity and metastatic pattern between these two murine lymphoma clones SL 12.3 and SL 12.4. Such variation in tumourigenicity, metastatic potential and pattern may be due to a certain subset of genes, which after either being activated or repressed, favour the selective growth of metastatic cells in organ specific environments. In addition, it is postulated that as the end result, differential expression of a series of critical genes allow tumour cells to evade the host's immune system and to "home" to and grow in distant target tissues.

As T and B lymphocytes are found to differ only in about 100 genes (Hedrick 1984), it is not surprising that such closely related clones as SL12.3 and SL12.4 cell lines might only differ in the expression of a few genes. Thus, these cell lines provide an attractive model for the study of differential genetic expression that might account for their in vivo metastatic behaviour.

The molecular approach to study SL 12.3 and SL 12.4 cells

Three major approaches to identify specific genes expressed in different cell lines are differential screening, subtractive hybridisation and more recently, differential display (Sunday 1995). All these approaches involved the basic

molecular techniques of messenger RNA (or mRNA) extraction and the synthesis of complementary DNA (or cDNA).

Messenger Ribonucleic Acids or mRNAs

When a cell produces a protein such as an enzyme or surface receptor, the DNA sequence responsible for the protein is used as a template for the synthesis of a complementary strand of nucleic acid called mRNA or messenger ribonucleic acid. These mRNAs move from the nucleus to the cytoplasm to be translated for protein synthesis in the ribosomes. mRNA, therefore, provides valuable information as it encodes the genetic information being processed in a cell at any one time.

It is known that cells of higher organisms contain about 100 000 different genes but only about 15 % (15 000) of these genes are expressed in an individual cell (Davidson 1976; Liang 1992). Any mRNAs that represent less than 0.5 % of the total mRNA population of the cell are classified as 'rare mRNA' or 'low abundance mRNA' (Maniatis 1983). Some of these rare mRNA sequences have been found to have short half-life and are not expressed all the time.

Using mRNA as a template and in the presence of an enzyme called reverse transcriptase, cDNAs (complementary deoxyribonucleic acids) can be synthesised. cDNAs have the same sequence as the initial gene segment which was expressed by the cell. Therefore, if all mRNAs of a cell line can be extracted, it is potentially possible to build a library of cDNA clones which represent the genes being expressed in a cell line at a particular time

point. Subsequently, comparison of cDNAs between cell lines could, theoretically, enable us to isolate cDNAs that are expressed exclusively in one cell line or tissue compared with another.

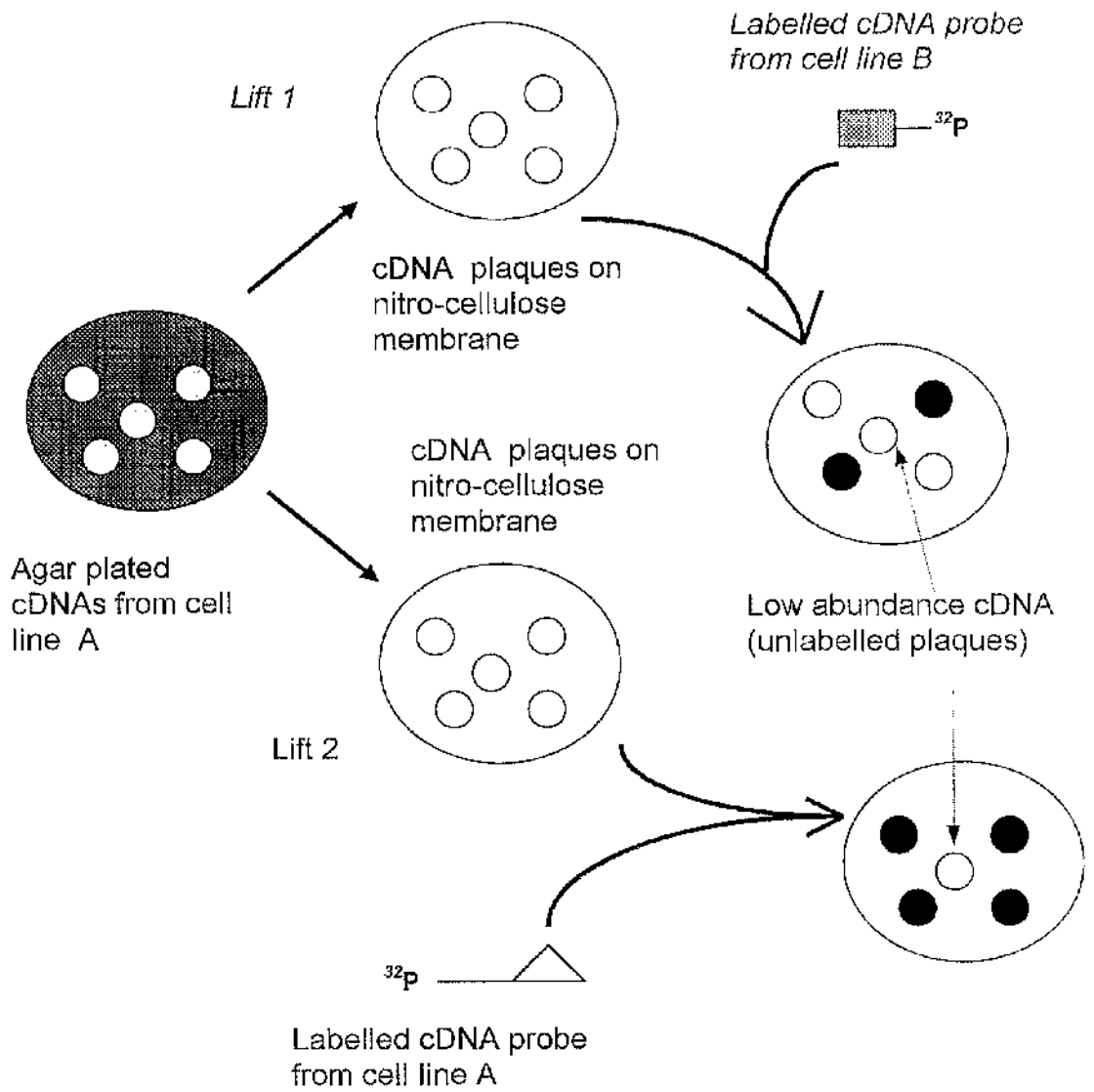
Methods for isolating genes that are exclusively expressed in one cell line

I. Differential Screening (Sunday 1995)

mRNAs of a cell line to be studied are reverse transcribed to their cDNAs. A cDNA library is then prepared in vectors such as Bluescript or Phage and plated onto an agar. The library is plated at a low enough density to visualise individual plaques representative as a single cDNA clone. “Lifts” or imprints of the agar-plated cDNAs are made onto nitro-cellulose membranes that are then screened with ^{32}P -labelled cDNA probes synthesised from cell lines of interest (Figure 8.1). Clones expressed in both cell lines will be identified as labelled plaques whereas plaques representing clones not expressed in the comparison cell line will not be labelled.

Despite being technically straightforward, this method is relatively insensitive. It is good for detecting high abundance mRNAs but rare mRNAs are undetectable because of the low copy number in the probe pool. Moreover, differential screening is very laborious and time consuming as it involves hundreds of duplicate lifts to identify cDNAs that are more strongly expressed in one cell line. Limitations lie in the variation of signal intensity and high background.

Figure 8.1 Differential screening.

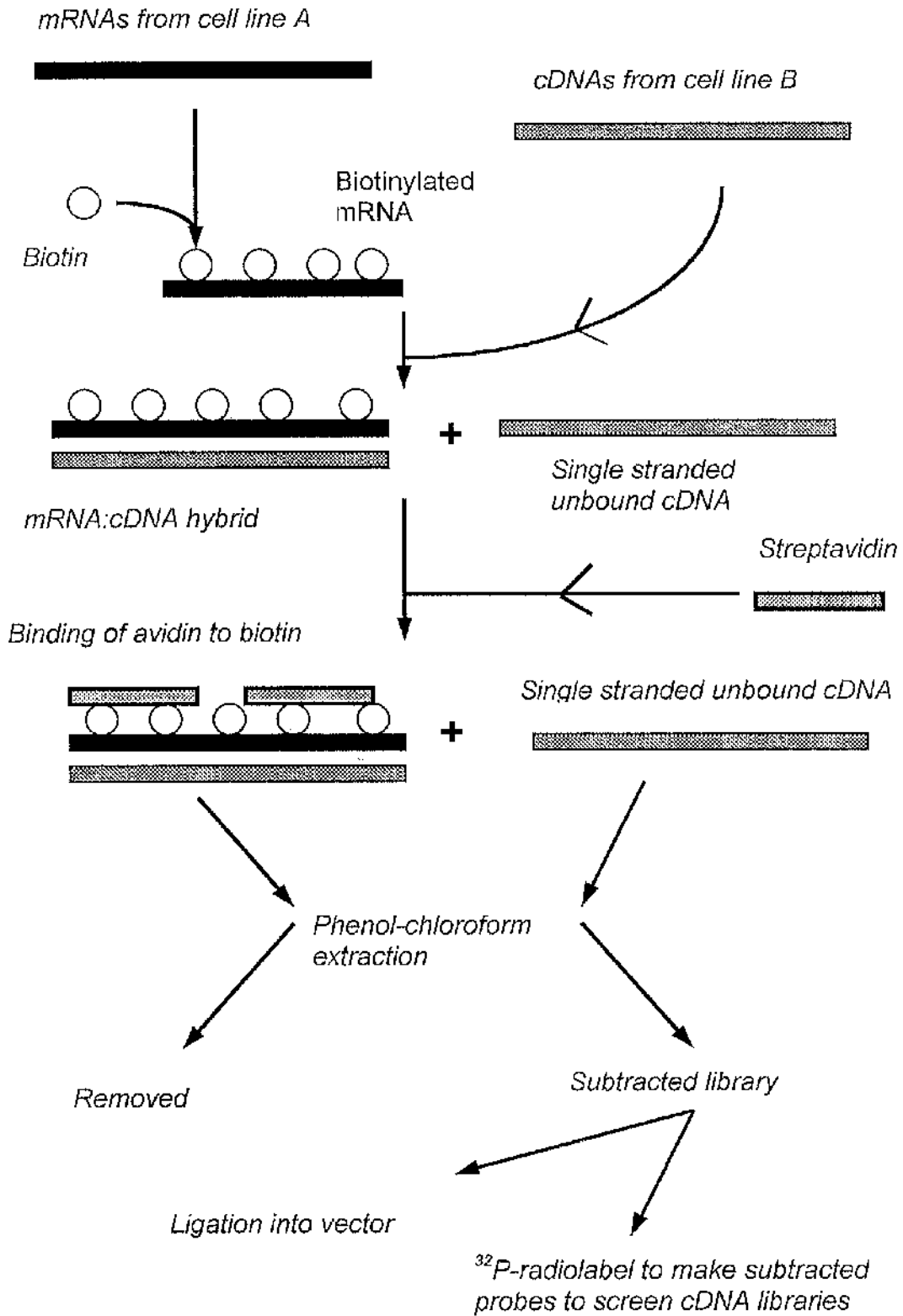


II. *Subtractive hybridisation*

Subtracted hybridisation is a well-established and sensitive method. A large amount of total RNA (~ 200 µg) from a cell line to be studied is biotinylated and hybridised with single stranded cDNA probes from cell lines of interest. The biotinylated mRNA:cDNA hybrids, thus, represents shared sequence expressed by both cell lines. These double stranded hybrids can be separated from unbound single stranded cDNAs by adding a large protein such as streptavidin to the mixture that binds to the biotin. The biotinylated sequences can then be extracted with phenol-chloroform where the sequences bound to avidin can be found at the interface between aqueous and the organic phase and the unbound single stranded cDNAs remain in the aqueous phase. These cDNAs can then be isolated and inserted into a suitable vector to make a subtracted library (Figure 8.2).

There are number of known variations to obtain the subtracted library and all of these can detect rare mRNAs (< 0.01 % abundance). However, subtraction hybridisation has its limitations. The construction of the cDNA library requires a large amount of total RNA and therefore, needs a large amount of cells or tissue. During this multistep process, there is a possibility of losing, contaminating or degrading the rare mRNAs.

Figure 8.2 Subtractive hybridisation



III mRNA Differential Display

A third technique, mRNA differential display was described by Liang and Pardee in 1992 (Liang 1992) to try to isolate and characterise genes that are differentially expressed in a particular cell line. This techniques involve two molecular tools: *Reverse Transcription and Polymerase Chain Reaction*.

Reverse Transcription-Polymerase chain reaction

1. Reverse transcription

Reverse transcription (RT) is a process where cDNAs are synthesised from mRNAs using an enzyme called reverse transcriptase that is found in retroviruses. An oligonucleotide primer is required to be attached to the end of the mRNA strand to initiate this process as the enzyme reverse transcriptase builds complementary nucleic acid strand by adding nucleotides to the primer. Fortunately, most eukaryotic mRNAs end in a string of 50-250 adenylate residues (poly-A tail) and as a result, a single oligonucleotide primer with a string of thymidylate residues (poly-T) is normally used for most reverse transcription processes.

Once the cDNAs are synthesised, the reverse transcription process is either terminated by denaturing the mRNA templates by an alkali treatment that does not affect the DNA or by denaturing the reverse transcriptase enzyme by heating the mixture to 94°C. This leaves a mixture of pure single stranded

cDNAs that are then used as templates for PCR.

II. Polymerase chain reaction

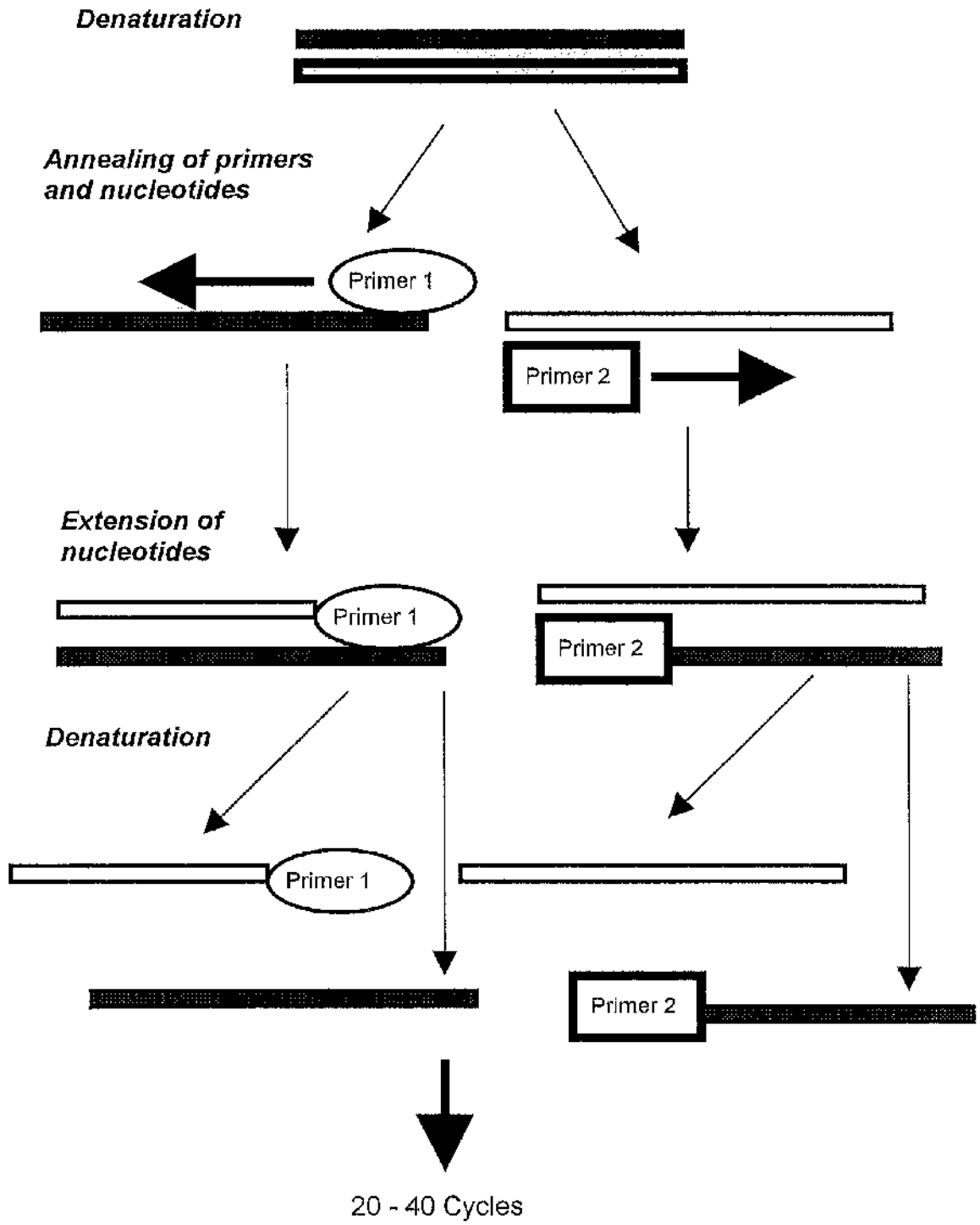
Polymerase chain reaction or PCR is an *in vitro* enzymatic method for the synthesis of specific DNA sequences. It involves repetitive cycles of 3 processes namely template denaturation, primer annealing and extension of annealed primers (Figure 8.3). Heated to 94⁰C, DNA strands are denatured to allow primers to anneal to them. The sequence of DNA of interest has to be known in order to prepare suitable pair of primers or amplimers to anneal and flank the region of the DNA for amplification. In the presence of DNA polymerase, nucleotides are then added to the initiating primer of one end. The nucleotides are then extended to build a complementary DNA strand.

In PCR, the end primer extension products in one cycle are used as templates for the next cycle, thus, approximately doubling the target DNA copies in every cycle. Therefore, a 20 cycle PCR would theoretically yield 2²⁰ amplifications of the target DNAs. This makes PCR a very sensitive process which only require a very small amount of DNA as the initial template. The cycle then repeats itself until specified or when all the nucleotides and enzyme are exhausted.

The yield of products in PCR depends on the reaction parameters such as enzyme, nucleotide, primer and Mg⁺⁺ concentrations. Every different DNA template requires different reaction parameters to achieve its maximum yield. The enzyme originally used in PCR for extending annealed primers was the Klenow fragment of E.Coli DNA polymerase I. Unfortunately, this

enzyme could be inactivated easily during the template denaturation process when the temperature required is about 94°C , thus, requiring fresh enzymes to be added for each cycle. The introduction of the thermostable DNA polymerase, Taq polymerase, isolated from *Thermus aquaticus*, transformed PCR. It makes PCR simple, robust and easily automated using a thermal cycling device. The reaction components (templates, dNTPs and buffers) can be added to a single tube and the amplification reaction carried out simply by cycling the temperatures within the tube.

Figure 8.3 A summary of Polymerase Chain Reaction (PCR)



Chapter 9 mRNA Differential Display

First described in 1992 by Liang and Pardee, mRNA differential display essentially displays the products of reverse transcription and polymerase chain reaction side by side on a sequencing gel. mRNAs can then be directly compared between cell lines and any mRNAs of interest can be cut out from the gel, reamplified and characterised (Liang 1992).

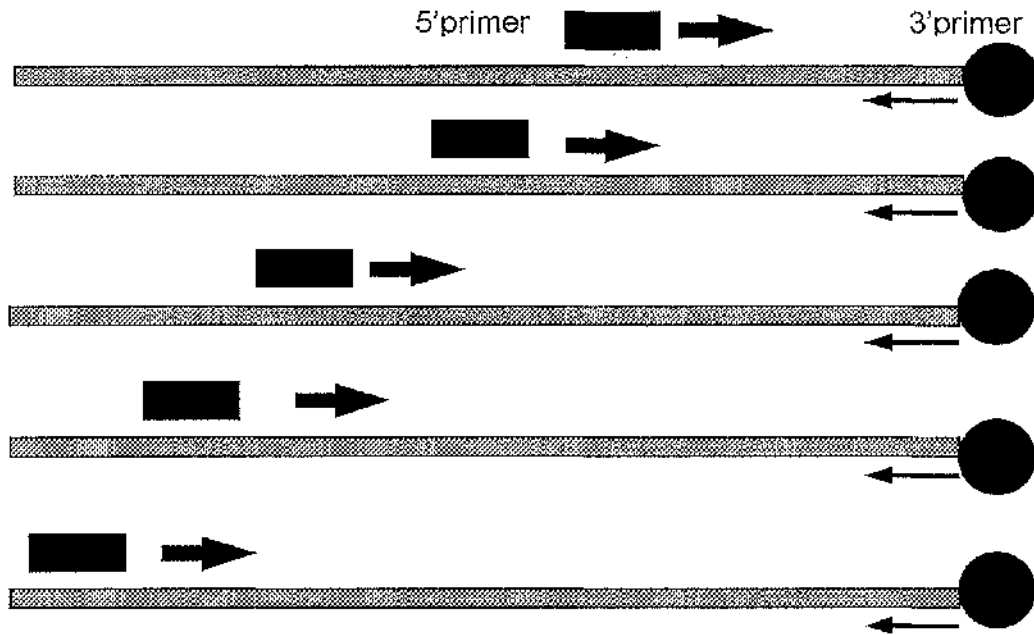
Basic concept of mRNA differential display

Based on the fact that a mammalian cell has 100 000 genes and only about 15 % (15 000) are expressed, Liang et al., used a pair of short and relatively non specific primers in the polymerase chain reaction. These short primers randomly amplify between 50 to 100 subsets of mRNAs of a cell. This number being optimal for display on a gel (Liang 1992).

The primers

Liang et al., use an anchoring 3'-primer and an arbitrarily chosen 5' primer which prime in random (Figure 9.1).

Figure 9.1 Primers used in differential display. The 3'-primer is an anchoring oligo(dTs) and the arbitrarily chosen 5'-primer anneal randomly.



Selection of the 3'-primer

Most eukaryotic mRNAs have a polyadenylated (poly-A) tail. Therefore a 3'-primer with oligo(dTs) such as 5'-T₁₁CA would be able to anchor and anneal to the 3' end of the mRNAs containing TG located upstream of their poly-A tail (Figure 9.2). By probability, oligo-dTs with extended two bases such as 5'T₁₁CA would recognise and amplify one twelfth of the total mRNA population because there are 12 different combinations of the last two 3' bases, omitting T as the penultimate base.

Figure 9.2 Selection of 3'-primer is based on the poly -A tail of mRNAs



Selection of the 5'-primer

To randomly prime, the arbitrarily selected 5'-primer should be very short such as 6 to 7 base pairs for it to anneal fairly frequently near the end of a cDNA strand (Table 9.1). Unfortunately, in experiments, primers shorter than 8 bases do not amplify well and primers with 10 bases amplify between 50 to 100 base pairs. For comparison, specific primers used in standard PCR are usually 20 or more base pairs in length.

Table 9.1. Theoretical calculation and experimental data of the number of mRNA species that could be amplified by arbitrary primers with different lengths in combination with an anchored oligo(dTs) that binds to 1/12 of mRNAs 3'termini
(From Liang et. al., 1992)

Length of arbitrary primer (bases)	Kilobases per binding site	Number of mRNAs displayed	
		<i>Theoretical</i>	<i>Experimental</i>
6	4	150	0
7	16	38	0
8	65	10	0
9	262	2	20-30
10	1049	<1	50-100

Liang et al., used a decamer, LTK3 (CTTGATTGCC), which is located 278 base pairs upstream of its poly-A tail of murine lymphocyte thymidine kinase mRNA as their arbitrary 5'-primer.

PCR parameters

For differential display, the following PCR parameters were first described by Liang. et al., (Liang 1992):

40 cycles of denaturation at 94⁰C for 30 seconds, annealing at 42⁰C for 1 minute and extension at 72⁰C for 30 seconds. This is followed by 5 minutes of elongation at 72⁰C. These parameters were subsequently optimised by Liang et al. when the annealing temperature was lowered to 40⁰C for two minutes (Liang 1993) to increase the sensitivity but at a cost of slight increased background.

The concentration of deoxynucleoside triphosphates (dNTPs) used was 2 μ M as this was found to be the ideal concentration for specific cDNA amplification and also optimal for labelling PCR-products with [³⁵S]-dATP. The reaction is carried out in the presence of 1 X PCR buffer, a pair of primers and Taq polymerase.

The Display

The process produces a series of randomly amplified radiolabelled cDNAs from which can be separated by polyacrylamide gel electrophoresis (PAGE). Inspection of the gel can identify cDNAs expressed in one cell line but not in another. cDNAs of interest can then be cut directly from the gel and eluted by boiling. cDNA of interest can then be reamplified and analysed.

Extraction of Total Cellular RNA from SL 12.3 and SL 12.4 cell lines

Method

Both SL 12.3 and SL 12.4 cells ($\sim 1 \times 10^6$ cells each) were pelleted and stored in ice for the whole procedure. 2 mls of a 4M Guanidinium Thiocyanate solution (containing 7 μ l/ml of 2-mercaptoethanol) was added to lyse and denature the cells to allow collection of total cellular RNA (nuclear and cytoplasmic RNA). 2-mercaptoethanol was used as an inhibitor to any ribonucleases present (Chomczynski 1987).

The total RNAs in the solution of cellular debris were extracted using 200 μ l of 2M sodium acetate followed by 2 mls of water saturated phenol. The total cellular RNAs will be present in the aqueous phase of the mixture while DNAs and proteins are soluble in the phenol phase. The aqueous phase was extracted twice with 400 μ l of chloroform / iso-amylalcohol solution before precipitating the RNAs using isopropanol at -20°C overnight. This

technique permits recovery of total RNAs from small quantities of tissues or cells and avoids the ultracentrifugation step of the Guanidinium - CsCl technique (Chomczynski 1987).

The purity and amount of the extracted RNAs were estimated using a spectrophotometer, based on the fact that pure RNA absorbs two times the amount of light at the wavelength of 260nm than at 280nm. Therefore a ratio of 260/280 of 2 represents pure RNA. Any contamination with proteins reduces this ratio. Furthermore, it is also known that for single stranded RNA, the absorbance of 1.0 at 260 nm corresponds to a concentration of 40µg/ml.

Results

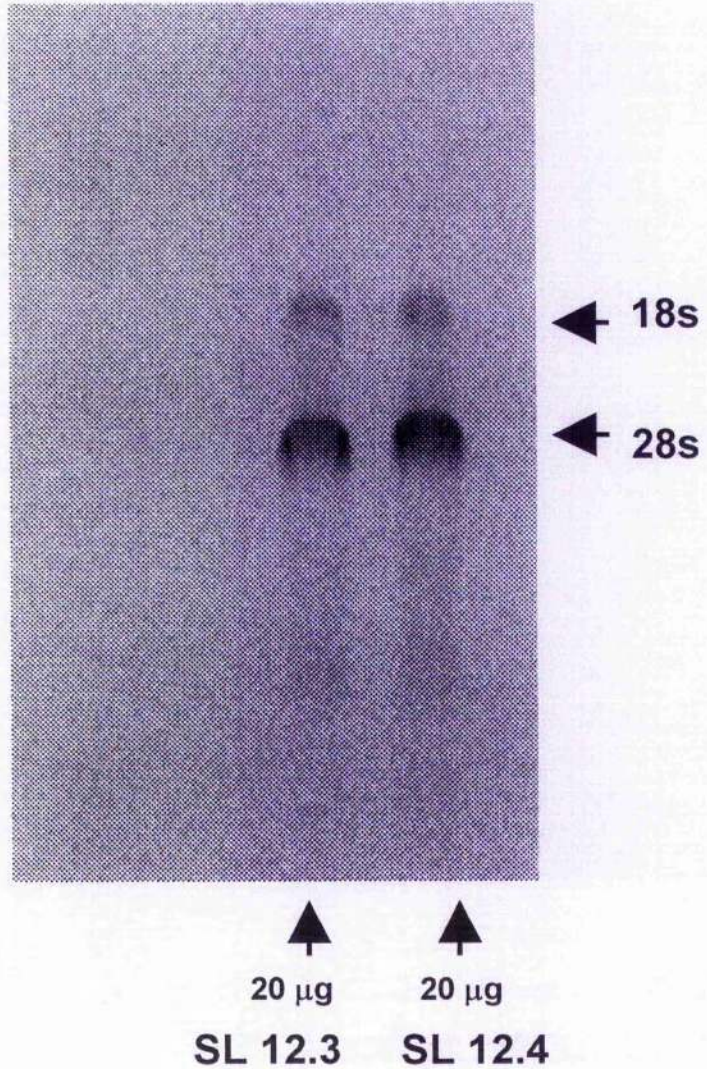
The amount and purity of total cellular RNA extracted from SL12.3 and SL12.4 cells (Table 9.2)

20 µg of total cellular RNA from SL 12.3 and SL 12.4 cell lines underwent electrophoresis in a denaturing Formamide/Formaldehyde 1 % agarose gel using 1 X MOPS (3-[N-morpholino]-propane sulphonic acid-sodium salt) as the running buffer and the results (Figure 9.3)

Table 9.2 Total Cellular RNA extracted from SL 12.3 and SL 12.4 cells

RNA	Reading	260 nm	280 nm	260/280	Concentration
12.3	1 st	0.180	0.090		
	2 nd	0.179	0.089		
	Average	0.1795	0.0895	2.0	7.18 µg/µl
12.4	1 st	0.121	0.049		
	2 nd	0.120	0.048		
	Average	0.1205	0.0485	2.5	4.82 µg/µl

Figure 9.3 Electrophoresis of total RNA of SL 12.3 and SL 12.4 cells in 1 % denaturing RNA agarose gel



Synthesis of first strand cDNA using reverse transcription

(Protocol supplied with the reverse transcription kit from Gibco BRL)

Method

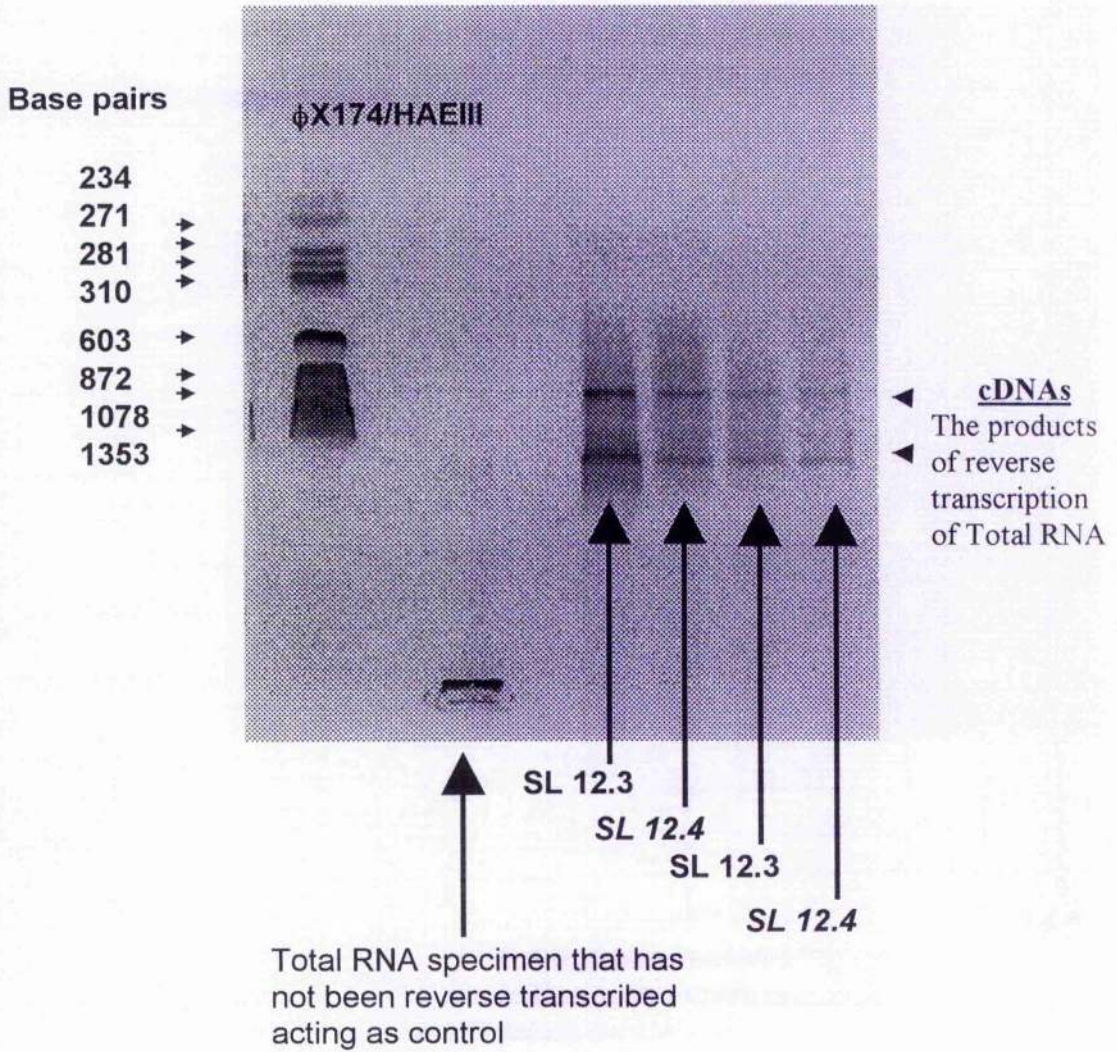
5 µg of total cellular RNA from each cell line was added to 2.0 µl of 25 µM T₁₂CA. Sterile distilled deionised water was used to bring the mixture final volume to 12.8 µls. The mixture was incubated at 70⁰C for 10 minutes and then cooled on ice immediately.

4.0 µls of 5X first strand buffer, 2.0 µls of 0.1M DTT and 0.2 µl of 2 mM dNTPs were added to the RNA solution and the mixture was spun briefly and then warmed at 37⁰C for 2 minutes. 1.0 µl (200 units) of SUPERScript REVERSE TRANSCRIPTASE (*Gibco BRL*) was then added to the solution to give a final volume of 20 µls mixture. The solution was then heated at 37⁰C for 60 minutes before terminated by heating at 94⁰C for 5 minutes.

Results

cDNA products from reverse transcription underwent electrophoresis in 1% agarose gel with 1 % TBE as running buffer. A specimen of total cellular RNA that was not reversed transcribed was also run in the agarose gel to act as negative control. This specimen should have no bands seen unless contaminated by cellular DNA (Figure 9.4)

Figure. 9.4 Electrophoresis of Reverse Transcription products of SL 12.3 and SL 12.4 cells (Total RNAs are successfully reversed transcribed to cDNAs as shown by the bands. Non reverse transcribed Total RNA acting as controls did not show any bands)



Lane 1 = 2 μ g of standard marker ϕ X174/HAEIII
 Lane 2 = 5 μ l of SL 12.4 Total RNA (Control)
 Lane 3 = 5 μ l of SL 12.3 (Set 1) cDNAs
 Lane 4 = 5 μ l of SL 12.4 (Set 1) cDNAs
 Lane 5 = 5 μ l of SL 12.3 (Set 2) cDNAs
 Lane 6 = 5 μ l of SL 12.4 (Set 2) cDNAs

Amplification and radiolabelling of cDNAs using Polymerase Chain Reaction

Method

The criteria of selecting the arbitrary 5' end primer is the same as Liang et al. However, the mRNA of CD 44 was used and a 10-mer sequence was chosen 851 base pairs upstream of EcoRI site (Figure 9.5) (Nottenburg 1989). CD44 was chosen as this adhesion molecule is found commonly in metastasising lymphoma cell lines. LTK3, the 10-mer used originally by Liang et al., was also used for comparison

Figure 9.5 mRNA of murine CD44 (Nottenburg 1989)

```
GAATTCTGCG CCCTCGGTTG GCTCCGGACG CCATGGACA AGTTTTGGTGG CACACAGCTT
GGGGACTTTG CCTCTTGCAG TTGAGCCTGG ACATCAGCA GATCGATTTG AATGTAACCT
GCCGCTACGC AGGTGTATTC CATGTGGAGA AAAATGGCCG CTACAGTATC TCCCGGACTG
GGCAGCTGA CCTCTGCCAG GCTTTCAACA GTACCTTACC CACCATGGAC CAAATGAAGT
TGGCCCTGAG CAAGGGTTTT GAAACATGCA GGTATGGGTT ATAGAAGGA AATGTGGTAA
TTCCGAGGAT TCATCCCAAC GCTATCTGTG CAGCCAACCA CACAGGAGTA TATATCCTCG
TCACGTCCAA CACCTCCCAC TATGACACAT ATTGCTTCAA TGCCTCAGCC CCTCCTGAAG
AAGACTGTAC TCAGTCACA GACCTACCCA ATTCCTTCGA TGGACCGGT ACCATAACTA
TTGTCAACCG TGATGGTACT CGCTACAGCA AGAAGGGCGA GTATAGAACA ACCAAGAAG
ACATCGATGC TTCAAACATT ATAGATGACG ATGTCAGCAG GGCTCCACC ATCGAGAAGA
GCACCCCAAG AGGCTACATT TTGCACACCT ACCTTCCTAC TGAACAGCCT ACTGGAGATC
AGGATGACTC CTTCTTTATC CGGAGCACCT TGGCCACCAG AGATCGAGAC
TCATCCAAGG ACTCCAGGGG GAGTTCCTGC ACTGTGACTC ATGGATCCGA ATTAGCTGGA
CACTCAAGTG CGAACCAGGA CAGTGGAGTG ACCACAACCT CTGGTCCTAT
AGGAGACCTCAGATTCCAG AATGGCTCAT 851CATCTTGGCA TCTCTCCTGG
CACTGGCTCT GATCTTGCC GTCTGCATCG CGGTCAATAG TAGGAGAAGG TGTGGGCAGA
AGAAAAAGCT GTGATCAAC GGTGGCAATG GGACAGTGGG AGACAGGAAA
CCCAGTGAGC TCAACGGGGAGCCAGCAAG TCTCAGGAAA TGGTGCATTT GGTGAACAAG
```

GAACCATCAG AGACCCCAGA CAGTGTATG ACAGCTGACG AGACCCGGAA TCTGCAGAGT
GTGGACATGA AGATTGGGGT GTAGTGCCTA CGCCATTAAC TTGAAAAGAC
AGCACGATTG GAAACGTCAT TGAATTC

Sterile distilled deionised water was added to 2 μ ls of the cDNA specimen to give a final volume of 12.9 μ ls. The cDNA solution was denatured by heating to 94°C.

A mixture of 2.0 μ ls 10 X PCR buffer (1 X PCR), 0.2 μ l 200 μ M dNTPs (2 μ M), 2.0 μ ls 25 μ M T₁₂CA (2.5 μ M), 0.4 μ l 25 μ M CD44 or LTK₃ (0.5 μ M), 1.0 μ l (5U/ μ l) Taq Polymerase and 1.5 μ ls [³⁵S]dATP α S (~0.5 μ M) was added to the cDNA solution. The mixture was covered with 30 μ ls of mineral oil before being subjected to the polymerase chain reaction parameters as follow: Template denaturation at 94°C for 30 seconds followed by 40 cycles of 94°C for 30 seconds, 40°C for 2 minutes and 72°C for 30 seconds. This was followed by an elongation period of 72°C for 5 minutes (Liang 1993). In experiments where a test gel was run without [³⁵S]dATP α S, its volume was replaced by 1.5 μ ls distilled water.

Results

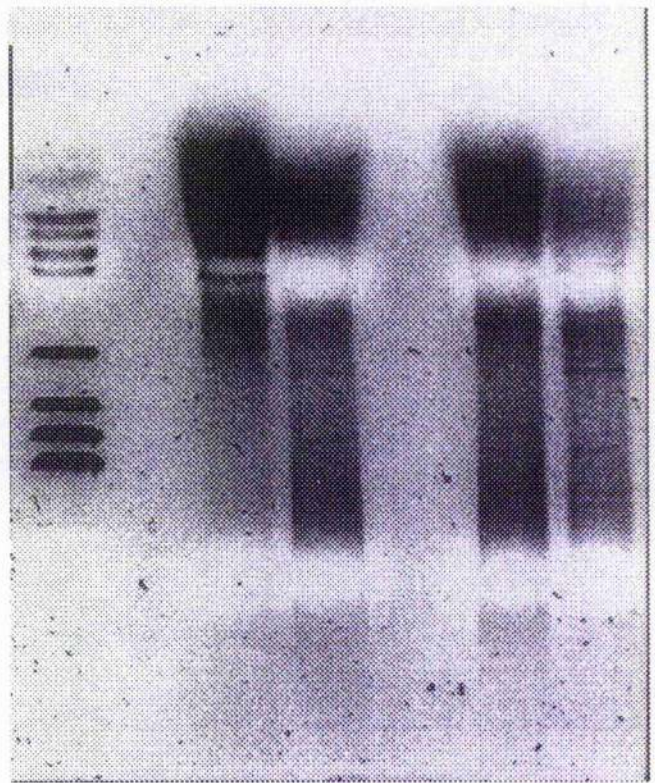
The products of PCR used for the test gel which did not use [³⁵S]dATP α S underwent electrophoresis in a 1 % agarose gel stained with Ethidium Bromide (Figure 9.6). It was found that the random 5'-primer based on the oligonucleotide CD 44 primed more efficiently than LTK3 (Figure 9.6). As a result, all subsequent PCRs with [³⁵S]dATP α S used CD 44 as the random

5'-primer and their products underwent electrophoresis in a DNA denaturing polyacrylamide sequencing gel as shown as an autoradiogram in Figure 9.7.

Figure 9.6 PCR products of SL 12.3 and SL 12.4 without [³⁵S]dATP α S using either CD44 or LTK3 primers

Base pairs

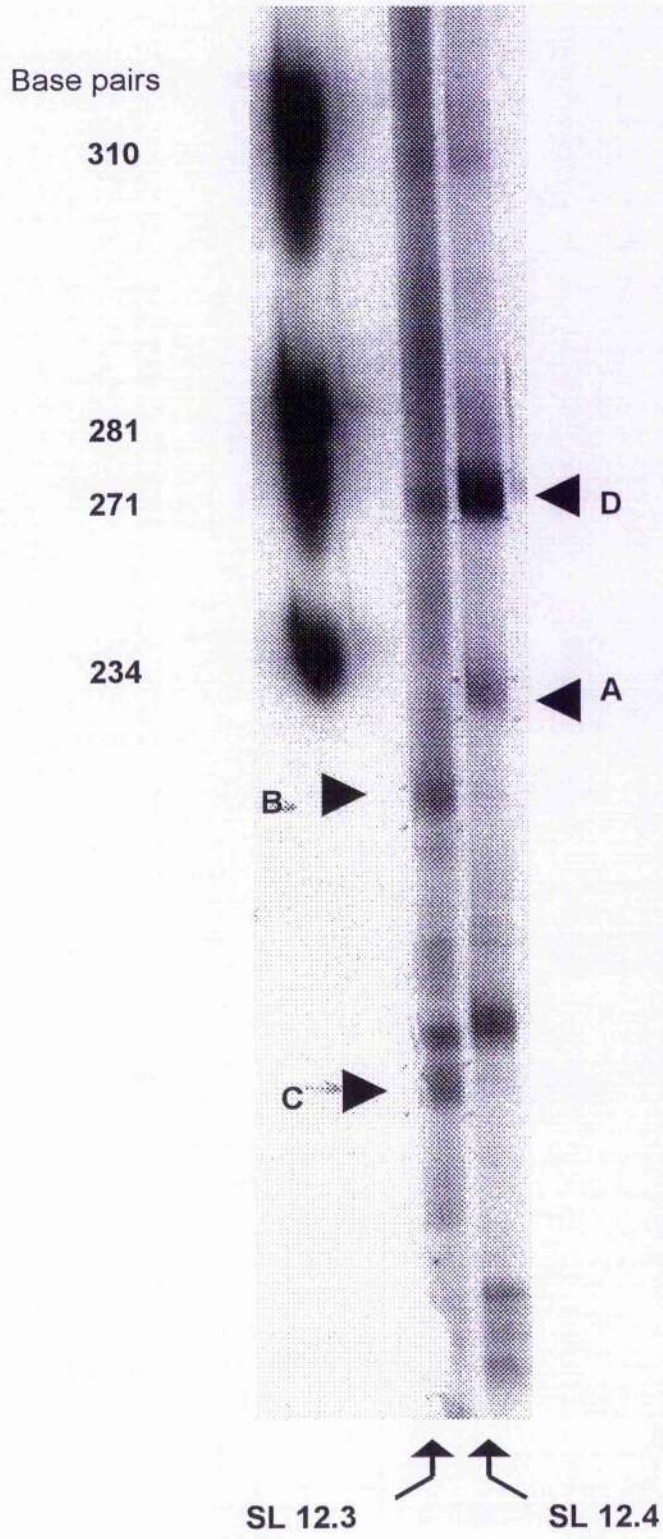
234 →
 271 →
 281 →
 310 →
 603 →
 872 →
 1078 →
 1353 →



SL12.3 SL12.4 SL12.3 SL12.4
 (CD44) (CD44) (LTK3) (LTK3)

- | | |
|----------|--|
| Lane 1 = | 500 ng of standard marker ϕ X174/HAEIII |
| Lane 2 = | 10 μ l SL 12.3 PCR products + 2 μ l 6X marker mixture (CD44) |
| Lane 3 = | 10 μ l SL 12.4 PCR products + 2 μ l 6X marker mixture (CD44) |
| Lane 4 = | 10 μ l SL 12.3 PCR products + 2 μ l 6X marker mixture (Ltk3) |
| Lane 5 = | 10 μ l SL 12.3 PCR products + 2 μ l 6X marker mixture (Ltk3) |

Figure 9.7 Autoradiogram showing the cDNA ladders of SL 12.3 & SL 12.4 cells using CD44



Four bands of cDNAs of interest were identified (Figure 9.7):

- Band A : Expressed exclusively in SL 12.4
- Band B : Expressed exclusively in SL 12.3
- Band C : Expressed exclusively in SL 12.3
- Band D : Expressed more in SL 12.4

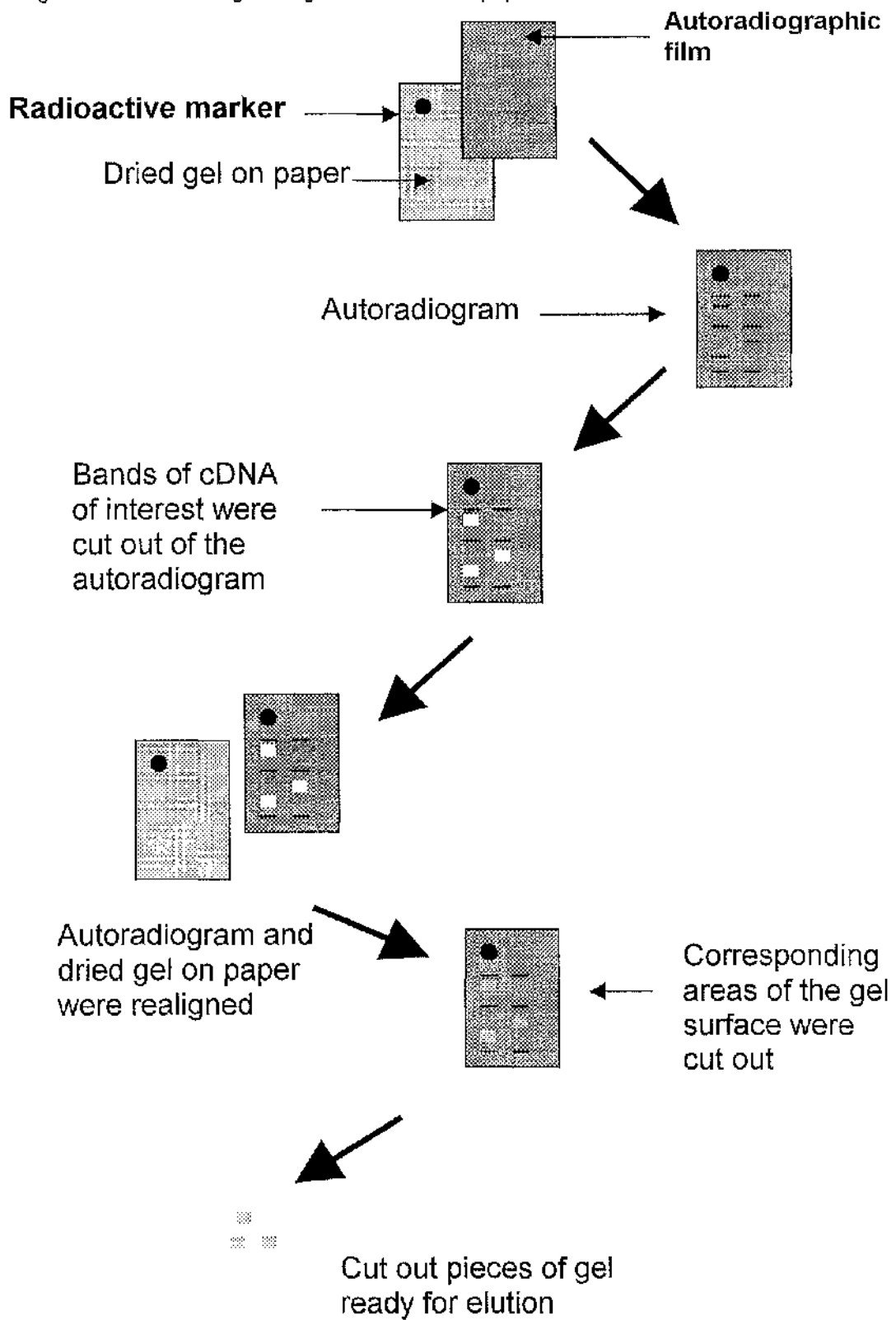
Elution of cDNAs of interest from dried polyacrylamide gel

Method

The gel containing cDNA band A, B, C and D was vacuumed dried onto 3MM paper. The dried gel on paper was covered with cling film and had one corner marked with radioactive ink for orientation before being exposed to autoradiographic film.

Having developed the autoradiogram, the cDNA of interest seen on the autoradiogram were cut out. The autoradiogram was then realigned with the dried gel on paper using the radioactive ink markings (Figure 9.8). The corresponding areas of the dried gel on paper were then cut out with a sharp scalpel and the piece of gel rehydrated by immersing in sterile TE buffer. The cDNAs in the gel were eluted out by incubating the mixture at 65°C for two hours. All tubes were then centrifuged at 13000 RPM for twenty minutes and 5 µls of the supernatant was used for reamplification.

Figure 9.8 Cutting dried gel out from 3 MM paper



Chapter 10 Characterisation of cDNAs of interest

Introduction

The isolated cDNAs have to be characterised before subjected to further analysis. Their sequence can then be compared to available cDNAs databases to identify previously characterised sequences.

To allow sequencing of cDNAs of interest, a reasonable amount of the cDNAs has to be available. The amount of cDNAs eluted from the dried gel is insufficient but one way of increasing the amount is to insert the cDNA into a vector such as a plasmid then allowing bacteria to replicate the vector.

TA Cloning

Introduction

TA cloning takes advantage of the nontemplate-dependent activity of thermostable polymerases in PCR which add a single deoxyadenosine (A) nucleotide at the 3'-end of duplex molecules of the PCR product. This 3' end A-overhangs is used to insert the PCR product into a vector which contains a single deoxythymidine (T) nucleotide at the insertion site (Figure 10.1)

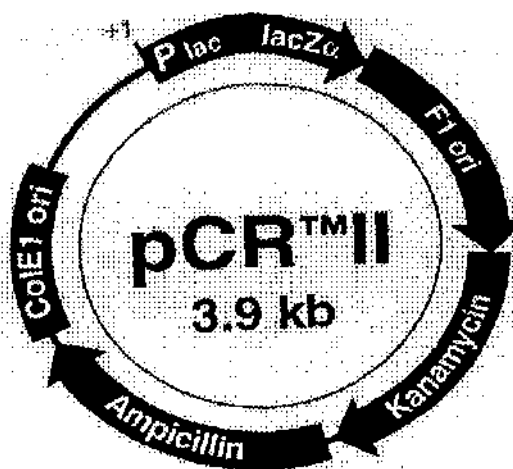
Figure 10.1 Insertion of PCR product into the vector using the overhang 3'-A tail (Insert) and the single 5'-T' nucleotide (vector)



Copied from Invitrogen Catalogue 1994

The vector used in this study, the plasmid pCR II (*Invitrogen*), has certain genes inserted into it as shown in Figure 10.2

Figure 10.2 pCRII vector with the different genes inserted into it.



Feature	Function
<i>lac</i> promoter	For bacteria expression of the <i>lacZα</i> fragment for α -complementation (blue-white screening)
the <i>lacZα</i> fragment	Encodes the first 146 amino acids of β -galactosidase. Complementation in <i>trans</i> with the Ω fragment gives active β -galactosidase for blue-white screening
Kanamycin and Ampicillin Resistance gene	Selection and maintenance in E.Coli, especially useful when cloning products amplified from penicillin resistant plasmids.

Copied from Invitrogen Catalogue 1994

This vector is designed to have a *lacZα* fragment, a gene for β-galactosidase expression. The insertion site is within this fragment so that a vector with no insert will have an uninterrupted *lacZα* fragment and thus, will be able to express β-galactosidase. If the agar medium that the colonies are grown on contains galactose, then the bacteria will be able to metabolise galactose forming blue colonies.

On the other hand, bacteria which has a vector with an insert will have an interrupted *lacZα* gene fragment. These bacteria cannot express β-galactosidase and hence, will be unable to metabolise galactose, forming white colonies.

As these vectors also carry amoxycillin and kanamycin resistant genes, they allow their host bacteria to grow in agar impregnated with antibiotics. This helps to eliminate growth of bacteria which does not contain the vector.

Method

The amount of PCR products required could be calculated using the formula provided by *Invitrogen* as below:

$$\begin{aligned}
 X \text{ ng PCR product} &= \frac{(Y \text{ base pair PCR product}) \times (50 \text{ ng pCRII vector})}{(\text{pCRII vector size in base pair})} \\
 &= Y \text{ base pair PCR product} \times (50/3900)
 \end{aligned}$$

(X ng is the amount of PCR product of Y base pairs to be ligated)

Three times X ng is used to give a 1:3 vector: PCR product ratio as recommended by *Invitrogen*. The PCR product that was about 500 base pair was added to a mixture of 1 μ l of 10 X Ligation Buffer, 2 μ l pCR II vector and 1 μ l of T4 DNA ligase. Sterile water was added to give a final volume of 10 μ l. All reagents were supplied in the TA cloning kit (*Invitrogen*). This ligation mixture was incubated at 14 - 15^oC overnight.

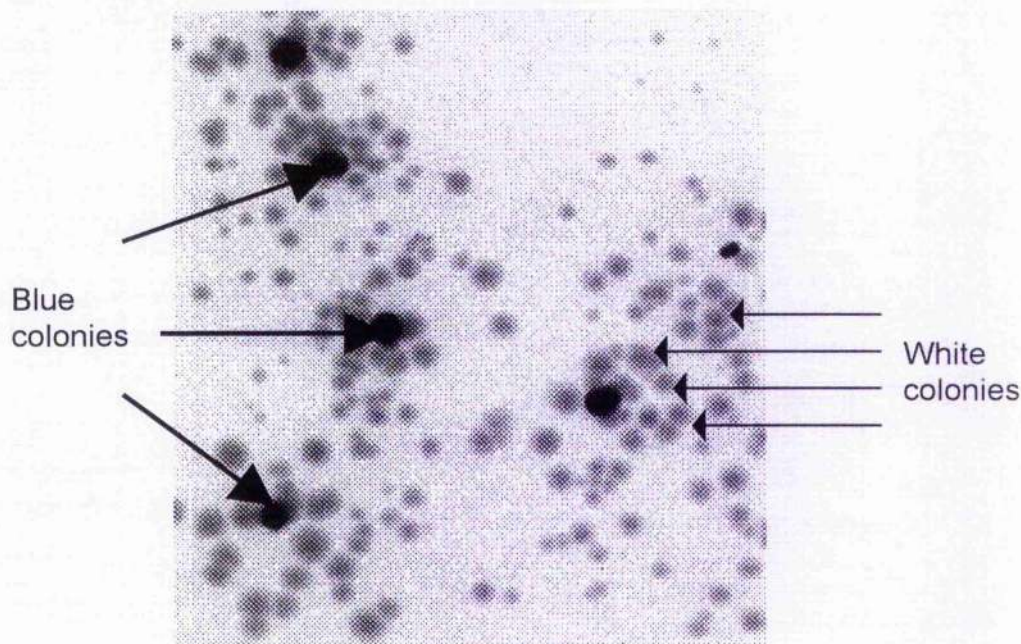
The supplied competent cells were added to 2 μ l of 0.5 M β -mercaptoethanol. 1 μ l of the ligation mixture was then added to the competent cells. The mixture was incubated in ice for 30 minutes, at 42^oC for 30 seconds and eventually back in ice for another 2 minutes. 450 μ l of prewarmed provided medium was added to this mixture. The cells were incubated at 37^oC for 1 hour with constant shaking at 225 RPM.

These cells were spread on an agar plate that contains amoxycillin and X-gal (galactose).

Results

Blue and white colonies were grown up as shown in figure 10.3. Blue colonies are bacteria with empty vectors (no insert), thus, able to metabolise galactose and turn blue. The white colonies, on the other hand, are bacteria with insert in vectors, thus, unable to metabolise galactose and turn white.

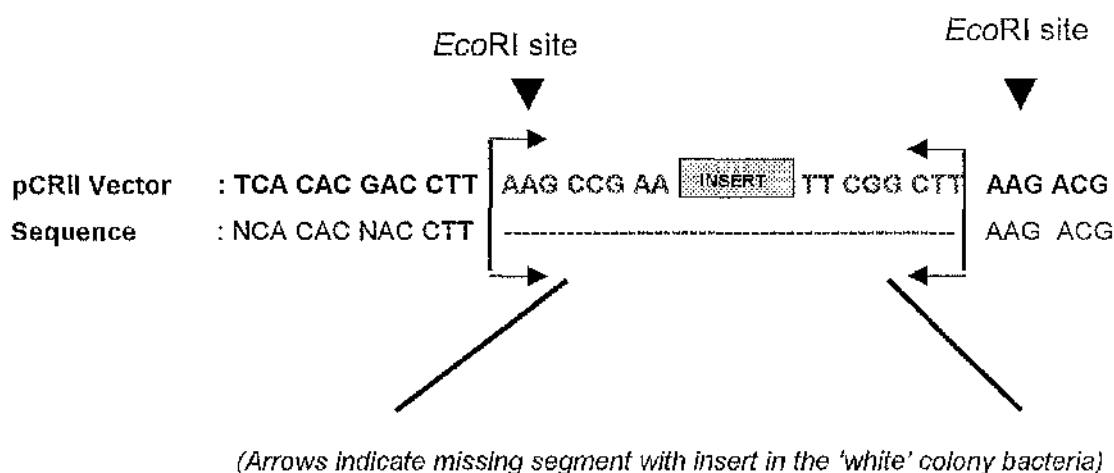
Figure 10.3 Agar plate showing white and blue colonies in TA cloning



A single white colony was transferred to 2 mls of LB medium and the mixture was incubated overnight at 37°C with constant shaking. 1.5 mls of this mixture was subjected to mini-prep to extract the vector from the bacteria. The 1.5 mls of bacteria mixture was pelleted and the medium aspirated. The pellet was resuspended in 100 µl of Glucose solution (50mM Glucose; 25 mM Tris-HCL at pH 8 & 10 mM EDTA at pH 8.0) and 200µl of sodium hydroxide solution (0.2 N NaOH & 1 % SDS). The solution was stored in ice for 5 minutes before mixing with 150 µl of potassium acetate solution (5 M potassium acetate & Glacial acetic acid). Having incubated in ice for 5 minutes, the solution was centrifuged and the supernatant added to equal volume of phenol chloroform solution. The mixture was centrifuged and the plasmid precipitated using 2 volumes of ethanol.

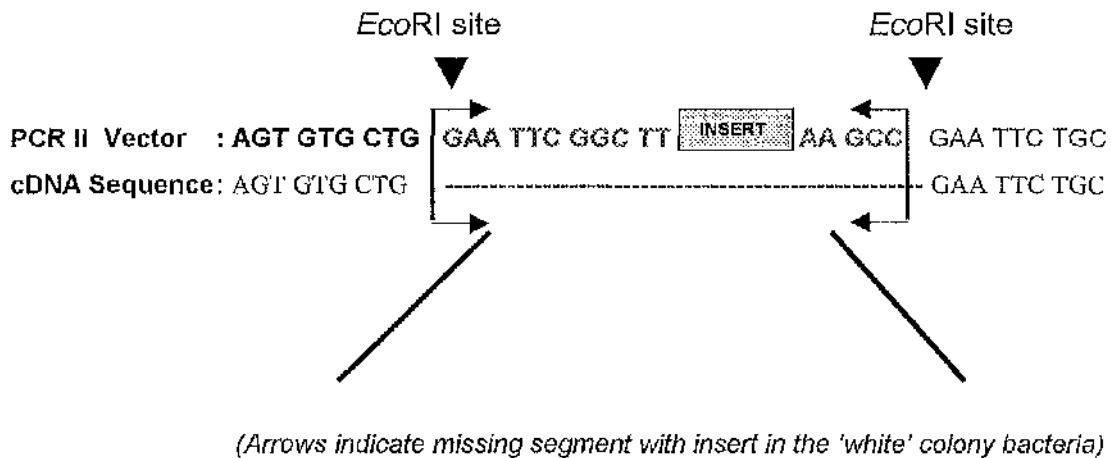
The extracted plasmid was sent to Dr. Fox, *Alta Bioscience*, Birmingham, UK for sequencing. The result of the sequence using M13 Forward Primer is as shown in Figure 10.4. No result for the sequence was available using the M13 Reverse Primer.

Figure 10.4 First specimen: Comparing sequence of vector PCR II (& insert) and sequence obtained



The whole procedure was repeated using a second white bacteria colony. The result of the sequence using M13 Reverse Primer is as shown in Figure 10.5. No result for the sequence was available using the T7 Promoter Forward Primer.

Figure 10.5 Second specimen: Comparing sequence of vector PCR II (& insert) and sequence obtained



Both specimens showed that the 'white' bacteria colonies sampled revealed false positives with blunt self-ligation of the nucleotides of the vectors. This self-ligation was unable to complete the *lacZα* gene fragment, thus, unable to express β -galactosidase and metabolise galactose ('white' colonies).

Furthermore, the inserted PCR product is flanked on each side by *EcoRI* sites. Therefore, treating any vectors with an insert with restriction enzyme *EcoRI* should reveal two distinct bands (insert + plasmid) on Agarose gel. Unfortunately, all 'white' colonies sampled did not reveal any insert. It is not surprising as the self-ligation happened to be around the *EcoRI* restriction site G AATTC as shown in Figure 10.4 and 10.5. Such high false positives were confirmed using another similar kit from Invitrogen and therefore, no further attempts to use TA cloning for this study.

Reamplification and direct sequencing

Introduction

Liang et al., used a pair short primers, a 10-mer and 13-mers in their differential display PCR. Unfortunately, these primers are too small to be successfully used as sequencing primers for the amplified-DNA using classical procedures. Therefore, to identify an amplified-cDNA, one has to insert in a vector prior to sequencing analysis, which could be time-consuming and labour intensive. One such technique, TA cloning, has been tried and described above.

Wenck et al., (Wenck 1995) described a simplified method using extended primers for the reamplification of the isolated cDNA bands from a differential display sequencing gel. These reamplified cDNAs and the extended primers are also suitable for direct sequence analysis.

Method

Wenck et. al., extended their 5'-decamer by adding an extra nine bases (GCGAATTCC) at its 5' end to become a 19-mer. An extra of 8 bases (CGGATCCC) was also added to the 5' end of the 3'-anchored primer to become a 22-mer.

The primers used in this reamplification were also extended similarly. The 5'-random decamer of CD 44 and the 3'-anchoring primer are extended as below :

CATCTTGGCA (5'-random decamer)



3'-CATCTTGGCA- CCTTAAGCG -5'

5'-TTTTTTTTTTTTTCA-3' (3'-anchoring primer)



5'- CGGATCCC TTTTTTTTTTTTTCA-3'.

Sterile distilled deionised water was added to 5 µls of the eluted cDNA specimen to give a final volume of 32.0 µls. The cDNA solution was denatured by heating to 94°C.

A mixture of 5.0 µls 10 X PCR buffer, 2.0 µls 200 µM dNTPs, 5.0 µls 25µM 22-mer, 1.0 µl 25 µM 19-mer, 5.0 µl (5U/µl) Taq Polymerase were added to the cDNA solution. The mixture is then covered with 50 µls of mineral oil before subjected to polymerase chain reaction for 40 cycles with

template denaturation temperature of 94⁰C for 30 seconds followed by the following parameters: 40 cycles of 94⁰C for 30 seconds, 40⁰C for 2 minutes and 72⁰C for 30 seconds. This is followed by an elongation period of 72⁰C for 5 minutes.

Purification of reamplified cDNAs

Method

Before the reamplified cDNA could be sequenced and further analysed, it requires to be purified from contaminant such as oligonucleotides and dNTPs.

The reamplified cDNAs for this study were purified using the *Promega* Magic™ PCR Preps DNA purification kit. 30 µls of the reamplified cDNA was added to the appropriate volume of the Direct purification buffer and resins following the protocol from the *Promega* kit. The cDNA would stick onto the resins and other contaminants such as dNTPs and oligonucleotides are then washed away with 80 % isopropanolol. The attached purified cDNA can then be eluted out with TE buffer and used for direct sequencing.

Sequencing of cDNAs

Unfortunately cDNA *B* was lost during its purification. Therefore, only cDNAs *A*, *C* and *D* were available for sequencing. Sequencing was performed by Dr. Fox, *Alta Bioscience*, Birmingham, UK. All cDNAs were

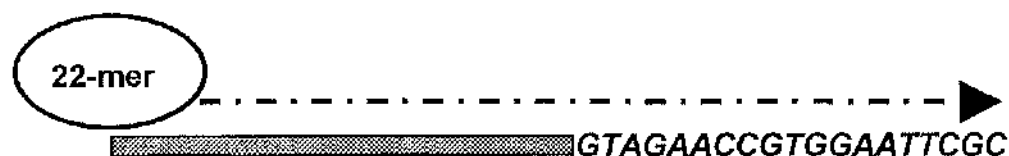
sequenced both up and downstream with the 22-mer and 19-mer primers. Sequencing using the 19-mer primer should end with a product flanked by a complementary oligonucleotide sequence of the 22-mer primer that was originally used: 3'-TGAAAAAAAAAAAAAGGGATCCG-5' (Figure 10.6).

Figure 10.6 Sequencing with 19-mers (5'-end primer)



Sequencing using the 22-mer primer should end with a product flanked by a complementary oligonucleotide sequence of the 19-mer primer that was originally used : GTAGAACCGTGGAATTCGC (Figure 10.7)

Figure 10.7 Sequencing with 22-mer (3'-end primer)



The results of sequencing of cDNAs A, C and D are shown in figures 10.8 to 10.13.

Figure 10.8 Sequence of cDNA A using 22-mers as the primer

10	20	30	40
ANGTGGAAAA	TTAAAATCAT	TCGAAAAGGT	TTAGACTGTC
50	60	70	80
AAGGGTATGT	AATGTTTGTG	ATCATAACTG	GCGAAAATAT
90	100	110	120
ATCTTCTAAT	AGATGGTCAC	CAATGGAAAC	AAGACACTGG
130	140	150	160
TTTGTAGAAG	AATAGAAATC	<u>ACAGTAGAAC CGTGGAATTC</u>	

CA

Figure 10.9 Sequence of cDNA A using 19-mers as the primer

10	20	30	40
CNGGNTTCGN	NACNTNTNTT	TTTCGTTGGT	GACCGTCTAT
50	60	70	80
GTAGAAGATA	GNTTTGGGTC	AGTTATGTAT	CGTGANCATT
90	100	110	120
ACTNGCCCTT	GACTGTCTAC	NCCTTNCGN	TNGATTTTNN
130	140	150	160
TTTNTANNA	TGTGAGAGTT	AAAATCTTTC	ATCCT <u>TGAANA</u>
170			
<u>AAAANGNNGG GATCCG</u>			

Figure 10.10 Sequence of cDNA C using 22-mers as the primer

10	20	30	40
TGGCCCTNNC	GTGGAATCCG	CACTTCCCAT	GATCGTNCAA
50	60	70	80
TTATNACAAT	CGTNATTTGA	TNGTGTNTGT	TGTANNCTTT
90	100	110	120
CACATNACNC	TTGAGAGAAC	GATTTATTCA	GTTTGTCAAG
130	140	150	
GGAAGTAGTA	TGNC <u>GNAAAA</u>	<u>CCGNGGAANT</u>	<u>CNC</u>

Figure 10.11 Sequence of cDNA C using 19-mers as the primer

10	20	30	40
TTNNNANGGC	CATTACNCNG	GGACNGCCGA	ACAAATGNAT
50	60	70	80
CTCNCATTTG	TNA'INTNAAN	NTTNACNNCT	TACTCGAACA
90	100	110	120
NNTNCAATNG	TNNTATNGAN	CCAATCAANG	GGAAGTATT
130	140	150	160
GTCACTGTGA	TTCCTGCC <u>NG</u>	<u>AAAAAAAAANNA</u>	<u>AGGGGANCCG</u>

Figure 10.12 Sequence of cDNA *D* using 22-mers as the primer

10	20	30	40
GNTCTNNCGT	GGATNNGNAN	TTTAAAATAT	GTATTCATT
50	60	70	80
TTCATAAATT	ACATGAGATT	ATATCACAAA	CTATAATAGA
90	100	110	120
AAATTAACAG	ATGACAGTAG	ACTTTAAATA	GAATTGTTGG
130	140	150	160
AAAATCTAAT	ACTCTTCAGA	AAAGATATAT	CACCCAGACT
170	180	190	
TTAACAAAAA	TATCCTCT <u>GT</u>	<u>AGAACCGTGG</u>	<u>AATTCGC</u>

Figure 10.13 Sequence of cDNA *D* using 19-mers as the primer

10	20	30	40
GCNNGNCATT	NTGNNGGNNN	GGGGTGATAT	ATCTTTTCTG
50	60	70	80
AAGAGTATTA	GATTTCCAN	CAATTCTATT	TAAAGTCTAC
90	100	110	120
TGTCATCTGT	TAATTTNCTA	TTATANTTTG	TGATATAATC
130	140	150	160
TCGTGTAATC	TATGANANAT	GAATACATAA	TTANATGTA
170	180	190	200
TATTTAATA	AAGATTNTG	<u>TGNNAAAAAN</u>	<u>ANNGGGACC</u>

CG

Chapter 11 Comparison sequences obtained with Genbank and Embank data

Searching through the Genbank (Genetic sequence database of nucleic acids) and Embl (European Molecular Biology Laboratory) (Pearson 1988), the following results have been obtained.

Band A : Exclusively expressed in SL 12.4

Using the 22-mer primer, the sequence of band A has the following homologies as shown in table 11.1:

Table 11.1 Homologies of Band A ~ 162 nucleotides (nt) (using 22-mer primer)

Databank entries	Nucleic acid	% Identity	Nt overlap
EM:BBPROMB M28681 GB:BORPROMB M28681	B.burgdorferi promoter region DNA (203 nt)	61.5	135 (20-155)
EM:CEUC18B10 U80024 GB:CELC18B10 U80024	Caenorhabditis elegans cosmid C18B (21185 nt)	59.8	132 (14910-15042)
EM:CEF59A1 Z81557 GB:CEF59A1 Z81557	Caenorhabditis elegans cosmid F59A1 (45300 nt)	64.8	88 (13430-13518)
GB:HSN114B2 Z73416 EM:HSN114B2 Z73416	Human DNA sequence from cosmid N114B2 (40523 nt)	66.7	84 (35730-35814)
GB:SCYJL109C Z49384 EM:SCYJL109C Z49384	S.cerevisiae chromosome X reading (6127 nt)	66.7	81 (2300-2381)
EM:HS597370 W74597 zd77h12.s1	Soares fetal heart NbHH1 (659 nt)	67.6	74 (70-144)
GB:W74597 W74597 zd77h12.s1	Soares fetal heart NbHH19W (659 nt)	67.6	74 (70-144)

Using the 19-mer primer, the sequence of band A has the following homologies as shown in table 11.2:

Table 11.2 Homologies of Band A ~ 176 nucleotides (nt) (using 19-mer primer)

Databank entries	Nucleic acid	% Identity	Nt overlap
GB:AA020100 AA020100 mh49d03.r1 EM:MMAA20759 AA020100 mh49d03.r1	Soares mouse placenta (265 nt)	75.3	150 (40-190)
EM:XMI17896 U17896 GB:XMU17896 U17896	Xiphophorus maculatus ERCC2/XPD gene (16840 nt)	55.9	145 (13740-13885)
GB:CELF28F9 U70850 EM:CEUF28F9 U70850	Caenorhabditis elegans cosmid F28F9 (31967 nt)	54.7	128 (12980-13108)
GB:CMU68290 U68290 EM:CMU68290 U68290	Chelonia mydas clone CM45 (618 nt) anonymous nuclear DNA sequence	58.3	127 (420-547)
M:RNTFPI D10926 GB:RATTFPI D10926	Rat mRNA for tissue factor in pathway inhibitor (1226 nt)	66.7	117 (1070-1187)
EM:MMGS00900 D19510 GB:MUSGS00900 D19510	Monse 3'-directed cDNA, MUSGS00900 (92 nt)	74.4	90 (2-90)
EM:PFHSP L02822 GB:PFAHSP L02822	Plasmodium falciparum heat-shock protein (2290 nt)	56.8	88 (370-458)
GB:NVU29474 U29474 GB:NVU29474 U29474	Nasonia vitripennis NATE P16 LTR (1071 nt)	63.4	82 (710-792)
EM:CEF23B2 Z82266 GB:CEF23B2 Z82266	Caenorhabditis elegans cosmid F23B2 (43589 nt)	58.9	73 (9380-9453)
GB:AXCELSYN X54676 EM:AXCELSYN X54676	A. Xylinum gene for cellulose biopsy (10094 nt)	66.2	71 (9970-10041)
EM:HYTYRKO6 M64611 GB:HYDTYRKINA M64611	Hydra vulgaris tyrosine kinase mRNA (1186 nt)	66.7	63 (100-163)
GB:CELF33G12 U41278 EM:CEF33G12 U41278	Caenorhabditis elegans cosmid F33G12 (31261nt)	63.8	58 (21890-21948)
EM:HSU47924 U47924 GB:HSU47924 U47924	Human chromosome 12p13 (79787 nt)	66.7	51 (74800-74851)

Band C : Exclusively expressed in SL 12.3

Using the 22-mer primer, the sequence of band C has the following homologies as shown in table 11.3:

Table 11.3 Homologies of Band C ~ 153 nucleotides (nt) (using 22-mer primer)

Databank entries	Nucleic acid	% Identity	Nt overlap
GB:SCYNL319W Z71595 EM:SCYNL319W Z71595 EM:SCYNL317W Z71593 GB:SCYNL317W Z71593	<i>S.cerevisiae</i> chromosome XIV reading frame ORF YNL319w (2064 nt)	57.4	115 (1880-1995)
EM:MM8CP2E14 X91151	<i>M.musculus</i> scp2 gene exon 14 (4825 nt)	55.7	115 (440-555)
GB:SCRPD3COS Z46259 EM:SCRPD3COS Z46259	<i>S.cerevisiae</i> FY1676 RPD3 gene (40050 nt)	57.4	115 (21730-21845)
EM:SC9346 Z48784 GB:SC9346 Z48784	<i>S.cerevisiae</i> chromosome IV cosmid 934 (19236 nt)	54.7	106 (19040-19146)
GB:W94205 W94205 zd30g09.r1 EM:HISW2053 W94205 zd30g09.r1	Soares fetal heart NbHH19 (461 nt)	58.6	99 (310-409)
EM:FH10292 U10292 GB:FH10292 U10292	<i>Fasciola hepatica</i> clone Fas 3-4 tran (439 nt)	58.5	82 (300-382)
EM:RNTCBC2 M63794	Rat T-cell receptor beta-chain complex (3203 nt)	65.5	55 (2260-2315)
GB:CCGHG X51969 EM:CCGHG X51969	<i>Cyprinus carpio</i> growth hormone gene (2838 nt)	63.6	77 (440-517)
EM:CPGCR L13196	<i>Cavia porcellus</i> glucocorticoid receptor (2316 nt)	61.0	77 (610-687)
EM:MMDP1 X72310	<i>M.musculus</i> mRNA for DRTF- polypeptide 1 (DP-1) (1700 nt)	60.5	76 (870-946)
EM:CEC08E8 Z81464 GB:CEC08E8 Z81464	<i>Caenorhabditis elegans</i> cosmid CO8E8 (7977 nt)	61.4	70 (84920-84990)

Using the 19-mer primer, the sequence of band C has the following homologies as shown in table 11.4:

Table 11.4 Homologies of Band C ~ 160 nucleotides (nt) (using 19-mer primer)

Databank entries	Nucleic acid	% Identity	Nt overlap
EM:SJPARA D28811 GB:SCMPARA D28811	Schistosoma japonicum mRNA for paramyosin (3514 nt)	52.7	129 (3320-3449)
EM:SJ11825 U11825 GB:SJU11825 U11825	Schistosoma japonicum structural mus (4022 nt)	53.5	127 (3360-3487)
GB:PVGLND5 X61293 EM:PVGLND5 X61293	P.vulgaris gln-delta gene for plastid-located glutamine synthetase (4695 nt)	53.2	124 (2310-2434)
EM:HS345XF1 Z51487 GB:HS345XF1 Z51487	H.sapiens (D12S1701) DNA segment containing (CA) repeat (373 nt)	53.0	115 (230-345)
GB:R51024 R51024 yg71b08.s1 EM:HS024119 R51024 yg71b08.s1	Homo sapiens cDNA clone 38646 3' (456 nt)	55.0	109 (160-269)
GB:CEF44D12 Z68298 EM:CEF44D12 Z68298	Caenorhabditis elegans cosmid F44D1 (31853 nt)	53.3	107 (24180-24287)
GB:CET19E10 Z46795 EM:CET19E10 Z46795	Caenorhabditis elegans cosmid T19E1 (19463 nt)	56.9	102 (14740-14842)
EM:RNCYPLA M14972	Rat cytochrome P-450-LA- omega (2462 nt)	53.9	102 (1980-2082)
EM:MMU70033 U70033	Mus musculus sodium calcium exchange (3180 nt)	60.7	61 (3060-3121)
GB:HSA1280 Z83307 EM:HSA1280 Z83307	Human DNA sequence from cosmid A1280 (22253 nt)	65.4	52 (10900-10952)
GB:AA048008 AA048008 mj26h10.r1 EM:MMAA48008 AA048008 mj26h10.r1	Soares monse embryo Nb (915 nt)	70.8	48 (560-608)

Band D: Expressed more in SL 12.4

Using the 22-mer primer, the sequence of band D has the following homologies as shown in table 11.5:

Table 11.5 Homologies of Band D ~ 197 nucleotides (nt) (using 22-mer primer)

Databank entries	Nucleic acid	% Identity	Nt overlap
GB:HSU78045 U78045 EM:HSU78045 U78045	Human collagenase and stromelysin g (79788 nt)	54.8	188 (42810-42998)
GB:AMFGENOM L06178 EM:MIAMMPGEN L06178	Apis mellifera mitochondrial genome (16343 nt)	59.4	180 (16010 - 16198)
EM:TTMIHILIN M87306 GB:TETMIHILIN M87306	Tetrahymena thermophila micronuclear linker histone polyprotein (3000 nt)	61.0	177 (660-837)
EM:BTCRYIIIA L03393 GB:BACCRYIIIA L03393	Bacillus thuringiensis insecticida (1692 nt)	62.4	170 (550-720)
EM:SDOXIIRF1 X95973 GB:SDOXIIRF1 X95973	S.douglasii mitochondrial OXII & R (2945 nt)	62.3	167 (100-267)
GB:TRBKPGEN M94286 EM:KTKPGEN M94286	Trypanosoma brucei brucei kinetoplast maxicircle genes (23016 nt)	59.1	164 (19610-19774)
EM:CEF59G1 U53332 GB:CEL59G1 U53332	Caenorhabditis elegans cosmid F59G1 (25642 nt)	60.7	163 (19240-19403)
EM:HVPFR1 X96551 GB:HVPFR1 X96551	H.vulgare Per1 gene (1994 nt)	62.7	158 (140-298)
EM:STSTHA M29041 GB:POTSTHA M29041	S.tuberosum pathogenesis-related protein (2896 nt)	58.6	152 (2580-2732)
EM:HSAC76 AC000076 00075; EM:HSAC76 AC000076 00075;	HTGS phase 3, complete sequence (41098 nt)	61.1	149 (17740-17889)
GB:MISCTRNA X06047 EM:MISCTRNA X06047	Yeast mitochondrial tRNA (1847 nt)	62.8	148 (540-688)
GB:BBU62901 U62901 EM:BBU62901 U62901	Borrelia burgdorferi thdF gene (4239 nt)	61.3	142 (430-593)
EM:CEF58G1 Z81556 GB:CEF58G1 Z81556	Caenorhabditis elegans cosmid F58G1 (42328 nt)	58.2	141 (27910-28051)

GB:CET05D4 Z81115 EM:CET05D4 Z81115	Caenorhabditis elegans cosmid (37039 nt)	58.2	141 (27910-28051)
EM:PML1PM62X M97517	Deer mouse (L1Pm62) (1825 nt)	61.2	139 (260399)
GB:CYLCPRECSL M59080 EM:CHCSRBCS M59080	Cylindrotheca sp. ribulose-1,5-bi (2517 nt)	62.7	134 (210-344)
EM:CFC25F6 U39742 GB:CELC25F6 U39742	Caenorhabditis elegans cosmid C25F6 (43803 nt)	62.6	131 (19690-19821)
GB:CET05D4 Z81115 EM:CET05D4 Z81115	Caenorhabditis elegans cosmid T05D4 (32612 nt)	66.4	128 (11890-12018)
EM:PFCOMPRA X95275 GB:PFCOMPRA X95275	P.falciparum complete gene map (15421 nt)	60.2	128 (13780-13908)
GB:CET06D8 Z49130 EM:CET06D8 Z49130	Caenorhabditis elegans cosmid T06D8 (32009 nt)	62.6	123 (22210-22333)
EM:HH43400 U43400 GB:HHU43400 U43400	Human herpesvirus-7 (HHV7) JI (65273 nt)	61.5	109 (136480-136589)
GB:PFU16955 U16955 EM:PF16955 U16955	Plasmodium falciparum ATPase 2 gene (5361 nt)	65.1	106 (5230-5336)
EM:CFORIDHER X94372	C.griseus DNA fragment 17kb downs (7321 nt)	64.2	106 (6600-6706)
EM:CEB0280 U10438 GB:CELB0280 U10438	Caenorhabditis elegans cosmid B0280 (41088 nt)	61.6	99 (10240-10339)
GB:SPAC4G8 Z56276 EM:SPAC4G8 Z56276	S.pombe chromosome I cosmid c4G8 (36933 nt)	69.7	89 (29110-29199)

Using the 19-mer primer, the sequence of band D has the following homologies as shown in table 11.6 :

Table 11.6 Homologies of Band D ~ 202 nucleotides (nt) (using 19-mer primer)

Databank entries	Nucleic acid	% Identity	Nt overlap
EM:SDMT2TRNA X95419 GB: SDMT2TRNA X95419	S.douglasii mitochondrial tRNA pro (932 nt)	59.4	187 (680-867)
EM:PKCYP73AA D82812 GB:POPCYP73AA D82812	Populus kitakamiensis cyp 73a (5167 nt)	53.3	180 (1760-1940)

GB:YSTMTTGD K03308 EM:MIYSTGD K03308	Saccharomyces cerevisia mitochondria (628 nt)	57.1	177 (380-557)
GB:MISCTRND X04564 EM:MISCTRND X04564	Yeast mitochondrial gene for transf (628 nt)	57.1	177 (380-557)
GB:MISC36 X00844 EM:MISC36 X00844	Yeast mitochondrial DNA with tRNA-Asp (628 nt)	57.1	177 (380-557)
GB:BMU07224 U07224 EM:BM07224 U07224	Brugia malayi a2 (IV) basement membrane(13007 nt)	57.2	173 (3780-3953)
GB:YSCMTCG03 L36887 EM:MISCCG03 L36887	Saccharomyces cerevisia mitochondria (6340 nt)	57.6	172 (2070-2243)
EM:HSU66059 U66059 GB:HSU66059 U66059	Human germline T-cell receptor beta (79783 nt)	55.3	170 (42560-42730)
FM:MIEGGU490 U49052 GB:EGU49052 U49052	Euglena gracilis cytochrome oxidase (2502 nt)	56.3	167 (70-237)
EM:RNAMPA01 M38061	Rattus norvegicus glutamate receptor (5787 nt)	60.4	164 (4130-4294)
GB:HUMLIMGP L04193 EM:HSLIMGP L04193	Human lens membrane protein (mp19) (8540 nt)	61.3	163 (1480-1643)
EM:CCPLAS X62578 GB:CCPLAS X62578	C.caldarium plastid genes ompR' (7462 nt)	56.2	160 (50-210)
EM:MMKPRLRP K03237	Mouse proliferin-related protein mRNA (972 nt)	59.7	159 (750-909)
EM:HS253J14 Z80771 GB:HS253J14 Z80771	Human DNA sequence from PAC 253J14 (79783 nt)	60.1	158 (3350-3508)
EM:MMMAL J02652	Mouse malate NADP oxidoreductase mRNA (3129 nt)	57.6	158 (1960-2118)
EM:MMMALEN M26756	Mouse malic enzyme mRNA1 (3071 nt)	57.6	158 (1900-2058)
EM:MISCTGT1 J01533 GB:YSCMTGT1 J01533	Yeast (S.cerevisiae) mitochondrial (716 nt)	62.2	156 (150-306)
GB:MISC10 V00691 EM:MISC10 V00691	Two yeast mitochondrial genes for tra (690 nt)	62.2	156 (150-306)
EM:HSMED Y00477 GB:HSMED Y00477	Human bone marrow serine protease gene (5292 nt)	60.1	153 (3580-3733)
GB:PFU48228 U48228 EM:PF48228 U48228	Plasmodium falciparum 5.8S	57.0	151

	ribosome (4639 nt)		(4360-4511)
GB:HSDNA11 X54282 EM:HSDNA11 X54282	Human chromosome 11 DNA (3750 nt)	56.8	148 (2180-2328)
GB:CEC41C4 Z48045 EM:CEC41C4 Z48045	Caenorhabditis elegans cosmid C41C4 (39750 nt)	56.1	148 (16510-16658)
GB:AA212895 AA212895 mw86e03.r1 EM:MMAA13252 AA212895 mw86e03.r1	Soares mouse NML Mus m (496 nt)	93.8	145 (330-475)
EM:MMD382 D78382	Mouse DNA for tob family (2338 nt)	59.4	138 (1490-1628)
EM:MMHSP70B M35021	Mouse heat shock protein 70.1 (hsp7) (3518 nt)	58.7	138 (730-868)
GB:CEF53H4 Z81089 EM:CEF53H4 Z81089	Caenorhabditis elegans cosmid F53H4 (40380)	56.8	132 (32070-32202)
GB:HSPHOSC X77337 EM:HSPHOSC X77337	H.sapiens gene for phosphate carrier (7969 nt)	60.8	130 (2500-2630)
EM:DDPHOSPHIC M95783 GB:DDIPHOSPHIC M95783	Dictyostelium discoideum phosphoin (2788 nt)	60.8	130 (140-270)
EM:MMCD18 X14951	M.musculus mRNA for CD18 antigen beta (2828 nt)	58.1	129 (2660-2789)
EM:MMHSP68C M12573 GB:MUSHSP68C M12573	Mouse heat shock protein (hsp68) mR (1330 nt)	61.4	127 (730-857)
EM:HSP91B7 Z80773 GB:HSP91B7 Z80773	Human DNA sequence from cosmid F91B7 (42613 nt)	64.7	119 (31770-31889)
EM:S85184 S85184	Cyclic Protein-2=cathepsin proenzyme (1790 nt)	60.9	115 (1370-1485)
GB:AA116330 AA116330 mp97e12.r1 EM:MMAA16330 AA116330 mp97e12.r1	Soares 2NbMT Mus muscu (163 nt)	95.6	114 (1370-1484)
GB:PEACPD2 M27309 EM:CHPSD201 M27309	Pea chloroplast photosystem II gene (4078 nt)	64.6	113 (3940-4053)
GB:HUMHPRTB M26434 BM:HSHPRT8A M26434	Human hypoxanthine phosphoribosyltr (56737 nt)	60.0	110 (12380-12490)
GB:XV18SRRN X74763 EM:XV18SRRN X74763	X.vesparum gene for 18S ribosomal R (2177 nt)	61.1	108 (200-308)
EM:VFVICG Y00506 GB:VFVICG Y00506	Vicia faba vicilin gene. (5327 nt)	60.2	103 (1420-1523)

EM:HS25J6 Z84476 GB:HS25J6 Z84476	Human DNA sequence (57949 nt)	65.9	91 (127350- 127441)
GB:HSJ180M12 Z82190 EM:HSJ180M12 Z82190	Human DNA sequence from clone J180 (47543 nt)	63.7	91 (126200- 126291)
EM:CEP40B5 U23182 GB:CEP40B5 U23182	Caenorhabditis elegans cosmid F40B5 (22237 nt)	64.4	90 (12640-12730)
EM:HSBPXIII M64554 GB:HUMBFXIII M64554	Human factor XIII b subunit gene (33206 nt)	67.1	82 (10840-10922)
GB:CELC49H3 U42436 EM:CEC49H3 U42436	Caenorhabditis elegans cosmid C49H3 (37516 nt)	65.4	78 (34340-34418)

Chapter 12 Discussion

The studies described have further characterised the SL 12 murine lymphoma model and resulted in the detection and characterisation of three unique cDNAs expressed in one of the cell lines versus the other.

The SL 12 murine lymphoma model was chosen for study as it shows the following features: Firstly, the lymphoma model is simple and clean with sister clones differing in their growth patterns, tumourigenicity, surface marker expression and metastatic pattern. Therefore, starting with 2 similar cell lines which were likely to be genetically similar should increased the chance of identifying important differences in gene expression.

Secondly, the lymphoma model is easy to maintain in tissue culture with a hundred percent cloning efficiency. The cell lines are stable with their tumourigenicity maintained even after multiple passages.

Thirdly, these lymphoma cell lines which grow in suspension provide an ideal system for reintroducing the cells back into the animal model using simple access such as tail vein injection.

Lastly, both SL 12.3 and SL 12.4 cells have an approximate doubling time of 48 hours in tissue culture and the median latent period for mice to deteriorate after tail vein injection is 17 days (11-24 days) for SL 12.3 cells and 56 days (22-56 days) for SL 12.4 cells. Comparing with known tumour models, the short doubling time and latent period provide a suitable in vivo

metastatic model. For example, the doubling time of the murine melanoma B16 cell line is 16 hours (Nicholson 1986) and the median doubling time of thirteen known human colorectal cell lines is 39 hours (24 to 110 hours) (McBain 1984; Morikawa 1988). Furthermore, in one hundred and twenty-seven human tumour cell lines studied, tumours could be harvested in 70 % of the cell lines within two months after subcutaneous inoculation and in the remaining 30 % of cell lines, tumours were harvested after two months of inoculation (Fogh 1977).

In vitro properties of SL 12.3 and SL 12.4

In tissue culture, both SL 12.3 and SL 12.4 cells grow in suspension. Morphologically, the SL 12.3 cells, however, tend to be more diffuse whereas SL 12.4 cells grow in clumps (Figure 5.1 and 5.2). There was no sign of either cell line developing attachment to the culture dishes and they are both anchorage independent. The differing morphology could be explained by the cell lines displaying differing cell surface adhesion molecules. For example, in epithelial cell lines, it is known that cells expressing E-Cadherins will bind to each other whereas cells that do not express or express poorly functioning E-Cadherins do not. Moreover, inactivation of other adhesion molecules has little effect on cell-cell interactions as long as the E-Cadherins adhesion molecules are functional (Pignatelli 1992). Lymphoma cell lines do not usually express E-Cadherins but the surface adhesion marker profile is as yet unknown for these two cell lines.

Morphological variation of cellular growth has also been observed in other tumour models. Out of twelve similar human colorectal cell lines established and characterised by McBain et al, two cell lines have monolayer epithelial cells, six cell lines have smooth surface multilayer spheroidal cells, two cell lines with tubular chain of cells and the last two cell lines with grape-like clumps. Similar morphological variations have been observed in cell lines established from human breast carcinomas (McBain 1984).

Under the same growth condition, both SL 12.3 and SL 12.4 cells appeared to have a similar exponential growth rate and doubling time (Figure 5.3). However, in the presence of such wide standard error of mean for each cell count, especially for SL 12.4 cells, it is not possible to conclude that the growth rate and doubling time are the same for the two cell lines.

Difficulties in counting technique maybe mainly responsible for this variation (Figure 5.3) and in particular clumping of SL 12.4 cells leads to potential dilution, pipetting and counting chamber errors. Further studies are required to eliminate these factors such as attempt at mechanical dispersion using repeated pipetting or pre-treatment of cell clumps with Trypsin.

Also, in view of the observed difficulties, other approaches should be considered in further studies such as the measuring of DNA produced from each line at defined time points. This would allow an indirect comparison of growth rate between SL 12.3 and SL 12.4 cells.

In vivo properties of SL 12.3 and SL 12.4

The tumourigenicity of SL 12.3 cells (10^6 cells injected intravenously) was 100 % with the mice deteriorating with a median of 17 days whereas the tumourigenicity of SL 12.4 cells (10^6 cells injected intravenously) was only 9 % at 8 weeks. The tumourigenicity of SL 12.4 cells could be increased by raising the number of cells inoculated such that after the injection of 10^7 cells 79 % of animals developed tumours but again with a longer latency period than SL 12.3 (48 days versus 17 days median). The latency period being similar between the 2 inoculae of SL 12.4 cells.

In the original studies by MacLeod et al., the tumourigenicity of SL 12.3 cells (10^6 cells injected intravenously) was 100 % with a latent period between 10 to 16 days post inoculation whereas the tumourigenicity of SL12.4 cells (10^6 cells injected intravenously) was 43.3 % with a latent period between 34 to 79 days post inoculation. (MacLeod 1985).

The tumourigenicity of SL 12.3 is therefore identical to that reported by MacLeod et al., but that of SL 12.4 lower at 1×10^6 cells. It is possible that mice preserved longer than eight weeks could have continued to develop tumours but timing of sacrifice in the present study was limited by protocol and Home Office regulations.

The lower tumourigenicity observed in 10^6 SL 12.4 cells maybe due to cells undergoing phenotypic drift reverting back to a less tumourigenic phenotype after repeated passages or storage. One way of regaining back the more aggressive phenotype is to reculture cells from organs of mice that develop

metastasis following an inoculation of SL 12.4 cells. However, this may potentially give rise to further subclones, thus, complicating the study.

On the other hand, the increased tumourigenicity observed after raising the number of SL 12.4 cells per inoculum to 10^7 cells is probably due to a higher number of viable tumour cells that have survived the tail vein injection and immune system to develop metastasis.

Macroscopic patterns of SL 12.3 and SL 12.4 cells

There were obvious macroscopic differences between the pattern of metastasis between the two cell lines. Mice injected with SL 12.3 cells characteristically developed massive hepatosplenomegaly with little obvious evidence of metastasis at other sites except in one mouse where renal and subcutaneous metastases were apparent.

In contrast mice injected with SL 12.4 developed less obvious hepatosplenomegaly but obvious metastases mainly in kidneys, ovaries and massive retroperitoneal lymph nodes enlargement with occasional subcutaneous and brain metastases. Most strikingly, the ovarian metastases were up to 1 cm in diameter whereas ovarian enlargement was never seen in SL 12.3. The pattern of metastasis between 10^6 and 10^7 SL 12.4 cells was not different although of course the low number of mice developing metastasis following 10^6 cells inoculated makes comparison difficult.

In the original studies by MacLeod et al., there were also macroscopic differences between SL 12.3 and SL 12.4 cell lines after intravenous inoculation of 10^6 cells. SL 12.3 cell line produced diffuse splenomegaly with occasional hepatomegaly whereas SL 12.4 cell line appeared to produce diffuse involvement of the liver (37 %) and the spleen (58 %) (MacLeod 1985).

In addition, mice injected with SL 12.4 cells developed extranodal tumours such as massive nodules in the kidneys, tumour mass in the thigh muscle and around the knee joint, subcutaneous tumour nodules, orbital and intracerebral tumours and massive bilateral ovarian tumours in about 95 % of animals (MacLeod 1985).

The metastatic patterns between the current studies and those previously are identical for SL 12.3. Where SL 12.4 is concerned, there were some variations between the current study and MacLeod's, in particular liver involvement is slightly higher macroscopically and ovarian involvement lower but these differences are not statistically significant. Differences might have been expected if there had been variation in the tumour genotype with time, as can occur within cells in culture. These results again suggest that the cell lines remain stable.

Microscopic analysis of SL 12.3 and SL 12.4 cells

Previous study has shown that all tumour cells including metastatic lesions have similar microscopic appearances. Cells were described as large with pleomorphic nuclei and were different from the typical AKR spontaneous

thymic lymphoma or the lymphomas developed after the primary explant of spontaneous lymphoma cells (MacLeod 1985). However, no attempt was made to analyse the metastatic patterns microscopically previously.

The macroscopic difference of lymphoblasts of SL 12.3 and SL 12.4 cells from normal lymphocytes makes the detection of these cells obvious in most tissues. It is, however, difficult to be confident of the nature of single cells and therefore, a cut off of eight or more lymphoblasts was chosen to score the slide as positive and any count of less than five lymphoblasts were scored as negative. When the scores are between these two limits further sections for the same organs were studied. Future studies might increase the accuracy using immunocytochemistry of protein specific to SL 12.3 and SL 12.4 cells, however, similar protein is likely to be expressed by other lymphocytes. There are no studies as yet identifying the potential marker proteins.

This microscopic analysis depends totally on the experience of the consultant histopathologist. To further reduce potential observer bias and errors, the observer randomly analysed the tissue sections without any information given whether the organs were from mice inoculated with SL 12.3 or SL 12.4 cells. Reproducibility studies were performed without observer's knowledge to check on consistency of the analysis. The sensitivity of this study could be further increased by performing statistical analysis of the observer as the whole analysis is observer dependent.

In the current study with SL 12.3 cells, it was found that there was commonly diffuse microscopic involvement of tissues that were not macroscopically enlarged. This was particularly apparent in renal, ovarian, lung, brain, thymus and retroperitoneal lymph nodes. The tissues commonly involved macroscopically in SL 12.3 such as the liver and spleen also showed microscopic involvement. Similarly with SL 12.4, diffuse microscopic involvement was also seen in liver, spleen, lung and thymus even where macroscopic involvement was not obvious.

These results suggest that both SL 12.3 and SL 12.4 cells are distributed to all tissues and the macroscopic differences are mainly due to the rapid development of hepatosplenomegaly and early death of the SL 12.3 inoculated mice. While there is no detectable difference between the *in vitro* growth rate of the two cell lines, it is possible that SL 12.3 is growing faster *in vivo* and that in particular the hepatic growth of SL 12.3 is faster than SL12.4. This could be either due to SL 12.3 cells expressing cellular growth factor receptors for hepatic growth factors or SL 12.4 cells failing to express functional growth factor receptors. An alternative explanation might be that the initial hepatic load of SL 12.3 cells is greater than SL 12.4, a phenomenon that may have resulted from homing of SL 12.3 cells to hepatic parenchyma. This possibility was further investigated by *in vivo* cellular tracking studies.

In vivo cellular tracking studies

Re-injecting labelled cells back into an animal model circulation allows the study of earlier stages of metastasis: tumour cell distribution, trapping and

extravasation. 5-(¹²⁵I)odo-2'-deoxyuridine (¹²⁵IUDR) has been found to be ideal in labelling cells (Fidler 1970; Hart 1981; Kjønniksen 1991) for cellular tracking studies as it is incorporated exclusively into DNA of actively dividing cells and is released without being re-utilised by other cells when the originally labelled cells died. The concentration of ¹²⁵IUDR to be used is critical. Sufficient ¹²⁵IUDR has to be used to increase the sensitivity for detecting small numbers of cells in tissues. However, over concentrated serum with ¹²⁵IUDR will be lethal to the cells. In the current study, 2.0 and 5.0 µCi/ml of ¹²⁵IUDR was found to produce optimal cell labelling without causing cell death (Chart 7.2, 7.3, 7.4 and 7.5). 2.0 µCi/ml rather than 5.0 µCi/ml was used for further study as the concentration producing minimum cellular toxicity is to be preferred to the maximum sensitivity for detection and 2.0 µCi/ml was more economical for isotope.

The percentage of incorporation of ¹²⁵IUDR into both cell lines was relatively low (6.9 % and 4.8 % for SL 12.3 and SL 12.4 cells respectively) as compared to the original study by Fidler (Fidler 1970). Furthermore, the percentage of incorporation is at least 50 % more in one set of cells compared to the other (Table 7.1).

As all cells were incubated together in the same environment and with the same batch of ¹²⁵IUDR, the difference in percentage of incorporation observed is most likely due to errors in washing and pelleting of cells (page 73) before being analysed by the gamma counter. These errors might be eliminated in further studies but in any biological systems there is likely to be variations that is beyond experimental control.

In the current study, autoradiograms confirmed that the radioactive iodine was taken into the nucleus of viable cells. This low percentage of incorporation is shown therefore to represent true cellular uptake rather than background contamination.

The current study showed that tumour cells circulated to all organs within fifteen minutes of inoculation but there is no significant difference in cellular dissemination in between SL 12.3 or SL 12.4 cells at fifteen minutes, one hour or three hours. Exceptions were of higher numbers of SL 12.4 cells seen in cerebral and thymus tissues at one hour post injection and also, higher number of SL 12.4 cells per gram of ovarian tissues at one hour but these differences were not apparent at fifteen minutes or three hours and therefore, it is unlikely that these are true differences explaining the distribution of metastasis.

Tumour cells passed the lungs and start to accumulate in the liver as early as fifteen minutes after tail vein injections (15.4% for SL 12.4 cells to 48.2 % for SL 12.3 cells in the liver). An hour after inoculation, labelled cells had already circulated to all organs but only 1.3 % of the original cells remained viable in tissues three hours post inoculation. Such rapid disappearance of radioactivity in organs could be due to rapid cell death after tail vein injection with the radioactive label being excreted from the system.

Pilot studies showed that no radioactivity was detected in mice 24 hours after cell injection. Injected in this way, cells may die rapidly and study by Fidler (Fidler 1970) has shown that only about 1 % of cells survived after 24 hours. The isotopes from dead cells are released into circulation and rapidly

excreted by the kidneys without being reutilized by other cells. The reason why other cells could not reutilize the isotope after the labelled cell died is not fully understood.

The percentage of incorporation of ^{125}I UDR in this study is low. This has reduced the sensitivity and accuracy of the technique producing wide variation in tissue counts. As a result, it is difficult to draw any firm conclusion from these data. However, this study appears to show similar tissue distribution of SL 12.3 and SL 12.4 following re-injection which is against the hypothesis that there is a difference in tissue homing between the two cell lines or that the phenomenon of homing exists within this model. Within the same cell line, there are differences between distribution of cells per gram of tissues within brain, lungs, liver, lymph nodes and ovaries. Similar differences are seen with both cell lines implying that the differences in tissue distribution are due to mechanical reasons rather than tissue specificity or homing. However, low incorporation of isotope and therefore, a reduction in accuracy of the technique means that the conclusion cannot be proved on the current data available.

As the histological studies show widespread microscopic dissemination of tumour cells in tissues, it is possible that in this model, components of both Mechanical and Seed and Soil hypothesis could explain the metastatic process. It seems that in the earlier stages of metastasis, the Mechanical hypothesis could be applied to explain the difference in the number of cells in different organs. However, despite poor data from the radioactive studies, both the macroscopic and microscopic analysis have shown that there are differences in the pattern of metastasis between the two cell lines that could

not be explained by the Mechanical Hypothesis only. The microscopic analysis has shown that the presence of tumour cells in tissues is not always followed by the formation of larger macroscopic metastasis. Some cells appear to stay dormant or probably grow at a slow rate, thus, giving rise to the observed different metastatic patterns between the two cell lines. This supports aspects of the Seed and Soil hypothesis in that there are differences or variations in the growth rate of cells in organs according to response to local tissue growth factors. On the other hand, failure of metastasis development in tissues maybe due to host immune factors.

Molecular experiments

Extraction of Total RNA / mRNA

Differential display, as a technique, allows us to identify cDNAs that are exclusively expressed in a cell line. It is totally dependent on the amount of cDNAs sequence amplified. Therefore, the sensitivity of the technique improves with the purity of mRNAs isolated as the quality of the mRNAs dictates the maximum amount of sequence information that can be converted to cDNA. Any degradation of RNA samples and DNA contamination leads to less reproducible bands resulting in the increase in the number of false positives.

High yield and pure undegraded total RNAs could be obtained from cells or tissues using the single step method of acid Guanidinium Thiocyanate-Phenol-Chloroform RNA extraction as described by Chomczynski

(Chomczynski 1987). However, despite careful technique, extracted RNA samples could occasionally be contaminated with cellular chromosomal DNAs (Liang 1993) which could give false positive results. This can be prevented by pre-treating the extracted total RNAs with DNase (Liang 1993) before subjecting to reverse transcription. The purity of total RNA specimens can further be assessed by running non-reversed-transcribed controls side by side with reversed transcribed products. Any band in the non reversed-transcribed controls would then represent samples contaminated with cellular chromosomal DNA that are independent of the reverse transcription process. The RNA specimens used in this study were shown to be free from DNA contaminants as shown in Figure 9.4.

Only 0.5 % to 2 % of total RNA population is mRNAs. Therefore, for the construction of a cDNA library a reasonable amount of total RNAs have to be extracted before sufficient mRNAs could be used to construct the cDNA library. Moreover, the extracted mRNAs has to be free from the degraded mRNAs, tRNAs and rRNAs.

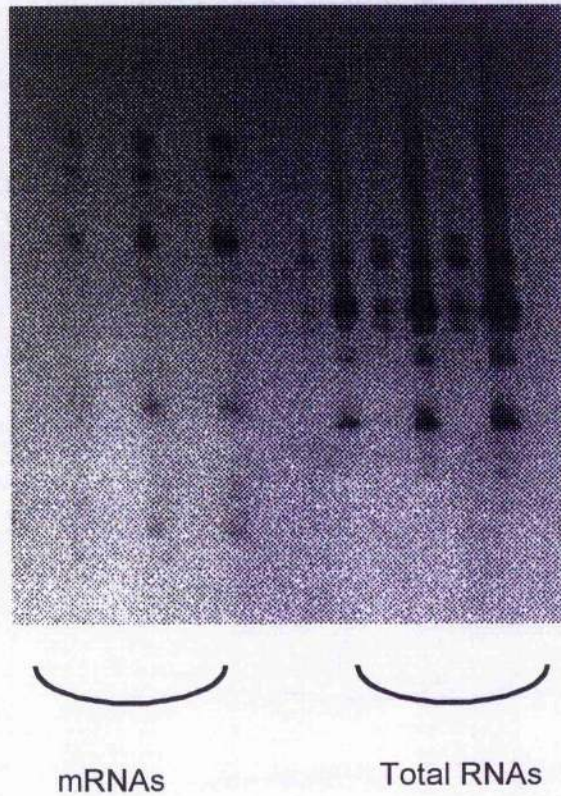
One way of extracting mRNAs directly from cellular or tissue samples is to use Dynabeads[®] biomagnetic separation system (*Dynal*[®])(Dynal). This technique makes use of the concept that mRNAs usually end with polyadenylated tails. Mixing dynabeads (beads that is covalently linked to a chain of 25 nucleotides long deoxythymidylates) with the lysates of cells or tissues allows base pairings between the poly-A tail of mRNAs and oligo (dT) residues that are bound to the beads. These bound products were removed from the rest of the mixture by using strong magnet to pull the beads. The mRNAs could then be eluted from the oligo-dTs and precipitated

out for further analysis. This technique is quick and reduces the chances of losing rare mRNAs.

The technique of differential display is not dependent on selective extraction of mRNA. In amplification, the presence of the polyadenylated tail of the mRNAs is used to anchor one of the primers. This has been confirmed by Liang et al., that there is no advantage of using mRNAs over total RNAs as a template for reverse transcription and polymerase chain reaction in the differential display method. The end results of cDNA bands were nearly identical (Liang 1993). This shows that the RT-PCR method is very specific for mRNAs even in the presence of ribosomal and transfer RNA, thus, further suggesting that PCR is a highly sensitive but not a quantitative reaction (Sunday 1995). Total RNAs are recommended to be used as templates as mRNAs can be contaminated with oligo-dTs by the isolation method resulting in exogenous priming in the reverse transcription step.

A comparison of mRNAs and total RNAs have been used as template for the RT-PCR in this series of study. It was found that fewer bands were produced in the mRNAs samples compared to total RNAs samples (Figure 12.1). One possible explanation is that rarer mRNAs can easily be lost during its extraction. Therefore, total RNAs rather than mRNAs have been used as templates in this study.

Figure. 12.1 PCR products using either mRNAs or total RNAs as template



Reverse Transcription

Liang et al., (Liang 1992) has shown that for a 20 μ l reverse transcription reaction, total RNA as low as 0.02 μ g (which is equivalent to RNA from 200 cells) would be sufficient to produce consistent pattern in the differential display. Lowering the RNA to 0.002 μ g of RNA caused sparser pattern of bands in the display probably due to loss of detection of rarer mRNAs. In fact, the intensity of bands displayed is totally independent of the

concentration of total RNA between 2 to 0.02 μg , thus, suggesting that under PCR conditions the display method is not very quantitative (Liang 1993).

The reverse transcription process was carried out in the presence of 2.5 μM of anchoring oligo-dTs and 20 μM dNTPs. The concentration of dNTPs is important, as any increase in its concentration would result in excess of dNTPs being carried forward to the subsequent PCR reaction, thus, producing a poorer yield in DNA amplification.

The enzymes most commonly used in reverse transcription are the reverse transcriptase from the Moloney murine leukaemia virus (MMLV) or from avian myeloblastosis virus (AMV). Reverse transcriptase, like any enzyme, is easily degraded if left for storage too long or underwent multiple thawing and freezing. A degraded enzyme yields low amount of cDNAs resulting in display failure. This enzyme should be aliquoted for further use to avoid repeated freezing and thawing process

Polymerase Chain Reaction (PCR)

In these studies, for the polymerase chain reaction we used an anchoring 3' end primer and a random 5' end primer to amplify all the reversed transcribed cDNAs. In general such a pair of primer set can amplify and display about 50 to 100 cDNA bands.

The 3' end anchoring primer was an oligo-dTs primer consisting of eleven or twelve 'T's with two additional non T bases at its 3' end such as T₁₂MN (where M may be dG, dA or dC and N maybe dG, dA, dT or dC). These two additional bases are important as they provide annealing specificity. It has been found that if these two additional bases were lacking, such as in degraded and old primers, the primer lost its anchoring device resulting in a smear being produced as opposed to defined band patterns (Figure 12.2) (Liang 1993). This is because the non anchoring 3' end primer anneals and prime at different sites of the poly-A tail of mRNA resulting in multiple transcript. An example of this is shown in figure 12.3 where older primers were used which may have become degraded and have lost the anchoring device. Smearing of the gel can also be due to the use of RNA specimens that are contaminated with oligo-dTs as in contaminated mRNA after its extraction using oligo-dTs.

Figure 12.2 The importance of the anchoring device in the 3'-end primer

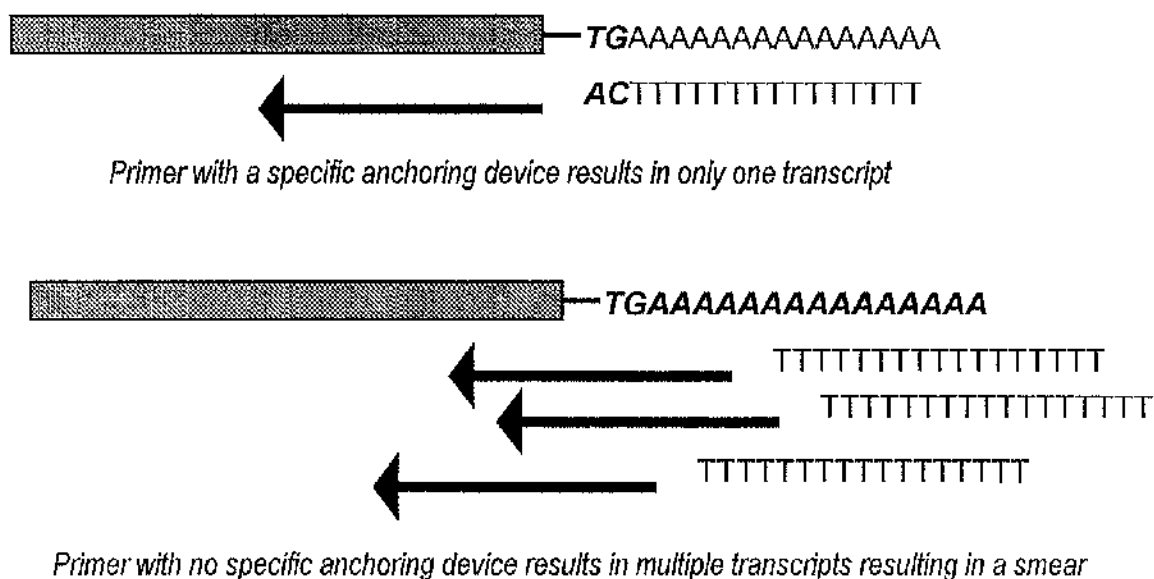
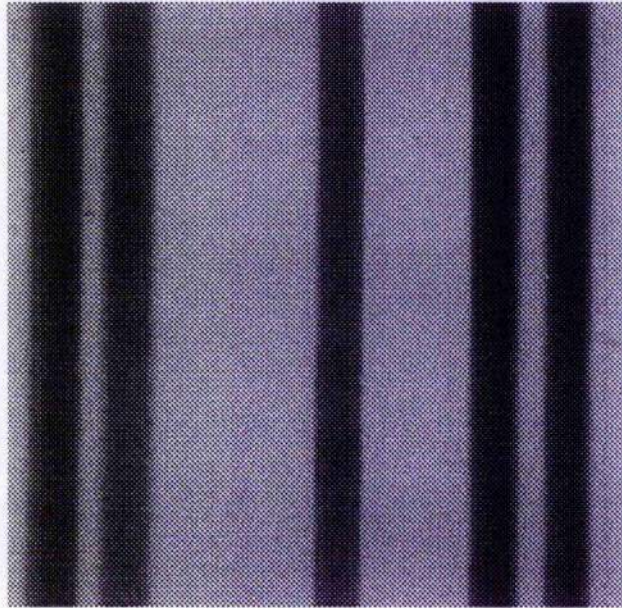


Figure 12.3 Smearing as a result of old 3'-end primers which have lost their anchoring device

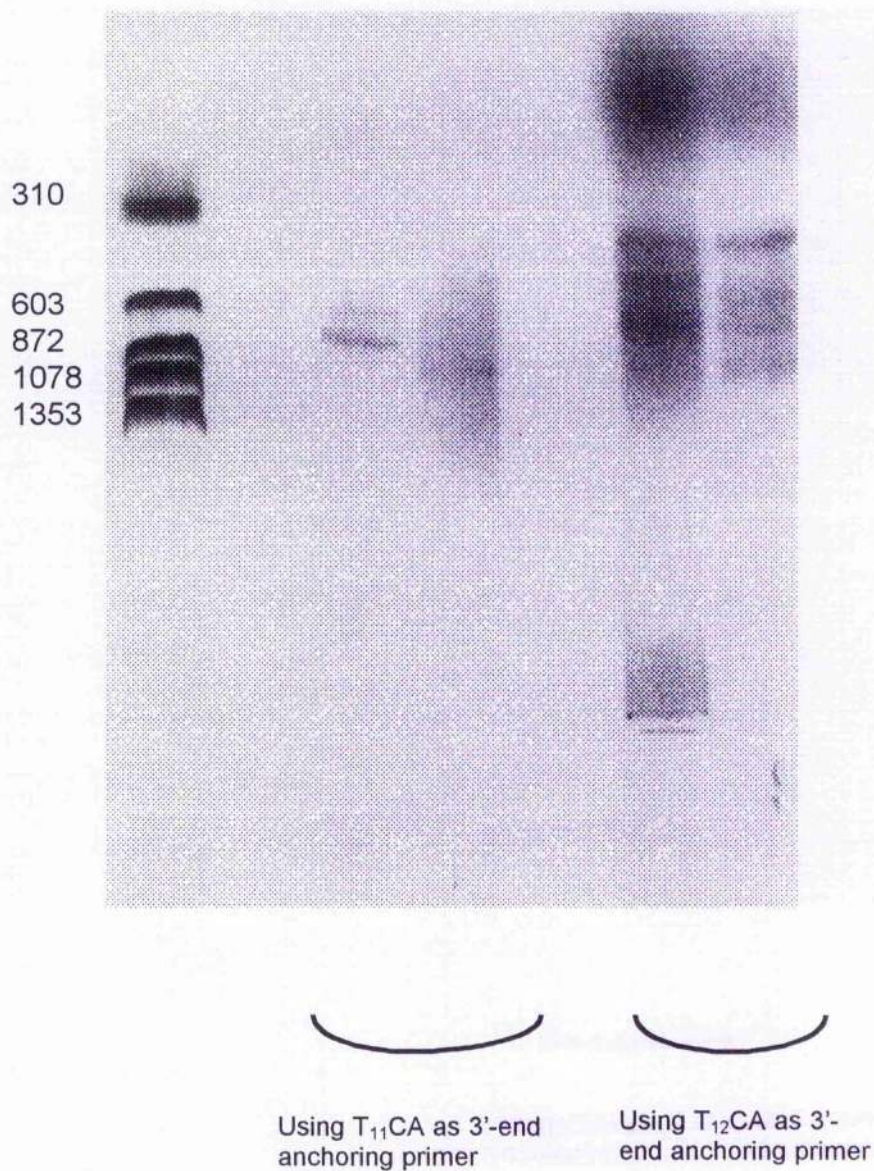


Furthermore, when $T_{12}MA$ primers were compared with $T_{12}CA$ primers in differential display, it was found that both primers have similar number of bands in the display. This suggests that the M base (where M may be dG, dA or dC) does not provide any specificity as $T_{12}MA$, theoretically, should produce three times the number of bands compared to $T_{12}CA$. This implies that the penultimate base from the 3' end of the $T_{12}MN$ primer may exhibit considerable degeneracy during priming in the reverse transcription step.

However, when the N base in the $T_{12}MN$ primer (where M may be dG, dA or dC and N maybe dG, dA, dT or dC) is changed, more bands were obtained compared to a change only in the 'M' base. This suggests that the specificity of the primer lies in the N base (Liang 1993) rather than the 'M' base. Therefore, instead of using twelve different anchoring primers to prime 10 000 mRNA species, only four anchored primers differing in the 'N' base

are sufficient. It has also been suggested that the longer the anchoring primers, the higher the background and fewer discrete bands produced. In this study comparison was made using T₁₁CA and T₁₂CA primers (Figure 12.4). T₁₂CA primers produced more bands than T₁₁CA despite having a slightly 'noisier' background (Figure 12.4). One explanation for this is that the longer primer anchors more efficiently than the T₁₁ base primer. Primers shorter than T₁₂ are unlikely to be useful but the background increases as the poly-t tail is lengthened. This has also been shown in other studies (Liang 1993).

Figure 12.4 PCR products on an Agarose gel using either T₁₁CA or T₁₂CA anchoring primers showing that as the primers are lengthened the anchorage efficiency increases but to the detriment to the increasing background



The specificity and sensitivity of the polymerase chain reaction are affected by the concentration of enzyme, primers and nucleotides, the number of cycles and denaturation, annealing and extension times.

The concentration of nucleotides and annealing temperature greatly influences the specificity of the reaction (Erlich 1991; Zimmermann 1996). The concentration of dNTPs is found to be important in both the reverse transcription and polymerase chain reaction. Liang et al., found that the optimum concentration dNTPs for reverse transcription is 20 μ M and 2 μ M for polymerase chain reaction. Lowering the concentration of dNTPs to 2 μ M improved the specificity of DNA amplification and was found to be necessary for labelling PCR products to a high enough specific activity with [α -³⁵S]-labelled ATP to provide high resolution on a DNA sequencing gel (Liang 1992). Too high dNTPs concentration in the reverse transcription caused over-excess dNTPs for the successive polymerase chain reaction. This results in direct competition with labelled dATP resulting in poor labelling of cDNAs.

To reduce excess dNTPs from contaminating subsequent polymerase chain reaction, it has been suggested that the reverse transcription products should run through cDNA spun columns. These columns, such as those from *Pharmacia*, are pre-packed with Sephacryl S-300 designed to purify cDNAs from smaller molecules such as oligonucleotides, nucleotides and phenol. However, in this study, this purification step was found not essential if the concentration of dNTPs was restricted to 20 μ M in the reverse transcription step. Moreover, in the purification process, the products can

easily be lost in the columns and not eluted out, thus, reducing the sensitivity of the method.

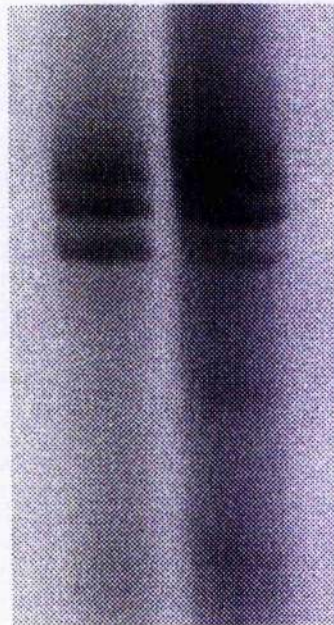
In a standard polymerase chain reaction, the annealing temperature for nucleotides is usually from 50°C to 70°C, depending on the melting temperature of the primers, T_m (the annealing temperature is usually about 50°C below the calculate T_m). In differential display, the T_m of the 5'-end short random decamer primer is low and, therefore, the annealing temperature for the polymerase chain reaction was suggested to be 42°C in the original studies (Liang 1992). Subsequently, it was found that lowering the annealing temperature down further to 40°C and increasing the annealing period from one to two minutes was optimum for the display (Liang 1993).

³⁵S nucleotide is the radioactivity of choice to label amplified cDNAs. It has low energy emission and produces high-resolution discrete bands that are ideal for display and direct comparison. Other alternatives include using ³²P and ³³P that are both of higher energy emissions and therefore, exposure time can be reduced. ³³P has lower emission energy compared to ³²P and theoretically, produces more discrete and higher resolution bands than ³²P. On the other hand, comparing to ³⁵S, both ³²P and ³³P have higher energy emissions, thus, producing less discrete bands and the higher background. Furthermore, these radionucleotides have a shorter half life compared to ³⁵S. In these studies, ³³P was originally used to label the nucleotide but the background was high and the bands produced were not discrete enough for further analysis.

The Display

The amplified and labelled cDNAs were displayed on a 6 % denaturing polyacrylamide sequencing gel. Any bands smaller than 300 base pairs can appear as doublets or triplets (Figure 12.5). The explanation for this is either the additional deoxyadenosine added by the Taq DNA polymerase or a slight difference in mobility between the two complementary strands on the denaturing gel. This phenomenon has been described in other study using differential display (Liang 1993).

Figure 12.5 Triplets seen in cDNAs less than 300 base pairs



The pattern of mRNAs in the differential display technique has been found to be highly reproducible between duplicate experiments (> 95 % reproducibility by counting discrete bands) (Liang 1993), thus, providing a good technique to isolate exclusively expressed genes

In this study, RNAs extracted from different batches of SL 12.3 and SL 12.4 cells that underwent differential display showed high reproducible rates of mRNA bands confirming the finding of Liang's original work (Liang 1993).

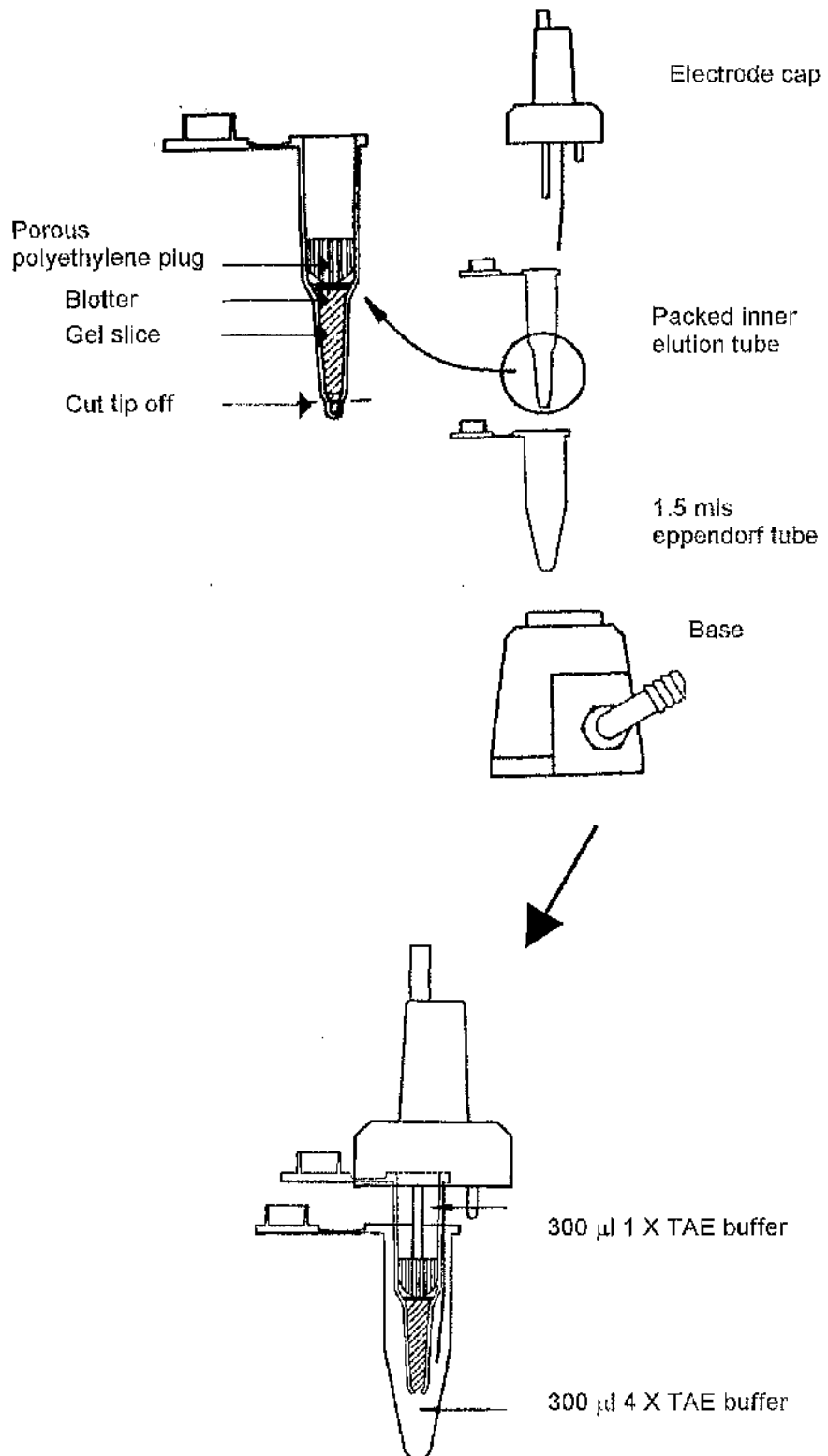
Recovery of cDNA from dried gel

The recovery of cDNA is important for further analysis and characterisation of the expressed mRNA. It has been suggested that the polyacrylamide gel with the displayed cDNAs should not be fixed with methanol/acetic acid solution before drying as this makes the recovery of cDNAs difficult. Liang et al., used the *Hoefers* gel eluter (Figure 12.6) to recover the cDNA segment from the dried gel in their original paper. Briefly, the cut gel/paper is inserted and packed into the conical end of the inner elution tube which is pre-filled with 300 µl of TAE buffer. Any bubbles are dislodged and a piece of blotter paper disk is placed into the tube on top of the gel / paper. A porous polyethylene plug is placed on top of the blotter paper (Figure 12.6). The tip of the inner elution tip is then cut off before applying current between the two electrodes. The cDNA are then eluted into the 1.5 ml eppendorf tube pre-filled with 4 X TAE buffer. Using this technique, Liang et al., is able to recover 50 % of the original cDNA. In this current study, this method of band purification and isolation using the *Hoefers* gel eluter

was tried but cDNAs were poorly recovered and insufficient for reamplification.

A second technique was therefore used for cDNA band recovery. Besides electroelution as above, cDNAs can also be recovered by rehydrating and incubating the gel / paper in sterile water. The cDNAs are then eluted out (Liang 1993; Mou 1994) by boiling. The eluted cDNAs can then be precipitated out with sodium acetate and reamplified with PCR. It has been shown that elution of cDNA from dried gel is possible in about 90 % and reamplification successful in 95 % of cases using these techniques (Liang 1993; Mou 1994). In the current studies, this method produces good cDNA band recovery. TE buffer was used in hydration and elution of the cDNAs in dried gel by incubating the paper / dried gel at 65⁰C for two hours and all four bands were successfully eluted.

Figure 12.6 The Hoefer's gel eluter



Reamplification

Having recovered the cDNA from the gel, it has to be reamplified and purified in order to sequence it. The process of TA cloning is described in Chapter 10. The advantages of using this method are that once the sequence is integrated into the plasmid, the product of the plasmid and its insert could then be replicated in bacteria easily. The cDNA can be directly sequenced within the plasmid as sequencing promoter sites are included in the plasmid's design. Also, the plasmids can be frozen down and stored indefinitely.

In the current study, despite incorporation of the cDNAs bands of interest within the plasmid obtaining white colonies the resulting plasmids, on testing, were unstable and sequencing revealed that the cDNA had been lost with self blunt ligation of the vector. Possible explanation of these is that the size of the insert and tertiary structure was not suitable for this method of cloning. Alternatively, the TA links necessary for plasmid stability may have been weak or the plasmid unstable at the ECoRI sites (See Chapter 10).

Repeated attempts were made varying the conditions for TA cloning. The vector: PCR product ratio was varied between 1:1 and 1:3. Studies were conducted both decreasing and increasing the number of PCR cycles and finally a different TA cloning kit were used with new batch of ligation enzymes and vectors. However, the cells still failed to yield plasmids with inserts when sequenced. On each occasion sequencing plasmids from bacteria of the 'white' and 'positive' colonies persistently showing no insert with the plasmid having been divided at ECoRI site. This was further

confirmed by adding EcoR1 restriction enzymes to these 'positive' plasmids. If the insert is present two bands should be seen where the enzymes cut out the insert at EcoR1 sites. These studies repeatedly produced only one band representing the plasmid suggesting that the blunt ligation at EcoR1 sites had already occurred before the plasmids were inserted into the bacteria.

Invitrogen was contacted regarding this problem but provided no further useful explanation regarding the observed phenomenon. TA cloning was repeated for more than six months until the isolated cDNA specimen run out.

During the course of these studies, a second method of amplification of cDNAs produced by differential display was published (Wenck 1995). This involves reamplification and resequencing with longer primers based on the initial primers used in differential display (See Chapter 10). This method was successful and allowed the direct sequencing of the products.

Sequences were produced for 3 bands isolated from the differential display. Band A was found expressed exclusively in SL 12.4 cells, Band C was expressed exclusively in SL 12.3 and Band D was expressed more in SL 12.4 than SL 12.3. Band B that was expressed exclusively in SL 12.3 was unfortunately lost during purification.

These sequences were used to search Embank and Genbank for homologies. Significant homologies are those that fall into exons of a gene that have high nucleotide overlap and strong identity.

The tables below detail the results of the searches with a description of likely significance and gene product under the heading homology.

Homologies of Band A ~ 162 nucleotides (nt) (using 22-mer primer)

Nucleic acid	% Identity	Nt overlap	Homology
B.burgdorferi promoter region DNA (203 nt)	61.5	135 (20-155)	Promoter region
Caenorhabditis elegans cosmid C18B (21185 nt)	59.8	132 (14910-15042)	Intron
Caenorhabditis elegans cosmid F59A1 (45300 nt)	64.8	88 (13430-13518)	Gene : F59A1.e Product unknown
Human DNA sequence from cosmid N114 B2 (40523 nt)	66.7	84 (35730-35814)	Intron
S.cerevisiae chromosome X reading (6127 nt)	66.7	81 (2300-2381)	Open Reading Frame
Soares fetal heart NbHH1 (659 nt)	67.6	74 (70-144)	Expressed sequence tag
Soares fetal heart NbHH19W (659 nt)	67.6	74 (70-144)	Expressed sequence tag

Band A (22-mers) has weak homology with an exon in *Caenorhabditis elegans* coding for an unknown protein, F59A1.e. The other homologous sequences detail above are either introns or EST (expressed sequence tags which are uncharacterised) or reading frames. This sequence could also be in the 3'-untranslated region.

Homologies of Band A ~ 176 nucleotides (nt) (using 19-mer primer)

Nucleic acid	% Identity	Nt overlap	Homologous Protein
Soares mouse placenta (265 nt)	75.3	150 (40-190)	Expressed sequence tag
Xiphophorus maculatus ERCC2/XPD gene (16840 nt)	55.9	145 (13740-13885)	Gene : ERCC2/XPD
Caenorhabditis elegans cosmid F28F9 (31967 nt)	54.7	128 (12980-13108)	Intron
Chelonia mydas clone CM45 (618 nt) - anonymous nuclear DNA sequence	58.3	127 (420-547)	Intron
Rat mRNA for tissue factor in pathway inhibitor (1226 nt)	66.7	117 (1070-1187)	Intron
Mouse 3'-directed cDNA, MUSGS00900 (92 nt)	74.4	90 (2-90)	Expressed sequence tag
Plasmodium falciparum heat-shock protein (2290 nt)	56.8	88 (370-458)	Intron
Nasonia vitripennis NATE P16 LTR (1071 nt)	63.4	82 (710-792)	Intron
Caenorhabditis elegans cosmid F23B2 (43589 nt)	58.9	73 (9380-9453)	Intron
A. Xylinum gene for cellulose biopsy (10094 nt)	66.2	71 (9970-10041)	Intron
Hydra vulgaris tyrosine kinase mRNA (1186 nt)	66.7	63 (100-163)	Gene : Tyrosine kinase
Caenorhabditis elegans cosmid F33G12 (31261nt)	63.8	58 (21890-21948)	Intron
Human chromosome 12p13 (79787 nt)	66.7	51 (74800-74851)	Intron

Baud A (19-mer) has weak homology to *X. maculatus* ERCC2/XPD exon and *H. vulgaris* tyrosine kinase exon. The other sequences detailed above are either introns or EST (expressed sequence tags which are uncharacterised).

Homologies of Band C ~ 153 nucleotides (nt) (using 22-mer primer)

Nucleic acid	% Identity	Nt overlap	Homology
<i>S.cerevisiae</i> chromosome XIV reading frame ORF YNL319w (2064 nt)	57.4	115 (1880-1995)	Open Reading Frame
<i>M.musculus</i> scp2 gene exon 14 (4825 nt)	55.7	115 (440-555)	Intron
<i>S.cerevisiae</i> FY1676 RPD3 gene (40050 nt)	57.4	115 (21730-21845)	Intron
<i>S.cerevisiae</i> chromosome IV cosmid 934 (19236 nt)	54.7	106 (19040-19146)	Intron
Soares fetal heart NbHH19 (461 nt)	58.6	99 (310-409)	Expressed sequence tag
<i>Fasciola hepatica</i> clone Fas 3-4 tran (439 nt)	58.5	82 (300-382)	Intron
Rat T-cell receptor beta-chain complex (3203 nt)	65.5	55 (2260-2315)	Intron
<i>Cyprinus carpio</i> growth hormone gene (2838 nt)	63.6	77 (440-517)	Intron
<i>Cavia porcellus</i> glucocorticoid receptor (2316 nt)	61.0	77 (610-687)	Gene : Glucocorticoid receptor
<i>M.musculus</i> mRNA for DRTF-polypeptide 1 (DP-1) (1700 nt)	60.5	76 (870-946)	Gene : Transcription factor
<i>Caenorhabditis elegans</i> cosmid CO8E8 (7977 nt)	61.4	70 (84920-84990)	Unfinished

Band C (22-mer) has weak homology to *Cavia porcellus* glucocorticoid receptor exon and *M. musculus* transcription factor exon. The other sequences detailed above are either introns or EST (expressed sequence tags which are uncharacterised).

Homologies of Band C ~ 160 nucleotides (nt) (using 19-mer primer)

Nucleic acid	% Identity	Nt overlap	Homology
<i>Schistosoma japonicum</i> mRNA for paramyosin (3514 nt)	52.7	129 (3320-3449)	Intron
<i>Schistosoma japonicum</i> structural mus (4022 nt)	53.5	127 (3360-3487)	Intron
<i>P. vulgaris</i> gln-delta gene for plastid-located glutamine synthetase (4695 nt)	53.2	124 (2310-2434)	Promoter
<i>H. sapiens</i> (D12S1701) DNA segment containing (CA) repeat (373 nt)	53.0	115 (230-345)	Intron
<i>Homo sapiens</i> cDNA clone 38646 3' (456 nt)	55.0	109 (160-269)	Expressed sequence tag
<i>Caenorhabditis elegans</i> cosmid F44D1 (31853 nt)	53.3	107 (24180-24287)	Intron
<i>Caenorhabditis elegans</i> cosmid T19E1 (19463 nt)	56.9	102 (14740-14842)	Gene : Transforming protein ctc2
Rat cytochrome P-450-I.A-omega (2462 nt)	53.9	102 (1980-2082)	Intron
<i>Mus musculus</i> sodium calcium exchange (3180 nt)	60.7	61 (3060-3121)	Intron
Human DNA sequence from cosmid A1280 (22253 nt)	65.4	52 (10900-10952)	Intron
Soares mouse embryo Nb (915 nt)	70.8	48 (560-608)	Expressed sequence tag

Band C (19-mer) has weak homology to *Caenorhabditis elegans* transforming protein exon. The other sequences detailed above are either introns or EST (expressed sequence tags which are uncharacterised).

Homologies of Band D ~ 197 nucleotides (nt) (using 22-mer primer)

Nucleic acid	% Identity	Nt overlap	Homology
Human collagenase and stromelysin g (79788 nt)	54.8	188 (42810-42998)	Intron
<i>Apis mellifera</i> mitochondrial genome (16343 nt)	59.4	180 (16010 - 16198)	Intron
<i>Tetrahymena thermophila</i> micronuclear linker histone polyprotein (3000 nt)	61.0	177 (660-837)	Intron
<i>Bacillus thuringiensis</i> insecticida (1692 nt)	62.4	170 (550-720)	Intron
<i>S.douglasii</i> mitochondrial OXII & R (2945 nt)	62.3	167 (100-267)	Intron
<i>Trypanosoma brucei brucei</i> kinetoplast maxicircle genes (23016 nt)	59.1	164 (19610-19774)	Intron
<i>Caenorhabditis elegans</i> cosmid F59G1 (25642 nt)	60.7	163 (19240-19403)	Intron
<i>H.vulgare</i> Perl gene (1994 nt)	62.7	158 (140-298)	Intron
<i>S.tuberosum</i> pathogenesis-related protein (2896 nt)	58.6	152 (2580-2732)	Intron
HTGS phase 3, complete sequenc. (41098 nt)	61.1	149 (17740-17889)	DiGeorge Critical Region of Human Chromosome 22
Yeast mitochondrial tRNA (1847 nt)	62.8	148 (540-688)	Intron

Borrelia burgdorferi tldF gene (4239 nt)	61.3	142 (430-593)	Intron
Caenorhabditis elegans cosmid F58G1 (42328 nt)	58.2	141 (27910-28051)	Intron
Caenorhabditis elegans cosmid (37039 nt)	58.2	141 (27910-28051)	Intron
Deer mouse (LIPm62) (1825 nt)	61.2	139 (260399)	Intron
Cylindrotheca sp. ribulose-1,5-biphosphate carboxylase/oxygenase small & large subunit genes (2517 nt)	62.7	134 (210-344)	Intron
Caenorhabditis elegans cosmid C25F6 (43803 nt)	62.6	131 (19690-19821)	Intron
Caenorhabditis elegans cosmid T05D4 (32612 nt)	66.4	128 (11890-12018)	Intron
P.falciparum complete gene map (15421 nt)	60.2	128 (13780-13908)	Gene : rpoD
Caenorhabditis elegans cosmid T06D8 (32009 nt)	62.6	123 (22210-22333)	Intron
Human herpesvirus-7 (HHV7) II (65273 nt)	61.5	109 (136480-136589)	Gene : II8 Product : Unknown
Plasmodium falciparum ATPase 2 gene (5361 nt)	65.1	106 (5230-5336)	Intron
C.griseus DNA fragment 17kb downs (7321 nt)	64.2	106 (6600-6706)	Gene : Dihydrofolate Reductase
Caenorhabditis elegans cosmid B0280 (41088 nt)	61.6	99 (10240-10339)	Intron
S.pombe chromosome I cosmid c4G8 (36933 nt)	69.7	89 (29110-29199)	Intron

Band D (22-mer) has weak homology to Plasmodium falciparum rpoD exon, H herpesvirus-7 H8 exon, Plasmodium falciparum ATPase2 exon and C. griseus Dihydrofolate Reductase exon. The other sequences detailed above are introns.

Homologies of Band D ~ 202 nucleotides (nt) (using 19-mer primer)

Nucleic acid	% Identity	Nt overlap	Homology
S.douglasii mitochondrial tRNA protein (932 nt)	59.4	187 (680-867)	Intron
Populus kitakamiensis cyp 73a gene for cinnamic acid 4-hydroxylase (5167 nt)	53.3	180 (1760-1940)	Intron
Saccharomyces cerevisia mitochondria Asp-tRNA (628 nt)	57.1	177 (380-557)	Intron
Yeast mitochondrial gene for transfer RNA (628 nt)	57.1	177 (380-557)	Intron
Yeast mitochondrial DNA with tRNA-Asp (628 nt)	57.1	177 (380-557)	Intron
Brugia malayi a2 (IV) basement membrane collagen gene (13007 nt)	57.2	173 (3780-3953)	Intron
Saccharomyces cerevisia mitochondria tRNA- Leu, Gln, Lys, Arg, Gly, Asp, Ser2, Arg2, Ala, Ile, Tyr, Asn genes. (6340 nt)	57.6	172 (2070-2243)	Intron
Human germline T-cell receptor beta (267156 nt)	55.3	170 (42560-42730)	Intron
Euglena gracilis cytochrome oxidase subunit 1 (2502 nt)	56.3	167 (70-237)	Intron
Rattus norvegicus glutamate	60.4	164	Intron

receptor (5787 nt)		(4130-4294)	
Human lens membrane protein (mp19) (8540 nt)	61.3	163 (1480-1643)	Gene : Human lens membrane protein
C. caldarium plastid genes ompR', psbD, psbC, rps16 and groEL (7462 nt)	56.2	160 (50-210)	Intron
Mouse proliferin-related protein mRNA (972 nt)	59.7	159 (750-909)	Gene : proliferin related protein
Human DNA sequence from PAC 253J14 on chromosome X (79783 nt)	60.1	158 (3350-3508)	Repeat region
Mouse malate NADP oxidoreductase mRNA (3129 nt)	57.6	158 (1960-2118)	Intron
Mouse malic enzyme mRNA1 (3071 nt)	57.6	158 (1900-2058)	Intron
Yeast (S.cerevisiae) mitochondrial THR-tRNA-1 and Val-tRNA-GUR genes (716 nt)	62.2	156 (150-306)	Intron
Two yeast mitochondrial genes for transfer RNA-Val (690 nt)	62.2	156 (150-306)	Intron
Human bone marrow serine protease gene (5292 nt)	60.1	153 (3580-3733)	Intron
Plasmodium falciparum 5.8S ribosome (4639 nt)	57.0	151 (4360-4511)	Gene : large subunit RNA
Human chromosome II DNA (3750 nt)	56.8	148 (2180-2328)	Intron
Caenorhabditis elegans cosmid C41C4 (39750 nt)	56.1	148 (16510-16658)	Intron
Soares mouse NML Mus m (496 nt)	93.8	145 (330-475)	EST
Mouse DNA for tob family (2338 nt)	59.4	138 (1490-1628)	Intron
Mouse heat shock protein 70.1 (hsp7) (3518 nt)	58.7	138 (730-868)	Intron

Caenorhabditis elegans cosmid F53H4 (40380)	56.8	132 (32070-32202)	Intron
H.sapiens gene for phosphate carrier (7969 nt)	60.8	130 (2500-2630)	Intron
Dictyostelium discoideum phosphoinositide-specific phospholipase (2788 nt)	60.8	130 (140-270)	Intron
M.musculus mRNA for CD18 antigen beta (2828 nt)	58.1	129 (2660-2789)	Intron
Mouse heat shock protein (hsp68) mR (1330 nt)	61.4	127 (730-857)	Intron
Human DNA sequence from cosmid F91B7 (42613 nt)	64.7	119 (31770-31889)	Intron
Cyclic Protein-2=cathepsin L proenzyme (1790 nt)	60.9	115 (1370-1485)	Intron
Soares 2NbMT Mus muscu (163 nt)	95.6	114 (1370-1484)	Expressed sequence tag
Pea chloroplast photosystem II gene (4078 nt)	64.6	113 (3940-4053)	Intron
Human hypoxanthine phosphoribosyltransferase (56737 nt)	60.0	110 (12380-12490)	Intron
X.vesparum gene for 18S ribosomal R (2177 nt)	61.1	108 (200-308)	Gene : 18s RNA
Vicia faba vicilin gene. (5327 nt)	60.2	103 (1420-1523)	Intron
Human DNA sequence from clone 25J6 (57949 nt)	65.9	91 (127350-127441)	Unfinished
Human DNA sequence from clone J180 (47543 nt)	63.7	91 (126200-126291)	Unfinished
Caenorhabditis elegans cosmid F40B5 (22237 nt)	64.4	90 (12640-12730)	Intron
Human factor XIII b subunit gene (33206 nt)	67.1	82 (10840-10922)	Intron
Caenorhabditis elegans cosmid C49H3 (37516 nt)	65.4	78 (34340-34418)	Intron

Band D (19-mer) has weak homology to Human lens membrane exon, Mouse proliferin related protein exon, *P. falciparum* rRNA exon, and *X. vesparum* RNA exon. The other sequences detailed above are introns or EST (expressed sequence tags which are uncharacterised).

The significant proteins coded by the homologous sequence are tyrosine kinase, ERCC2, transforming protein and proliferin-related protein. All these proteins are known to play important roles in metastasis.

Tyrosine kinase

Tyrosine kinase catalyses the transfer of the γ phosphate of adenosine triphosphate to the tyrosine residues. This results in conformational changes of the target protein that modulate its activity.

The tyrosine kinase receptor contains an extracellular ligand recognition site, a single membrane spanning and cytoplasmic protein kinase domain. The primary structure of this kinase domain consists of the catalytic core embedded within regulatory sequences, that determines the activity of the kinase. When bound to ligand, tyrosine kinase phosphorylates the assembled proteins, allowing the transmission of signal from the environment into the cell. Tyrosine kinase receptors are essential for normal growth and mutations of the kinase domain could result in uncontrolled cell growth (Cadena 1992).

ERCC

The function of ERCC1 protein is essential for repair of damaged DNA by ultraviolet light and chemicals. ERCC1 deficient mice are unable to repair DNA damage and cross-links resulting in accumulation of unrepaired lesions and double strands break of DNAs. This leads to an increased mutation frequency and genome instability of cells (Weeda 1997).

Transforming protein

These are cytoplasmic proteins that could transform a cell to become cancerous. An example is v-src, a mutant of the normal cellular protein c-src. It is not known how v-src transforms the cells but direct interaction between this protein and the cellular plasma membrane is essential before the cell become transformed or malignant (Darnell 1990).

Proliferin-related protein

These proteins are expressed by several murine cell lines during active growth and found to be in abundance in mouse placenta. Their function as a placental hormone is unknown but they are homologous to all the family of the prolactin family (Linzer 1985). As prolactin has been associated with tumours such as breast carcinoma (Reynolds 1997), proliferin related protein might be important in tumour biology.

Chapter 13 Conclusions

This thesis investigates the molecular pathology of metastasis focusing on the mechanisms and differential gene expression responsible for the differing observed metastatic patterns of SL 12.3 and SL 12.4 cell lines. The first section of this study was to re-establish the metastatic model and to compare the growth patterns and morphology of the two cell lines. In the second section, the pattern of metastasis of the two cell lines was analysed both macroscopically and microscopically and the cellular dissemination to different organs was studied using radiolabelled ^{125}I UDR tumour cells. Lastly, in the third section, molecular tools such as differential display were used to identify, isolate and characterise possible cDNAs being differentially expressed by the SL 12.3 and SL 12.4 cell lines.

Section 1

In vitro studies : Tissue culture and growth characteristics

Aim

Tissue culture studies were done to re-establish and to study the growth patterns of the SL 12.3 and SL 12.4 cell lines

Approaches used

Both cell lines were grown in culture and environment as originally described (MacLeod 1984). Their morphology in tissue culture was documented and their growth patterns were determined by daily cellular count for five consecutive days.

Results

Both cell lines grow well in suspension in tissue culture. SL 12.3 cells grow diffusely whereas SL 12.4 cells grow in clumps. Under the same growth condition, both cell lines appeared to have similar growth patterns.

Discussion

In tissue culture, both SL 12.3 and SL 12.4 cell lines are stable with a hundred per cent cloning efficiency. Despite similar appearance in their growth patterns, it was not possible to conclude that the growth rate and doubling time are the same for the two cell lines as daily cell count showed wide standard error of mean for SL 12.4 cells. This variation is mainly due to difficulties in counting technique and in particular, clumping of SL 12.4 cells leads to potential pipetting and counting chamber errors. Further studies are required to eliminate these factors such as attempt at mechanical dispersion using repeated pipetting or pre-treatment of cell clumps with Trypsin.

Further studies

In view of the difficulties and to further compare the growth patterns of the two cell lines, other approaches should be considered such as the measuring of the amount of DNA produced from each cell line at defined time points. This would allow an indirect comparison of growth rate between SL 12.3 and SL 12.4 cells

Section 2

In vivo studies – Macroscopic and microscopic studies

Aim

The pattern of metastasis of the two cell lines analysed macroscopically were compared with the microscopic findings.

Approaches used

SL 12.3 and SL 12.4 cells were injected into the tail veins of AKR mice to mimic circulating metastatic cells. Autopsies were performed on any mice showing signs of distress or surviving beyond 8 weeks. Macroscopic findings of the organs were recorded for comparison with the microscopic analysis of the same organs by a consultant histopathologist.

Results

The tumourigenicity of 10^6 SL 12.3 cells was 100 % of 11 mice compared to only 9 % of 11 mice with 10^6 SL 12.4 cells. However, when the SL 12.4 cells were increased ten fold (10^7 cells per inoculum), the tumourigenicity was increased to 79 %.

Macroscopically, 10^6 SL 12.3 cells appeared to produce metastasis mainly in the spleen (100 %) and liver (100 %) whereas 10^7 SL 12.4 cells injected mice developed large ovarian metastasis and retroperitoneal nodes in addition to hepatosplenomegaly (78.5 %).

In addition to confirming the macroscopic findings, microscopic analysis showed that SL 12.3 and SL 12.4 lymphoblasts are present in organs that are not involved macroscopically. Furthermore, the infiltration pattern of the two cell lines differs between organs.

Discussion

Unlike SL 12.3 cells, the tumourigenicity of SL 12.4 cells was lower compared to original study (MacLeod). It is possible that mice preserved longer than eight weeks could have continued to develop tumours but the timing of sacrifice in the present study was limited by protocol and Home Office regulations.

Another explanation is that the SL 12.4 clone underwent phenotypic drift reverting to a less tumourigenic phenotype. One way to regain the more

aggressive phenotype is to culture cells from metastatic deposits of organs following an inoculation of SL 12.4 cells. However, this may give rise to further subclones, thus, confusing the study.

To allow comparison of metastatic pattern with SL 12.3 cells, SL 12.4 cells were increased to 10^7 cells per inoculum resulting in an increased in tumourigenicity from 9 % to 79 %. This may be due to an increase bolus of viable cells in circulation that have higher chances to lodge at capillary sites and to evade rapid cell death caused by tail vein injection and the immune system.

The microscopic analysis depends totally on the experience of the observer and attempts were made to further reduce any observer bias and errors by randomisation of the tissue sections without any information given whether the organs were from the mice inoculated with SL 12.3 or SL 12.4 cells. Reproducibility studies were performed without the observer's knowledge to check on consistency of the analysis.

Further studies

Since microscopic evidence of widespread tumour cells was found, the observed metastatic pattern from the macroscopic studies is more likely to be due to differing in vivo growth factors and host immune system. The sensitivity of this study could be further increased by performing statistical analysis of the observer and by using immunocytochemistry to identify cells directly from the slides. Further in vivo studies need to be performed to

study the different growth rates of SL 12.3 and SL 12.4 in relation to differing growth factors and possibly tissue extracts.

In vivo studies – Cellular tracking studies

Aim

A cellular tracking study using radiolabelled $^{125}\text{TUDR}$ tumour cells was performed to investigate the possibility that the difference in metastatic pattern observed is due to the initial load of cells reaching some organs being higher, a phenomenon that might result from homing of tumour cells to a specific tissue site.

Approaches used

Daily cell counts were performed for five days on viable cells that were incubated with medium containing various concentrations of $^{125}\text{TUDR}$. Having determined the incorporation rate and the optimum dose of $^{125}\text{TUDR}$ for cell labelling, both the cell lines were labelled and injected into the tail vein of mice randomly. The mice were then sacrificed at different time point and the harvested organs were washed before analysed with a gamma counter.

Results

The mean percentage of incorporation of ^{125}I UDR into both cell lines was relatively low (6.9 % and 4.8 % for SL 12.3 and SL 12.4 cells respectively) and the percentage of incorporation was at least 50 % more in one set of cells compared to the other.

There are no significant differences in cellular dissemination detected between SL 12.3 and SL 12.4 cells at fifteen minutes, one hour and three hours. Exceptions were of higher numbers of SL 12.4 cells seen in cerebral and thymic tissues at one hour post injection and also higher number of SL 12.4 cells per gram of ovarian tissues at one hour but these differences were not apparent at fifteen minutes or three hours.

Discussion

The mean percentage of incorporation of ^{125}I UDR was low and this reduced the sensitivity and accuracy of the technique producing wide variation in tissue counts. As a result, it is difficult to draw any firm conclusions from the data. However, this study appears to show similar tissue distribution of SL 12.3 and SL 12.4 cells following reinjection which is against the hypothesis that there is a difference in tissue homing between the two cell lines or that the homing phenomenon exists within the model.

There are differences observed between distribution of cells per gram of tissues in brain, lungs, liver, lymph nodes and ovaries within both cell lines

implying that the differences in tissue distribution are due to mechanical reasons rather than tissue specificity or homing. However, these conclusions cannot be proved on the current data available as the low incorporation of isotope reduces the accuracy of the technique.

As all cells were incubated together in the same environment with the same batch of ^{125}I UDR, the difference in percentage of incorporation observed is most likely due to errors in washing and pelleting of cells before being analysed by the gamma counter. This could improve with more practice and experiment but in any biological systems there are always going to be variation beyond experimental control.

Further studies

In vivo cellular tracking can be studied using another approach such as fluorescent labelling technique. Molecule such as PKH26 can be used to label cells by incorporating into the lipid bilayer of cytoplasmic membranes. The labelled cells can be detected sensitively in various organs using the flow cytometry and fluorescence (Johnsson 1997; Horan 1990). Problems, however, may still be encountered during this technique if labelling is not as high and small number of cells being present in different organs.

Section 3

Molecular Studies

Aim

Having shown that SL 12.3 and SL 12.4 cell lines have different metastatic patterns, molecular tools are used to isolate and characterise any genes that are differentially expressed in a cell line.

Approaches used

Total RNAs extracted from both cell lines were reversed transcribed to cDNAs. These cDNAs were amplified and labelled with polymerase chain reaction (PCR) using an anchoring 3'-end primer and a arbitrary 5'-end primer based on CD44 and LTK3 (Lymphocyte thymidine kinase sequence). The products were displayed along each other for comparison in a polyacrylamide gel. cDNAs of interest were cut out, reamplified and sequenced. Initial reamplification was attempted using the TA cloning system without any success. Subsequent reamplification was then carried out successfully using PCR and a pair of extended primers. The cDNAs were then compared to known sequences in genetic databases.

Results

Three cDNAs (Band A, C and D) were isolated and sequenced. Band A was exclusively expressed by SL 12.4 cells and has weak homology to ERCC/XPD and tyrosine kinase exons. Band C was exclusively expressed by SL 12.3 cells and has weak homology to exons coding for glucocorticoid receptor, transcription factor and transforming proteins. Lastly, band D was expressed more in SL 12.4 cells than SL 12.3 cells and has weak homology to exons coding for rpoD, ATPase2, dihydrofolate reductase and proliferin related protein.

Discussion

The differential display technique was used to isolate cDNAs that are exclusively expressed because this method was 'state of the art' at the time this work was produced. The technique is easily reproducible and requires very low concentration of RNAs. The gene products can be compared directly and cut out for further reamplification. Unfortunately, the difficulties lie in reamplification and sequencing as the primers used were too short for conventional technique. Attempts to reamplify using the TA cloning system failed because false positives were produced as a result of self blunt ligation at ECoRI sites of the plasmid. Reamplification was, however, successfully performed using the extended primers that also allowed subsequent conventional sequencing technique.

Further Studies

The three cDNAs isolated merit further study. Northern blot analysis is required to confirm their differential expression. Using them as probes, fuller cDNA sequences can be extracted from mouse cDNA libraries for characterisation. For further investigation of the role of this longer sequence on the in-vivo and in-vitro growth rates of the two cell lines and subsequent pattern of metastasis, the gene can be inserted (transfection) into the genome of the other cell line or deleted (knock-out) from the genome of the corresponding normal cell in the mice.

Other approaches to identify differential expressed gene (Carulli 1998) such as serial analysis of gene expression or SAGE (Velculescu 1995) and representational difference analysis (Lisitsyn 1995) could be applied to this model.

Conclusion

Having established the methods, this thesis will be the foundation to further studies on the differential gene expression in human tumour model such as colorectal cancer. Primary tumours from the left and the right side of the colon, despite similar histological appearance, are known to behave differently in metastasis clinically. Differential expression of these primary tumours, liver and nodal metastasis may help in isolating genes that are responsible for their different tumourigenicity and pattern of metastasis.

References

- Albelda, S. (1993). "Role of integrins and other cell adhesion molecules in tumour progression and metastasis." Lab Invest **68**: 4-17.
- Alessandro, R. and E. C. Kohn (1995). "Tumour invasion and angiogenesis." Cancer **76**(10): 1874-1877.
- Alexander, P. (1974). "Proceedings: Escape from immune destruction by the host through shedding of surface antigens: is this a characteristic shared by malignant and embryonic cells?" Cancer Res **34**: 2077-2082.
- Alexander, P. (1976). "Dormant metastases which manifest on immunosuppression and the role of macrophages in tumours." Book : Fundamental aspects of metastasis(ed. L. Weiss), North-Holland, Amsterdam: 227-239.
- Aruffo, A., I. Stamenkovic, et al. (1990). "CD 44 is the principal cell surface receptor for hyaluronate." Cell **61**: 1303-1313.
- Auerbach, R., W. Lu, et al. (1987). "Specificity of adhesion between murine tumour cells and capillary endothelium : an in vitro correlate of preferential metastasis in vivo." Cancer Res **47**: 1492-1496.
- Bancroft, J. D. and A. Stevens (1990). "Theory and Practice of Histological Techniques." Book 3rd Edition Churchill Livingstone.
- Bartgatze, R., N. Wu, et al. (1987). "High endothelial venule binding as a predictor of the dissemination of passaged murine lymphomas." J Exp Med **166**: 1125-1131.
- Batson, O. V. (1940). "The function of the vertebral veins and their role in the spread of metastasis." Ann. Surg **112**: 138-49.
- Behrens, J. (1993). "The role of cell adhesion molecules in cancer invasion and metastasis." Breast-Cancer-Res-Treat **24**: 175-184.
- Cadena, D. and G. Gill (1992). "Receptor tyrosine kinase." Faseb J **6**: 2332-2337.
- Carulli, J., M. Artinger, et al. (1998). "High throughput analysis of differential gene expression." J Cell Biochem Suppl **30-31**: 286-296.

Chew, E. C., R. L. Josephson, et al. (1976). "Morphological aspects of the arrest of circulating cancer cells." Book : Fundamental Aspects of Metastasis ed. L. Weiss: 121-150.

Chomczynski, P. and N. Sacchi (1987). "Single-Step Method of RNA isolation by Acid Guanidinium Thiocyanate-Phenol-Choloroform Extraction." Analytical Biochemistry **162**: 156-159.

Cifone, M. A. and I. J. Fidler (1981). "Increasing Metastatic Potential is Associated with Increasing Genetic Instability of Clones Isolated from Murine Neoplasms." Proc Nat Acad Sci, USA **78**: 6949-6952.

Coman, D. (1944). "Decreased mutual adhesiveness, a property of cells from squamous cell carcinoma." Cancer Res **1**: 625-629.

Coman, D. R. (1953). "Mechanisms responsible for the origin and distribution of blood-borne tumour metastasis : A Review." Cancer Research **13**: 397-404.

Coman, D. R., R. P. DeLond, et al. (1951). "Studies on the mechanism of metastasis. The distribution of tumours in various organs in relation to the distribution of arterial emboli." Cancer Research **11**: 648-651.

Cotmore, S. F. and R. L. Carter (1973). "Mechanisms of enhanced intrahepatic metastasis in surfactant-treated hamsters; an electron microscope study." International Journal of Cancer **11**: 725-738.

Currie, G. and P. Alexander (1974). " Spontaneous shedding of TSTA by viable sarcoma cells : its possible role in facilitating metastatic spread. " Br. J. Cancer **29**: 72-75.

DeBryun, P. and Y. Cho (1979). "Entry of metastatic malignant cells into the circulation from a subcutaneously growing myelogenous tumour." J. Natl. Cancer. Inst **62**: 1221-1228.

Darnell, J., H. Lodish, et al. (1990). Molecular cell biology, Scientific American Books.

Davidson, E. H. (1976). Gene activity in early development. New York, Academic Press.

Dexter, D. L. and P. Calabresi (1982). "Intraneoplastic diversity." Biochimica et Biophysica Acta **695**: 97-112.

Dingermans, K. P. and V. d. B. Weerman (1980). "Metastasis - Clinical and Experimental Aspects." Hellmann, K, Hilgard, P, Eccles, S 2nd edition: 194-198.

Donati, M. B. and A. Poggi (1980). "Malignancy and haemostasis." British Journal of Haematology **44**: 173-182.

Dorland (1981). Dorland's Illustrated Medical Dictionary 28th Edition. Philadelphia, WB Saunders.

Dorudi, S., J. Sheffield, et al. (1993). "E-Cadherin expression in colorectal carcinoma." Am J Pathol **142**: 981-986.

Dougherty, G., S. Dougherty, et al. (1992). "Expression of human CD 44R1 enhances the metastatic capacity of murine fibrosarcoma cells." Proc Am Assoc Cancer **33**: 34.

Dynal Technical handbook Molecular Biology.

Eisenbach, L., S. Segal, et al. (1985). "Proteolytic enzymes in tumor metastasis. I. Plasminogen activator in clones of Lewis lung carcinoma and T10 sarcoma." J. Nat Cancer Inst **74**: 87-93.

Elvin, P. and E. CW (1982). "The adhesiveness of normal and SV40-transformed BALB/C 3T3 cells : effects of culture density and shear rate." European Journal of Cancer and Clinical Oncology **18**: 669-675.

Erlich, H. A., D. Gelfand, et al. (1991). "Recent advances in the polymerase chain reaction." Science **252**: 1643-1651.

Evans, C. (1991) The metastatic cell, Chapman & Hall.

Ewing, J. (1928). "Neoplastic Diseases(A treatise on tumours)." W,B Saunders, Philadelphia 3rd Edition: 86.

Fidler, I. J. (1970). "Metastasis : Quantitative analysis of distribution and fate of tumour emboli labelled with ¹²⁵I-5-Iodo-2'-deoxyuridine." Journal of the National Cancer Institute **45**: 773-782.

Fidler, I. J. (1973b). "The relationship of embolic homogeneity, number, size and viability to the incidence of experimental metastasis." European Journal of Cancer **9**: 223-227.

Fidler, I.J (1978). "Tumour heterogeneity and the biology of cancer invasion and metastasis." Cancer Reserch **38**: 2651-2660.

Fidler, I. J. (1985). "Macrophages and metastasis - A biological approach to cancer therapy." Cancer Research **45**: 4714-4726.

Fidler, I.J (1990). "Critical factors in the biology of human cancer metastasis : twenty-eight GHA Clowes memorial award lecture." Cancer Res **50**: 6130-6138.

Fidler, I.J and C. Batch (1987). The Biology of cancer metastasis and implications for therapy, Year book medical publisher.

Fidler, I. J. and M. L. Kripke (1977). "Metastasis results from pre-existing variant cells within a malignant tumour." Science **197**: 893-895.

Fidler, I. and M. Kripke (1980). Metastatic heterogeneity of cells from K-1735 melanoma. Stuttgart, Gustav Fischer Verlag.

Fidler, I. J. and M. L. Kripke (1988). "Biology of Cancer Metastasis." Book : Cancer, the outlaw cell 2nd edition: 164.

Fidler, I. and J. Talmadge (1986). "Evidence that intravenously derived murine pulmonary metastases can originate from the expansion of a single tumour cell." Cancer Res **46**: 5167-5171.

Fogel, M., E. Gorelik, et al. (1979). "Differences in cell surface antigens of tumour metastases and those of the local tumour." J. Nat. Canc. Inst **62**(585-588).

Fogh, J., J. Fogh, et al. (1977). "One hundred and twenty-seven cultured human tumour cell lines producing tumours in nude mice." J Natl Cancer Inst **59**: 221-225.

Folkman, J., K. Watson, et al. (1989). "Induction of angiogenesis during the transition from hyperplasia to neoplasia." Nature **339**: 58-61.

Foulds, L. (1949). "Mammary tumours in hybrid mice : growth and progression of spontaneous tumours." Br. J. Cancer **3**: 345-375.

Foulds, L. (1969). Neoplastic development. New York, Academic Press.

Foulds, L. (1975). Neoplastic development. New York, Academic Press.

Frost, P. and R. S. Kerbel (1983). "Immunology of metastasis : can the immune system response cope with disseminated tumour?" Cancer Metastasis Review **2**: 239-256.

Garrod, D. R. (1993). "Cell to cell and cell to matrix adhesion." BMJ **306**: 703-705.

Gastpar, H. (1982). "Platelet aggregation inhibitors and cancer metastasis." Annales Chirurgiae et Gynaecologiae **71**: 142-150.

- Gehlsen, K., W. Argraves, et al. (1988). "Inhibition of in vitro tumour cell invasion by Arg-Gly-Asp-containing peptides." J. Cell Biol **106**: 925-930.
- Greene, H. and E. Harvey (1964). "Relationship between the dissemination of tumour cells and the distribution of metastases." Cancer Res **24**: 799-811.
- Gunthert, U., M. Hofman, et al. (1991). "A new variant of glycoprotein CD44 confers metastatic potential to rat carcinoma." Cell **65**: 13-24.
- Guo, Y., J. Ma, et al. (1994). "Inhibition of Human Melanoma Growth and Metastasis in Vivo by anti-CD 44 Monoclonal Antibody." Cancer Res **54**: 1561-1565.
- Hanna, N. (1982a). "Role of natural killer cells in control of cancer metastasis." Cancer Metast Rev **1**: 45-64.
- Hanna, N. and I. Fidler (1980). "Role of natural killer cells in the destruction of circulating tumor emboli." J. Nat. Cancer. Inst **65**: 801-809.
- Hart, I. R. (1982). "Seed and soil' revisited : Mechanisms of site specific metastasis." Cancer Metastasis Rev **1**: 5-16.
- Hart, I. and I. Fidler (1981). "Role of organ selectivity in the determination of metastatic patterns of B16 melanoma." Cancer Res **41**: 1281-1287.
- Hart, I. and N. Goode (1989). "Molecular aspect of metastatic cascade." Biochim Biophys Acta **989**: 65-84.
- Hart, I. and A. Saini (1992). "Biology of tumour metastasis." Lancet **339**: 1453-1457.
- Hart, I. R., J. E. Talmadge, et al. (1981). "Metastatic behaviour of a murine reticulum cell sarcoma exhibiting organ-specific growth." Cancer Research **41**: 1281-1287.
- Haynes, B., E. Harden, et al. (1983). "Differentiation of human T-lymphocytes. I. Acquisition of a novel human cell surface protein(p80) during normal intrathymic T-cell maturation." J Immunol **131**: 1195-1199.
- Hays, E. F., N. Margaretten, et al. (1982). "Spontaneous leukaemia viruses : lymphomagenic ecotropic viruses of the AKR mice." Journal of the National Cancer Institute **69**: 1077-1082.
- Hedrick, S. M., D. L. Cohen, et al. (1984). "Isolation of cDNA clones encoding T cell-specific membrane associated proteins." Nature(Lond) **308**: 149-153.

- Heppner, G. (1984). "Tumour heterogeneity." Cancer Research **44**: 2259-2265.
- Horak, E., D. L. Darling, et al. (1986). "Analysis of organ-specific effects on metastatic tumour formation by studies in vitro." Journal of the National Cancer Institute **76**: 913-922.
- Horan, P., M. Melnicoff, et al. (1990). "Flourescent cell labelling for in vivo and in vitro cell tracking." Methods in Cell Biology **33**: 469-490.
- Horst, E., C. Meijer, et al. (1990). "Adhesion molecules in the prognosis of diffuse large cell lymphoma: expression of a lymphocyte homing receptor(CD 44), LFA-1(CD11a/CD18) and ICAM-1(CD54)." Leukaemia(Baltimore) **4**: 595-599.
- Humphries, M. J., K. Olden, et al. (1986). "A synthetic peptide from fibronectin inhibits experimental metastasis of murine melanoma cells." Science **233**: 467-469.
- Hynes, R. (1987). "Integrins: a family of cell surface receptors." Cell **48**: 549-544.
- Hynes, R. (1992). "Integrins: Versality, Modulation and signalling in cell adhesion." Cell **69**: 11-25.
- Hynes, R. and A. Lander (1992). "Contact and adhesive specificities in the associations, migrations, and targeting of cells and axons." Cell **68**: 303-322.
- Ishikawa, F (1989). "Identification of angiogenic activity and the cloning and expression of platelet-derived endothelial cell growth factor." Nature **338**: 557-562.
- Jalkanen, S., H. Joensuu, et al. (1992). "Lymphocyte homing and clinical behaviour of non-Hodgkin's lymphoma." J Clin Invest **87**: 1853-1840.
- Jaques, G., B. Auerbach, et al. (1993). "Evaluation of serum neural cell adhesion molecule as a new tumour marker in small cell lung cancer." Cancer **72**: 418-425.
- Jiang, W., M. Puntis, et al. (1994). "Molecular and cellular basis of cancer invasion and metastasis : implications for treatment." Br. J. Surg **81**: 1576-1590.
- Jiang, W. G. (1996). "E-Cadherin and its associated protein catenins, cancer invasion and metastasis." Br. J. Surg. **83**: 437-446.

Johnsson, C., R. Festin, et al. (1997). "Ex vivo PKH26-labelling of lymphocytes for studies of cell." Scandinavian Journal of Immunology **45**(5): 511-514.

Johnson, J., B. Stade, et al. (1989). "De novo expression of intracellular-adhesion molecule in melanoma correlates with increased risks of metastasis." Proc. Natl. Acad. Sci. USA **86**: 641-644.

Juneja, H., F. Schmalsteig, et al. (1993). "Vascular cell adhesion molecule-1 and VLA-4 are obligatory adhesion proteins in the heterotypic adherence between human leukaemia/lymphoma cells and marrow stromal cells." Exp Haematol **21**: 444-450.

Kahn, P. (1992). "Adhesion protein studies provide new clue to metastasis." Science **257**: 614.

Kaminski, M. and R. Auerbach (1988). "Tumour cells are protected from NK-cell-mediated lysis by adhesion to endothelial cells." Int. J. Cancer **41**: 847-849.

Kerbel, R. S. (1990). "Growth dominance of the metastatic cancer cell : cellular and molecular aspects." Advances in cancer research **55**: 87 - 132.

Kim, U., A. Baumler, et al. (1975). "Immunological escape mechanism in spontaneously metastasizing mammary tumors." Proc Nat Acad Sci **72**: 1012-1016.

Kinsella, A. R., B. Green, et al. (1993). "The role of the cell-cell adhesion molecule E-cadherin in large bowel tumour cell invasion and metastasis." Br. J. Cancer **67**: 904-909.

Kinsey, D. (1960). "An experimental study of preferential metastasis." Cancer **13**: 674-676.

Kjonnixsen, I., H. K. Hoifodt, et al. (1991). "Different metastasis patterns of a human melanoma cell line in nude mice and rats : Influence of microenvironments." Journal of National Cancer Institute **14**: 1020-1024.

Kowitz, A., G. Kadmon, et al. (1993). "Expression of L1 cell adhesion molecule is associated with lymphoma growth and metastasis." Clin Exp Metast **11**: 419-429.

Kull, F., D. Brent, et al. (1987). "Chemical identification of a tumor-derived angiogenic factor." Science **236**: 843-845.

Lauri, D., L. Needham, et al. (1991). "Tumour cell adhesion to endothelial cells : Endothelial leucocyte adhesion molecule-1 as an inducible adhesive receptor specific for colon carcinoma cells." J. Natl. Cancer. Inst **81**: 1321-1324.

- Lesley, J., R. Schulte, et al. (1990). "Binding of hyaluronic acid to lymphoid cell lines is inhibited by monoclonal antibodies against Pgp-1." J Exp Cell Res **187**: 224-233.
- Liang, P., L. Averboukh, et al. (1992). "Differential display and cloning of messenger RNAs from human breast cancer versus mammary epithelial cells." Cancer Res **52**: 6966-6968.
- Liang, P., L. Averboukh, et al. (1993). "Distribution and cloning of eukaryotic mRNAs by means differential display : refinements and optimisation." Nucleic Acids Research **21**(14): 3269-3275.
- Liang, P. and A. B. Pardee (1992). "Differential display of eukaryotic mRNA by means of the polymerase chain reaction." Science(257): 967-971.
- Linzer, D., S. Lee, et al. (1985). "Identification of proliferin mRNA and protein in mouse placenta." Proc Natl Acad Sci USA **13**(82): 4356-4359.
- Liotta, L., J. Kleinermann, et al. (1974). "The significance of haematogenous tumour cell clumps in the metastatic process." Cancer Res **34**: 997-1004.
- Liotta, L. A. (1985). "Mechanisms of cancer invasion and metastases." Book : Important advances in oncology (Eds : Devita VT Jr, Hellman S, Rosenberg S) Philadelphia : Lippincott: 25-41.
- Liotta, L. A. (1986). "Tumour invasion and metastases - role of the extracellular matrix: Rhoads memorial award lecture." Cancer Res **46**: 1-7.
- Liotta, L. A., S. Abe, et al. (1979). "Preferential digestion of basement membrane collagen by an enzyme derived from a metastatic murine tumour." Proceedings of the National Academy of Sciences, USA **76**: 2268-2272.
- Lisitsyn, N. (1995). "Representational difference analysis : finding the differences between genomes." Trends Genet **11**(8): 303-307.
- McArdle, C., D. Hole, et al. (1990). "Prospective study of colorectal cancer in the West of Scotland: 10 year follow-up." Br. J. Surg **77**: 280-282.
- McBain, J. A., L. L. Weese, et al. (1984). "Establishment and characterisation of human colorectal cancer cell lines." Cancer research **44**: 5813-5821.
- MacLeod, C. L., A. M. Fong, et al. (1990). "Isolation of Novel Complementary DNA Clones from T Lymphoma Cells : One Encodes a Putative Multiple Membrane-spanning Protein." Cell Growth and Differentiation **1**: 271-279.
- Macleod, C. L., E. F. Hays, et al. (1984). "A New Murine Model for the in Vitro Development of Thymoma Cell Heterogeneity." Cancer Res **44**: 1784-1790.

- MacLeod, C. L., S. E. Weinroth, et al. (1985). "SL 12 Murine T-lymphoma : A New Model for Tumour Cell Heterogeneity." Journal of National Cancer Institute **74**: 875-882.
- Maemura, M. and R. Dicksin (1994). "Are cellular adhesion molecules involved in the metastasis of breast cancer." Breast cancer research and treatment **32**: 239-260.
- Maniatis, T., E. F. Fritsch, et al. (1983). Molecular Cloning : A laboratory Manual. Cold Spring Harbour, New York, Cold Spring Harbour Laboratory Press.
- Matsumura, Y. and D. Tarin (1992). "Significance of CD 44 gene products for cancer diagnosis and disease evaluation." Lancet **340**: 1053-1058.
- Mignatti, P., E. Robbins, et al. (1986). "Tumour invasion through the Human Amniotic Membrane : Requirement for a proteinase cascade." Cell **47**: 487-498.
- Miyasaka, M. (1995). "Cancer metastasis and adhesion molecules." Clinical orthopaedics and related research **312**: 10-18.
- Morikawa, K., S. Walker, et al. (1988). "Influence of organ environment on the growth , selection and metastasis of Human Colon Carcinoma Cells in Nude Mice." Cancer Res **48**: 6863-6871.
- Mou, L., H. Miller, et al. (1994). "Improvements to the differential display method for gene analysis." Biochemical and biophysical research communcations **199**(2): 564-569.
- Nagase, H., A. Barratt, et al. (1992). "Nomenclature and glossary of the matrix metalloproteinases." Matrix **1**: 421-424.
- Naito, S., R. Giavazzi, et al. (1987). "Correlation between the in vitro interactions of tumour cells with an organ microenvironment and metastasis in vivo." Invasion Metastasis **7**: 126-129.
- Namec, R., B. Toole, et al. (1987). "The cell surface hyaluronate binding sites of invasive human bladder carcinoma cells." Biochem Biophys Res Commun **149**: 249-257.
- Natali, P., M. Nicotra, et al. (1990). "Differential expression of ICAM-1 in primary and metastatic melanoma lesions." Cancer Res **50**: 1271-1278.
- Neri, A. and G. L. Nicholson (1981). "Phenotypic drift of metastatic and cell-surface properties of mammary adenocarcinoma cell clones during growth in vitro." International Journal of Cancer **28**: 731-738.

Netland, P. and B. Zetter (1984). "Organ specific adhesion of metastatic tumour cells in vitro." Science **224**: 1113-1115.

Nicholson, G. L. (1982). "Cancer metastasis : organ colonisation and the cell-surface properties of malignant cells." Biochemical Biophysica Acta **695**: 113-176.

Nicholson, G.L and S. Custead (1982). "Tumour metastasis is not due to adaptation of cells to a new organ environment." Science **215**: 176-178.

Nicholson, G. L. and K. M. Dulski (1986). "Organ specificity of metastatic tumour colonisation is related to organ-selective growth properties of malignant cells." International Journal of Cancer **38**: 289-294.

Nigam, A., M. Pignatelli, et al. (1994). "Current concept in metastasis." Gut **35**: 996-100.

Nigam, A., F. Salvage, et al. (1993). "Loss of cell-cell and cell-matrix adhesion molecules in colorectal cancer." Br J Cancer **68**: 507-514.

Nottenburg, C., G. Rees, et al. (1989). "Isolation of mouse CD 44 cDNA: structure features are distinct from the primate cDNA." Proc. Natl. Acad. Sci. USA **86**: 8521-8528.

Nowell, P. C. (1976). "The clonal evolution of tumour cell populations." Science **194**: 23-28.

Ossowski, L. and E. Reich (1983b). "Antibodies to plasminogen activator inhibit human tumor metastasis." Cell **35**(611-619).

Paget, S. (1889). "The distribution of secondary growths in cancer of the breast." Lancet **i**: 571-573.

Pauli, B. and C. Lee (1988). "Organ preference of metastasis." Lab Invest **58**: 379-387.

Pearson, W. R. and D. J. Lipman (1988). "Improved tools for Biological Sequence Comparison." Proc. Natl. Acad. Sci **85**: 2444-2448.

Picker, L. J. and E. C. Butcher (1992). "Physiological and Molecular Mechanisms of Lymphocytes Homing." Annu. Rev. Immunol. **10**: 561-591.

Pignatelli, M., D. Liu, et al. (1992). "Morphoregulatory activities of E-Cadherins and beta-1 integrins in colorectal tumour cells." Br. J. Cancer **66**: 629-634.

Poste, G. and I. Fidler (1980). "The pathogenesis of cancer metastasis." Nature **283**: 139-146.

Reclamer, J. C. A. (1829). "Recherches sur le Traitement du Cancer par la Compression Methodique Simple ou Combinee et sur l'Histore Generale de la Meme Maladie." Chez Gabor, Paris **2**: 110. (Reviewed By Paget, 1889)

Reynolds, C., K. Montone, et al. (1997). "Expression of prolactin and its receptor in human breast carcinoma." Endocrinology **12**(138): 5555-5560.

Roos, E. (1991). "Adhesion moleculaes in lymphoma metastasis." Cancer and metastasis reviews **10**: 33-48.

Roosien, F., D. Rijk, et al. (1989). "Involvement of LFA-1 in lymphoma invasion and metastasis demonstrated with LFA-1-deficient mutants." J. Cell. Biol **108**: 1079-1085.

Salsbury, A. J. (1975). "The significance of the circulating cancer cell." Cancer Treatment Reviews **2**: 55-72.

Schackert, G. and I. Fidler (1988). "Site-specific metastasis of mouse melanomas and a fibrosarcoma in the brain or the meninges of syngeneic animals." Cancer Res **48**: 3478-3483.

Scheele, J. (1993). "Hepatectomy for liver metastasis." Br. J. Surg. **80**: 274-276.

Schirmacher, V. (1985). "Cancer Metastasis : experimental approaches, theoretical concepts, and impacts for treatment strategies." Book : Advances in cancer research(ed. G. Klein and S.Weinhouse), Academic Press, London **43**: 1-73.

Schmidt, M. D. (1903). "Die Verbrietungswege der Karcinome und die Beziehung generalisierter Sarkome zu den leukamischen Neubildungen." Jena, Gustav Fisher, Jean.

Seiter, S., R. Arch, et al. (1993). "Prevention of tumour metastasis formation by anti-variant CD 44." J Exp Med **177**: 443-447.

Seki, H., J. Tanaka, et al. (1993). "Neural cell adhesion molecule (NCAM) and perineural invasion in bile duct cancer." J. Surg. Oncol **53**: 78-83.

Shing, Y., J. Folkman, et al. (1985). "Angiogenesis is stimulated by a tumor-derived endothelial cell growth factor." Cell Biochem **29**: 275-287.

Shing, Y., J. Folkman, et al. (1984). "Heparin affinity: purification of a tumor-derived capillary endothelial cell growth factor." Science **223**: 1296-1298.

- Sloane, B. and K. Hohn (1984). "Cysteine proteinases and metastasis." Cancer Metast Rev **3**: 249-263.
- Sloane, B., J. Rozhin, et al. (1986). "Cathepsin B: association with plasma membrane in metastatic tumors." Proc. Natl. Acad. Sci **83**: 2483-2487.
- Stamenkovic, I., M. Amiot, et al. (1989). "Lymphocyte molecule implicated in lymph node homing is a member of the link protein family." Cell **56**: 1047-1053.
- Stamenkovic, I., A. Aruffo, et al. (1991). "The haemopoietic and epithelial forms of CD 44 are distinct polypeptides with different adhesion potentials for hyaluronate-bearing cells." EMBO J **10**: 343-348.
- Sugarbaker, E. (1981). "Pattern of metastasis in human malignancies." Cancer Biol Rev **2**: 235-303.
- Sunday, M. E. (1995). "Differential display RT-PCR for identifying novel gene expression in the lung." Am. J. Physiol. **269**: L273-L284.
- Takeichi, M. (1991). "Cadherin cell adhesion receptors as a morphogenetic regulator." Science **251**: 1451-1455.
- Talmadge, J. and I. Fidler (1982). "Cancer metastasis is selective or random depending on parent tumour population." Nature **297**: 593-594.
- Tanabe, K., L. Ellis, et al. (1993). "Expression of CD 44R1 adhesion molecule in colon carcinomas and metastases." Lancet **341**: 725-726.
- Tang, D. G. and K. V. Honn (1994). "Adhesion molecules and tumour metastasis: an update." Invasion metastasis **14**: 109-122.
- Taptiklis, N. (1968). "Dormancy by dissociated thyroid cells in the lungs of mice." Eur J Cancer **4**: 59-66.
- Taptiklis, N. (1969). "Penetration of the vascular endothelial barrier by non-neoplastic thyroid cells in circulation." Eur J Cancer **5**: 445-457.
- Tarin, D., J. E. Price, et al. (1984b). "Mechanisms of human tumour metastasis studied in patients with peritoneovenous shunts." Cancer Res **44**: 3584-3592.
- Underhill, C. (1992). "CD 44: the hyaluronan receptor." J Cell Sci **103**: 293-298.
- Underhill, C. and B. Toole (1980). "Physical characteristic of hyaluronate binding to the surface of simian virus 40 transformed 3T3 cells." J Biol Chem **155**: 4544-4551.

Underhill, C. and B. Toole (1981). "Receptor for hyaluronate on the surface of parent and virus-transformed cell lines; binding and aggregation studies." Exp Cell Res **131**: 419-425.

Velculescu, V., L. Zhang, et al. (1995). "Serial analysis of gene expression." Science **270**(5235): 484-487.

Wang, B., G. McLoughlin, et al. (1980). "Correlation of plasminogen activator with tumour metastasis in B16 mouse melanoma cell lines." Cancer Res **40**: 280-292.

Warren, B. (1980). Extravasation of cancer cells with special references to brain metastasis and the arrest and microinjury hypothesis. Boston, Massachusetts, G.K Hall.

Warren, R. (1995). "Regulation of vascular endothelial growth factor of human colon cancer and tumorigenesis in a mouse model of experimental liver metastasis." J. Clin. Invest. **95**: 1789-97.

Waxman, J. and H. Wasan (1992). "The architecture of cancer." BMJ **305**: 1306-1307.

Weeda, G., I. Donker, et al. (1997). "Disruption of mouse ERCC1 results in a novel repair syndrome with growth failure, nuclear abnormalities and senescence." Curr Biol **7**(6): 427-439.

Wenck, A. R. and M. Laszlo (1995). "Direct sequencing of DNA isolated from mRNA differential display." Biotechniques **18**: 48-53.

Willis, R. A. (1973). "The spread of tumours in the human body." **3rd edition.**

Weiss, L. (1985). Principles of Metastasis. Orlando, FL, Academic Press.

Weiss, L. (1994). "Cell adhesion molecules : A critical examination of their role in metastasis." Invasion Metastasis **14**: 192-197.

Yoneda, T., A. Sasaki, et al. (1994). "Osteolytic bone metastasis in breast cancer." Breast cancer and Treatment **32**: 73-84.

Zetter, B. R. (1990). "The cellular basis of site-specific tumour metastasis." N. Engl. J. Med **332**: 605-612.

Zimmermann, K. and W. Mannhalter (1996). "Technical Aspects of quantitative Competitive PCR." Biotechniques **21**: 268-279.

